US 20230255479A1

(19) United States

(12) Patent Application Publication (10) Pub. No.: US 2023/0255479 A1

Holland et al. (43) Pub. Date: Aug. 17, 2023

(54) SYSTEM AND METHOD FOR EYE REGION VISUALIZATION IN A LASER SURGICAL SYSTEM

(71) Applicant: **ViaLase, Inc.**, Aliso Viejo, CA (US)

(72) Inventors: **Guy Holland**, San Juan Capistrano, CA (US); **Tibor Juhasz**, San Clemente, CA (US); **Wesley W. Lummis**, Rancho Santa Margarita, CA (US); **Eric R. Mikula**, Aliso Viejo, CA (US); **Ferenc Raksi**, Mission Viejo, CA (US); **Manu Sharma**, Ladera Ranch, CA (US); **Hadi Srass**, Yorba Linda, CA (US); **Carlos G. Suarez**, Tustin, CA (US)

(21) Appl. No.: **17/671,496**

(22) Filed: **Feb. 14, 2022**

Publication Classification

(51) **Int. Cl.**

A61B 3/14	(2006.01)
H04N 5/232	(2006.01)

(52) **U.S. Cl.**

CPC ***A61B 3/14*** (2013.01); ***H04N 5/232125*** (2018.08); ***H04N 5/23299*** (2018.08); *H04N 5/2256* (2013.01)

(57) **ABSTRACT**

A system for imaging a region of an eye includes a laser source that outputs a laser beam; a first optical subsystem that couples to the eye; a focusing objective coupled with the first optical subsystem and the laser source; a visualization system having a depth of field and a field of view; a movement subsystem that moves the focusing objective and the visualization system; and a control system that controls the movement subsystem and the visualization system to: place the depth of field and the field of view at respective positions relative to a target volume so the volume is within the depth of field and the field of view, obtain an image of the region of the eye, and maintain the position of the field of view of the visualization system relative to the target volume during movement of a laser focus through the target volume.

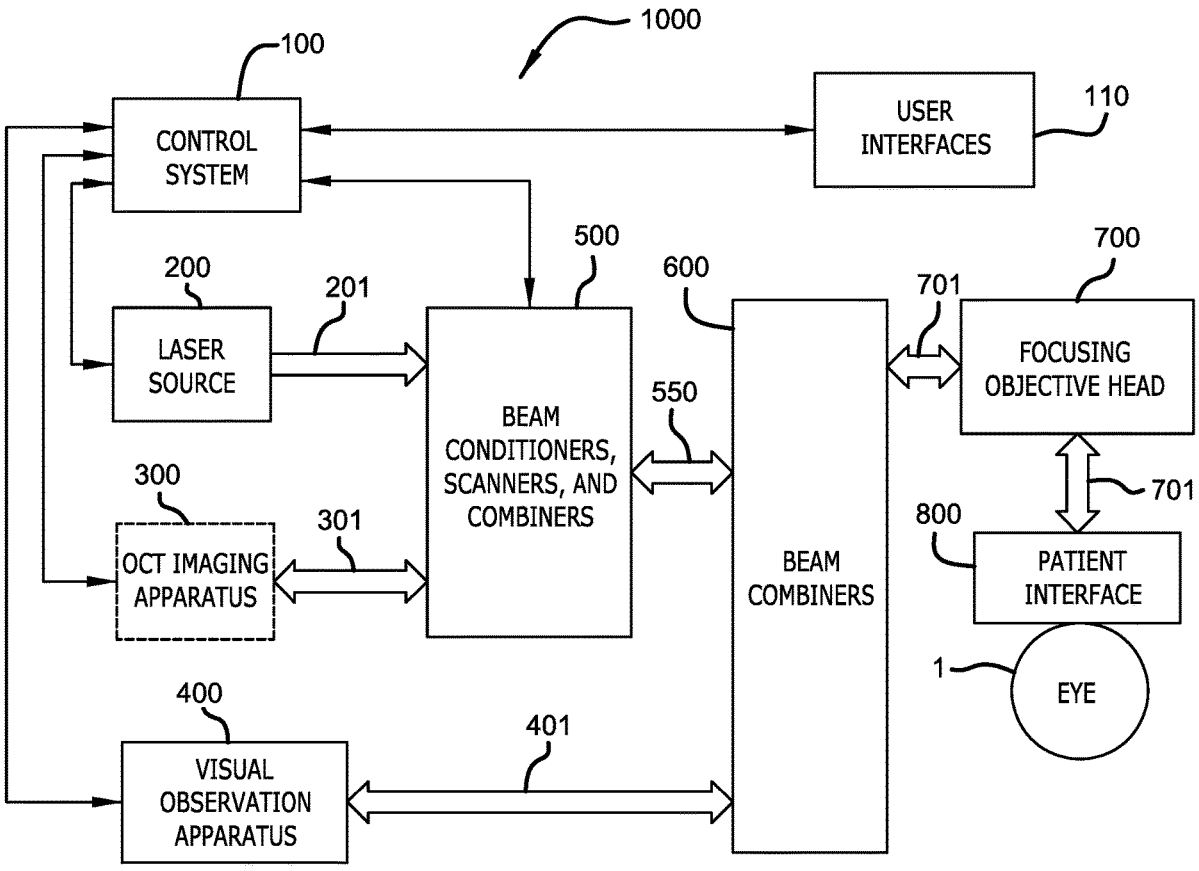

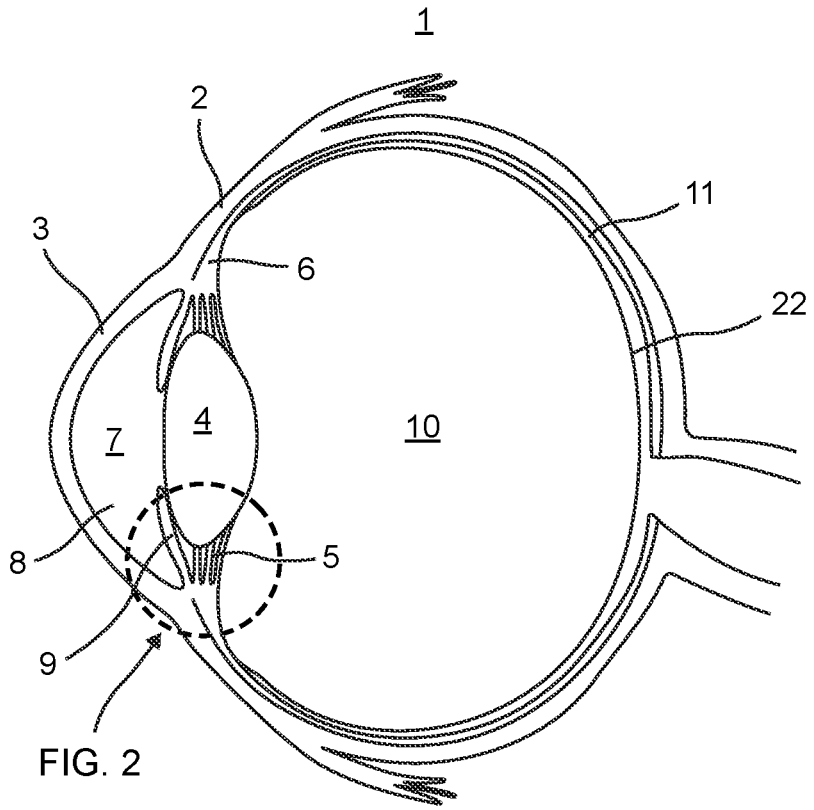

FIG. 2

FIG. 1
(Prior Art)

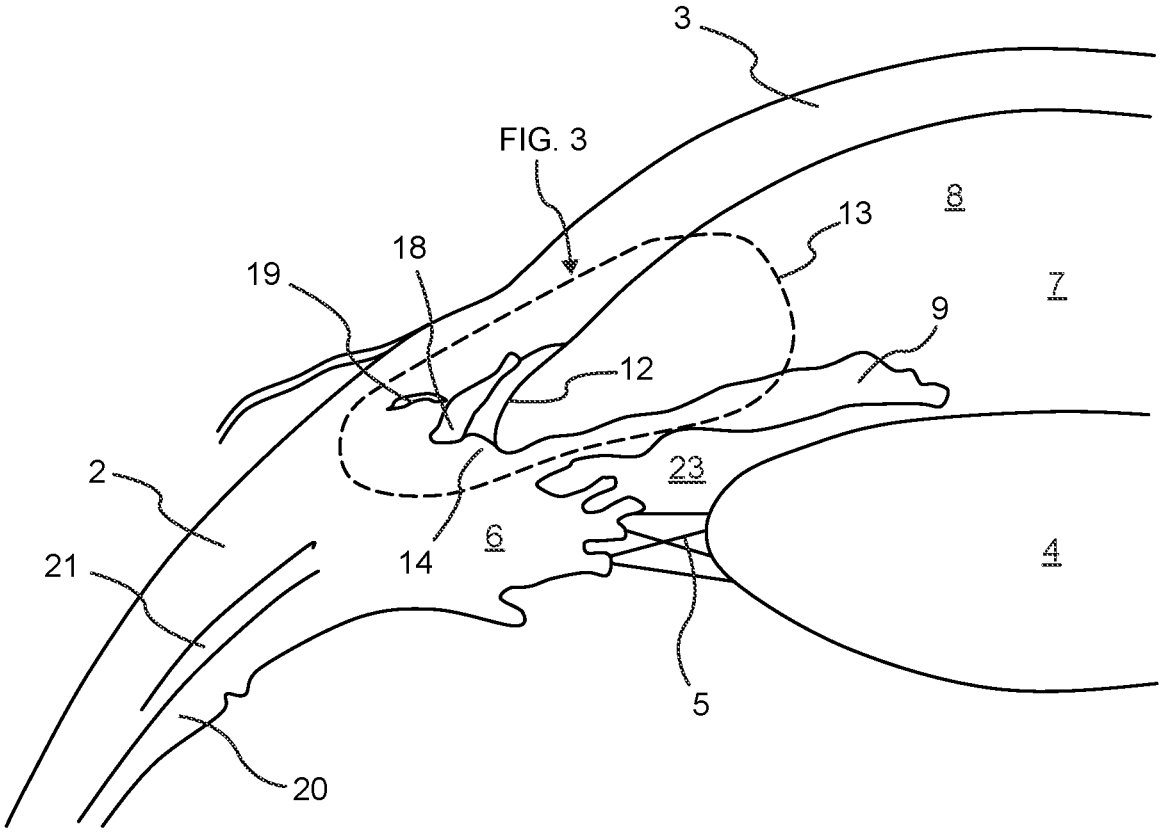

FIG. 2
(Prior Art)

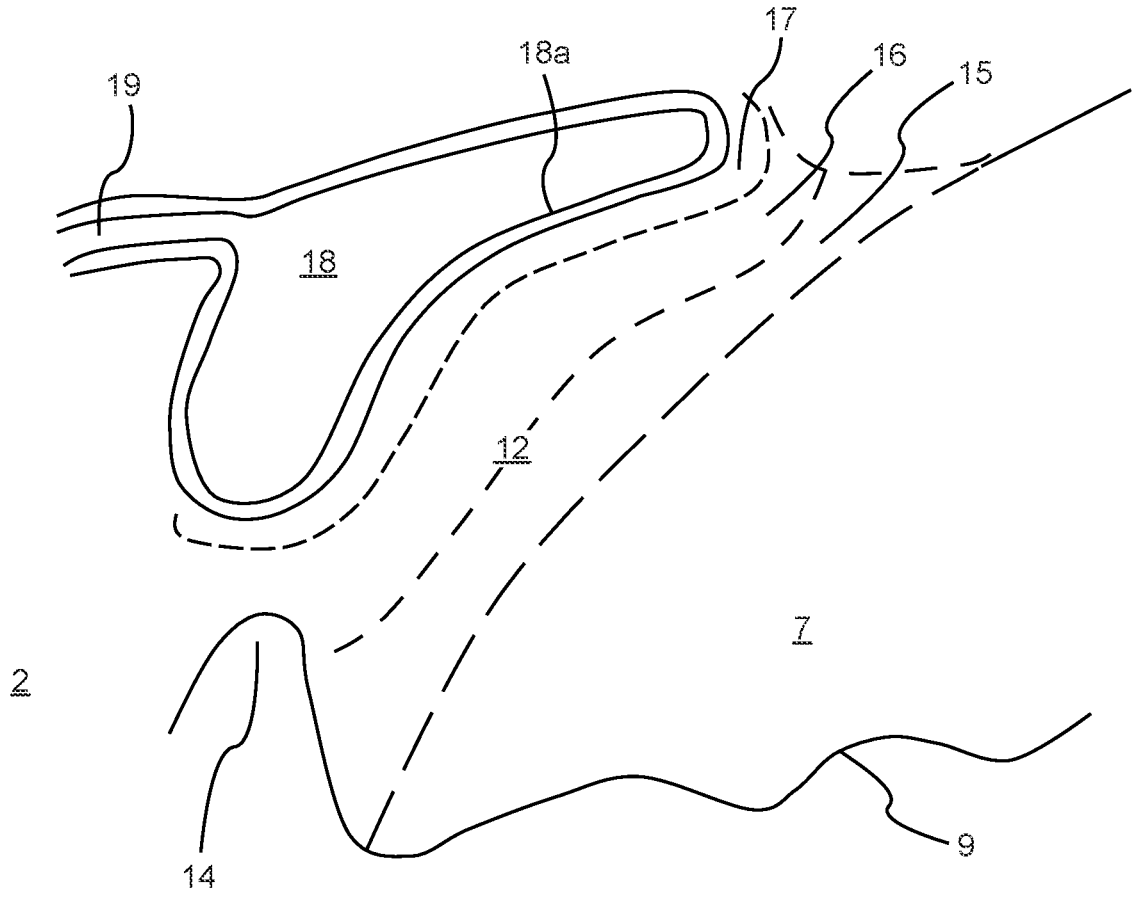

FIG. 3
(Prior Art)

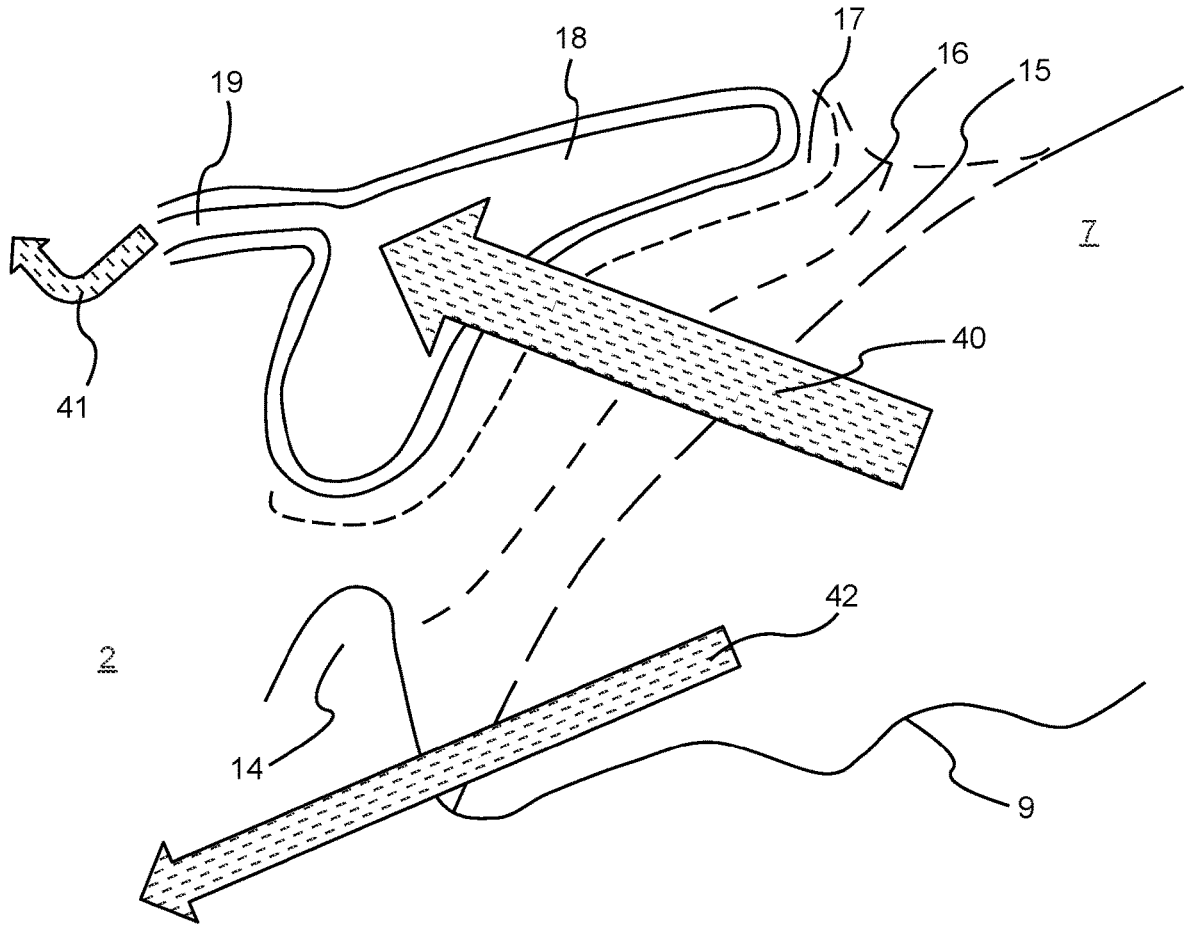

FIG. 4
(Prior Art)

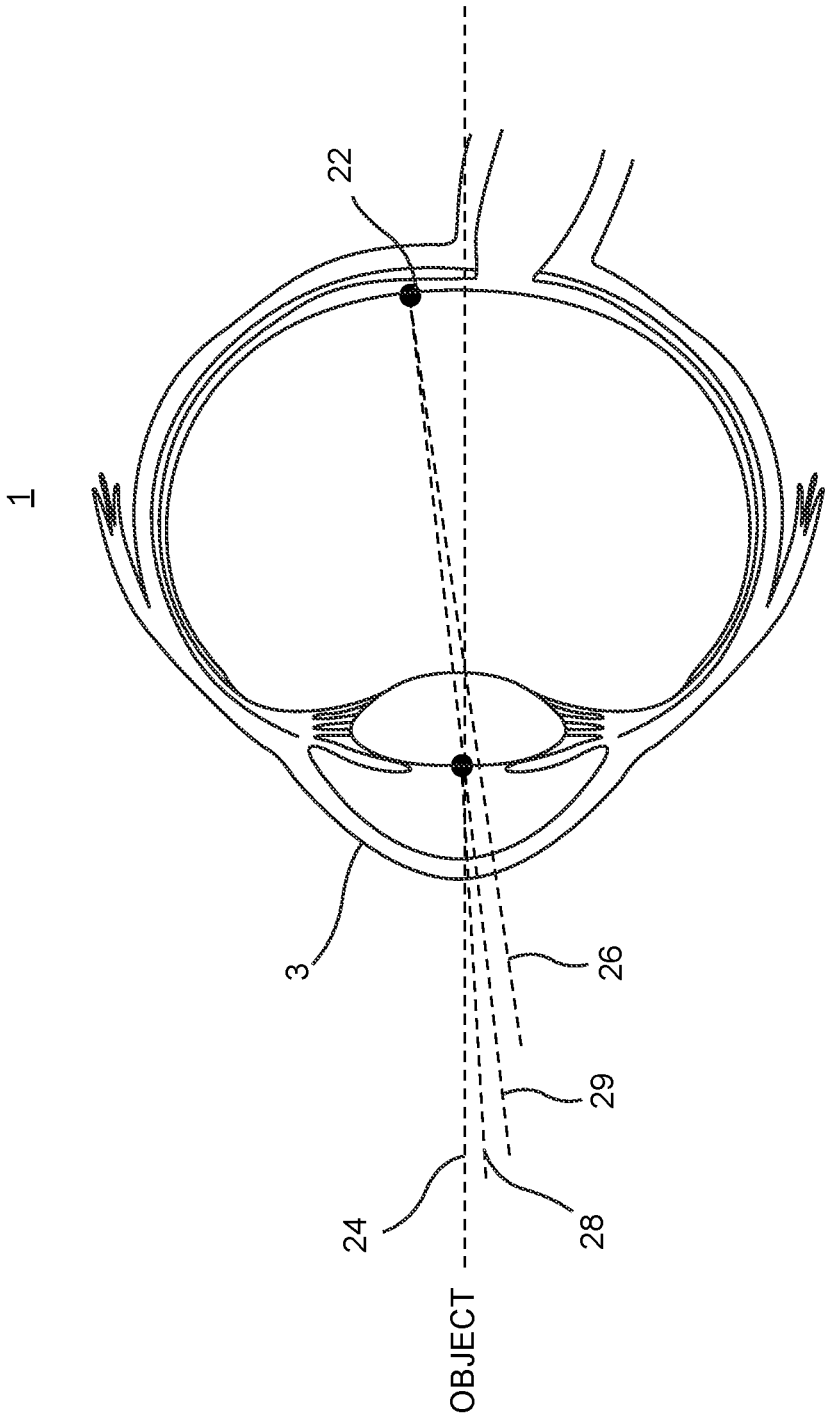

FIG. 5
(Prior Art)

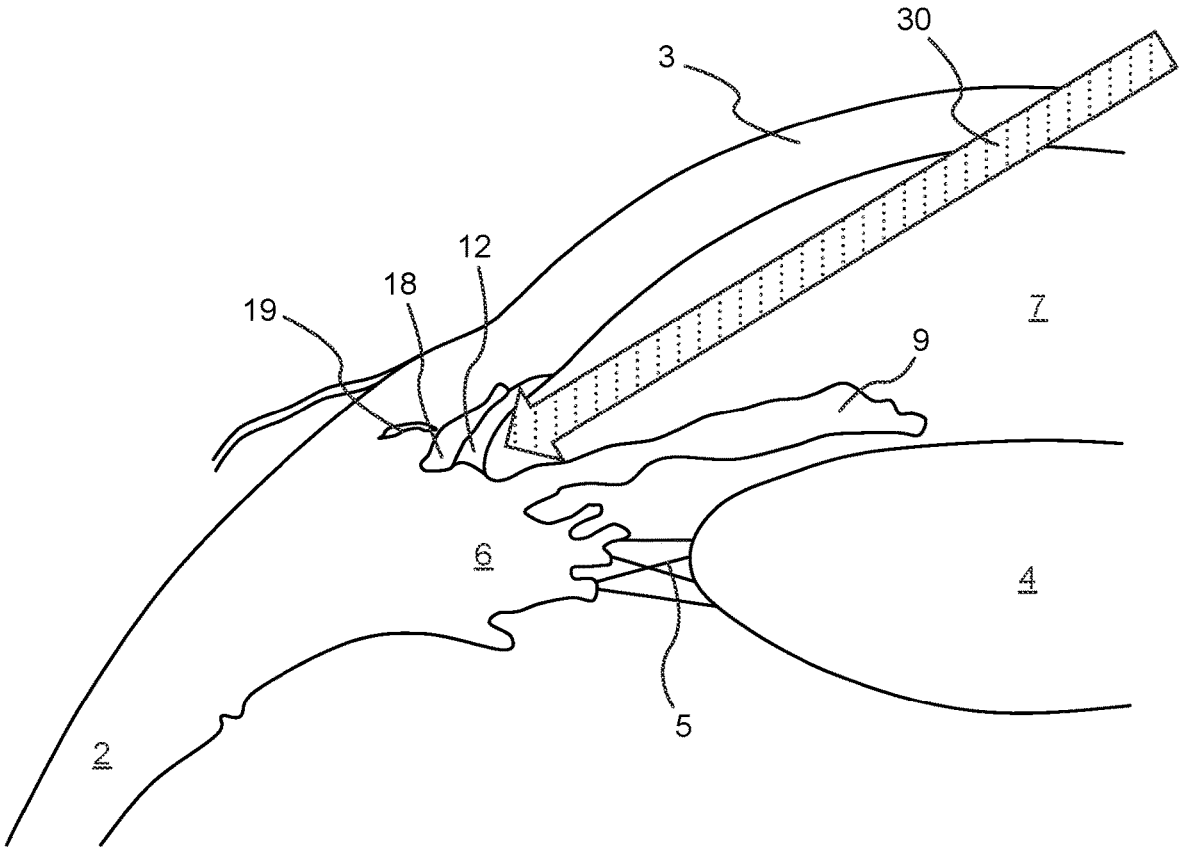

FIG. 6

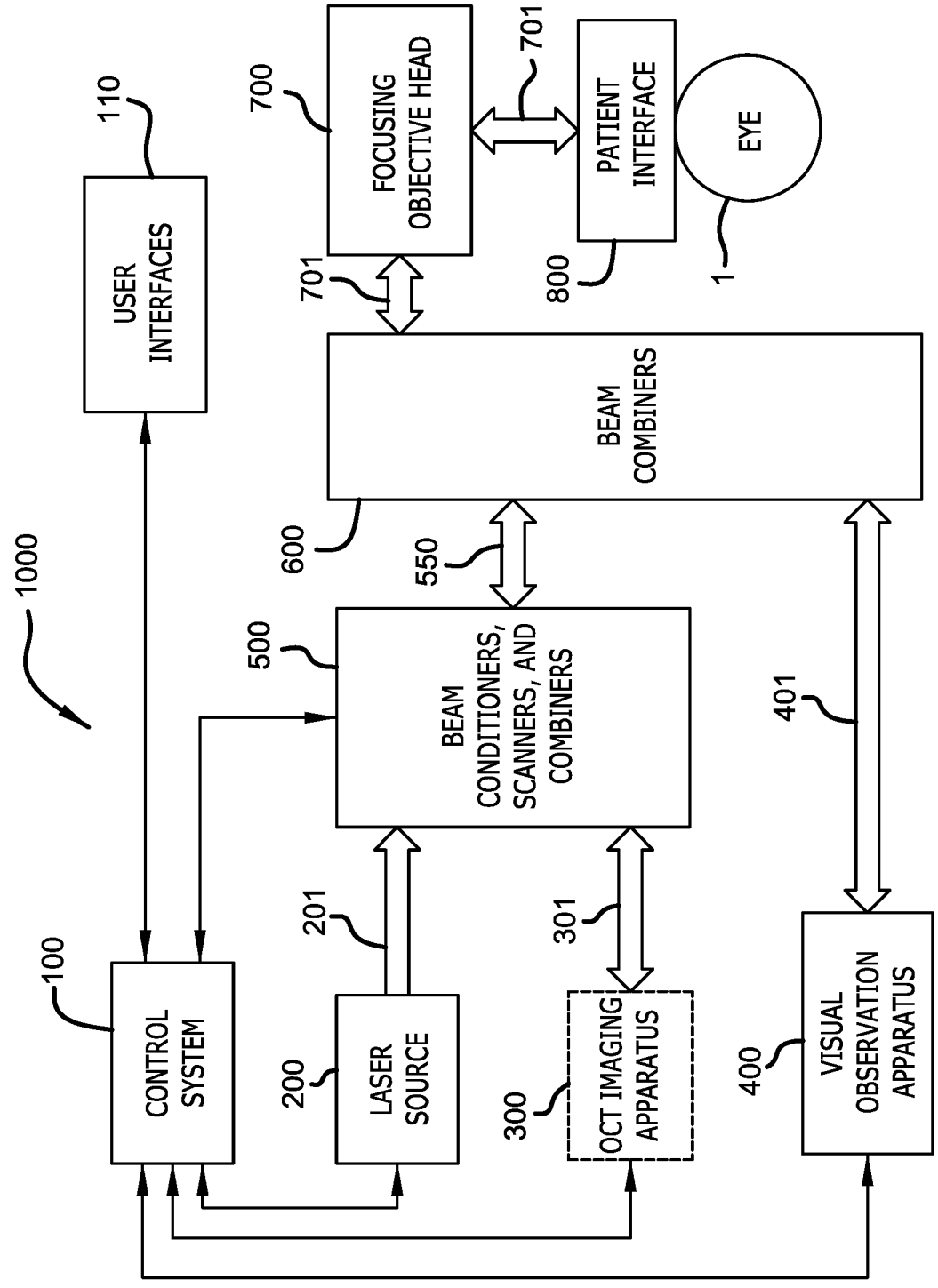
1000
100
CONTROL SYSTEM
110
USER INTERFACES
200
LASER SOURCE
201
300
OCT IMAGING APPARATUS
301
400
VISUAL OBSERVATION APPARATUS
401
500
BEAM CONDITIONERS, SCANNERS, AND COMBINERS
550
600
BEAM COMBINERS
700
FOCUSING OBJECTIVE HEAD
701
701
800
PATIENT INTERFACE
EYE
1

FIG. 7

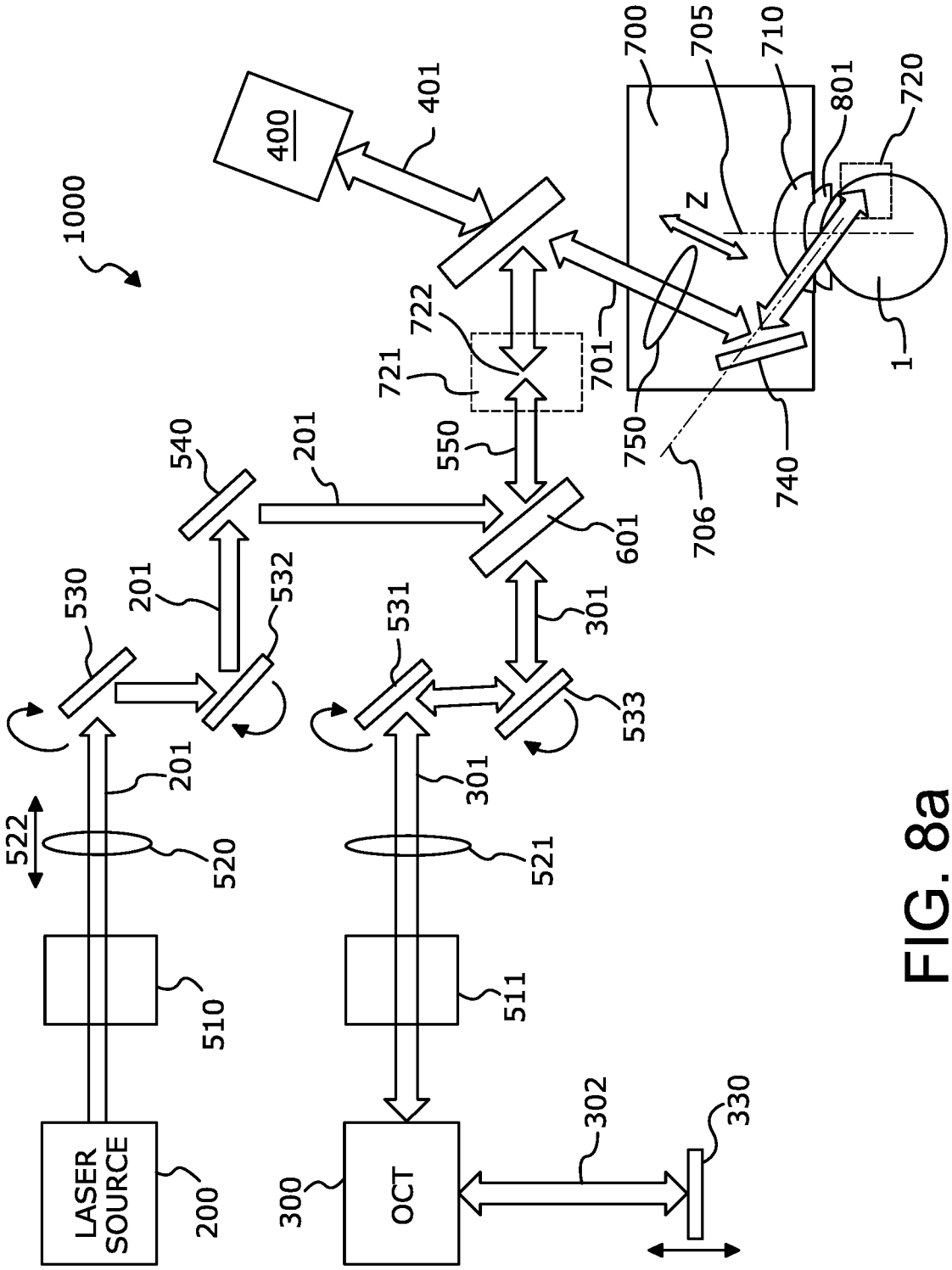
1000
400
401
700
705
710
801
720
z
722
721
701
1
750
706
740
550
540
201
601
530
532
531
301
533
522
520
521
510
511
LASER SOURCE
200
300
OCT
302
330

FIG. 8a

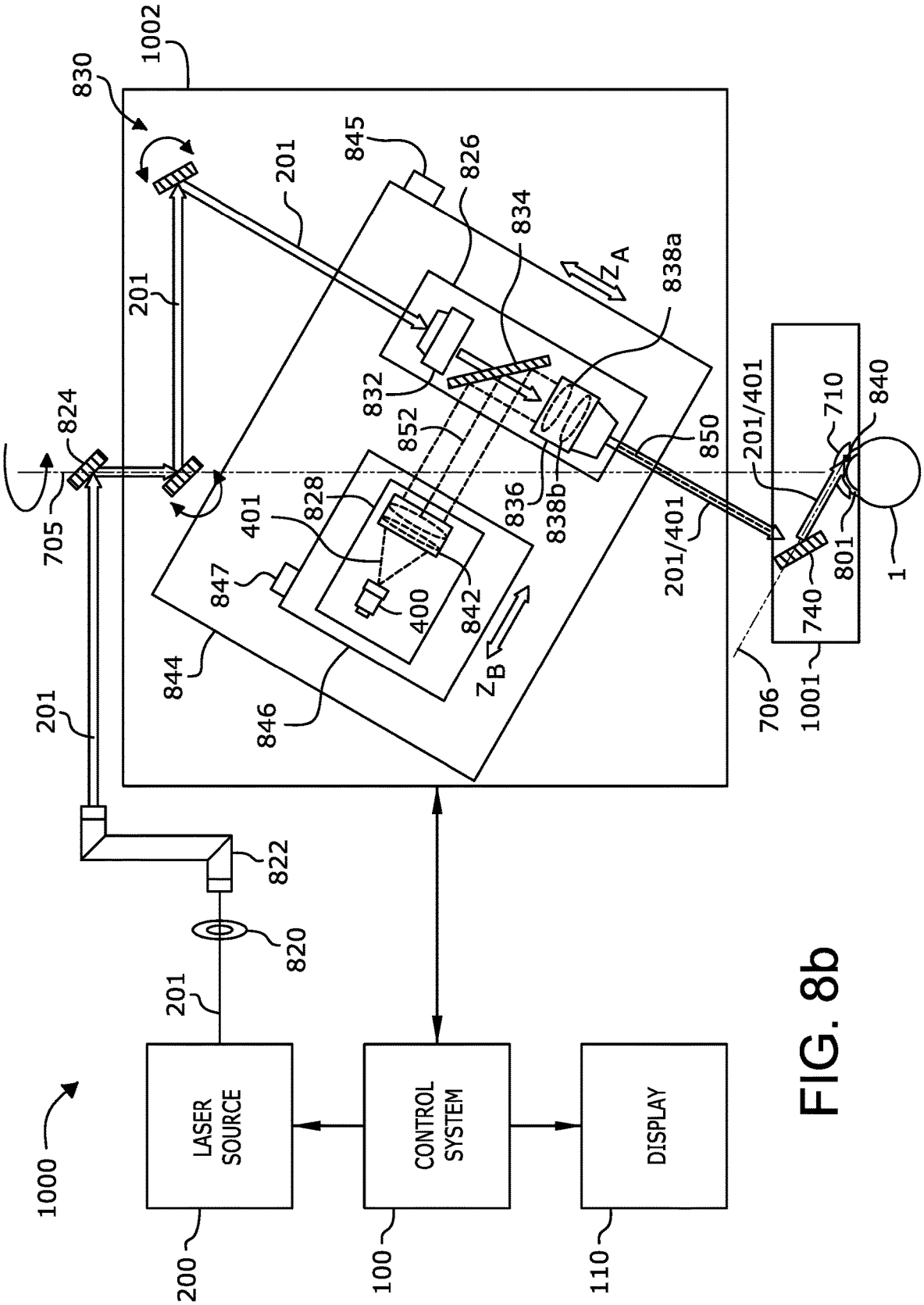
1000
LASER SOURCE
CONTROL SYSTEM
DISPLAY
200
100
110
1002
830
201
845
826
834
838a
Z_A
832
852
850
824
705
828
836
838b
401
847
400
842
Z_B
844
846
201/401
710
840
801
740
1001
706
1
822
820

FIG. 8b

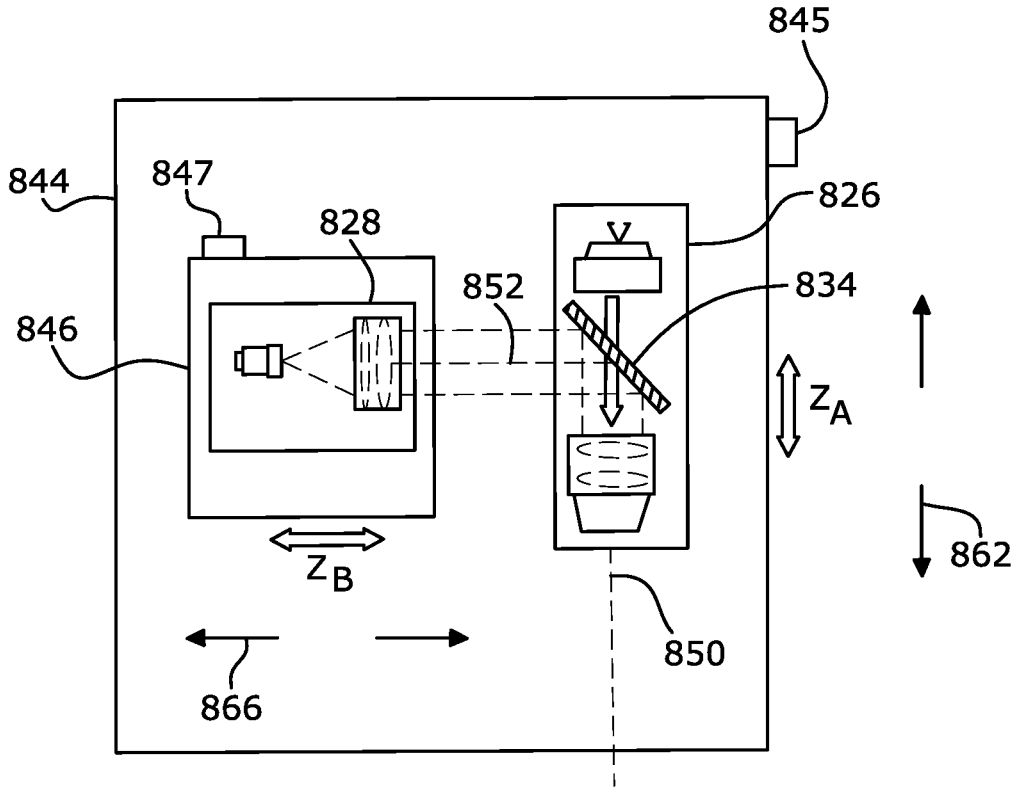
845
844
847
828
826
852
834
846
Z_A
862
Z_B
850
866

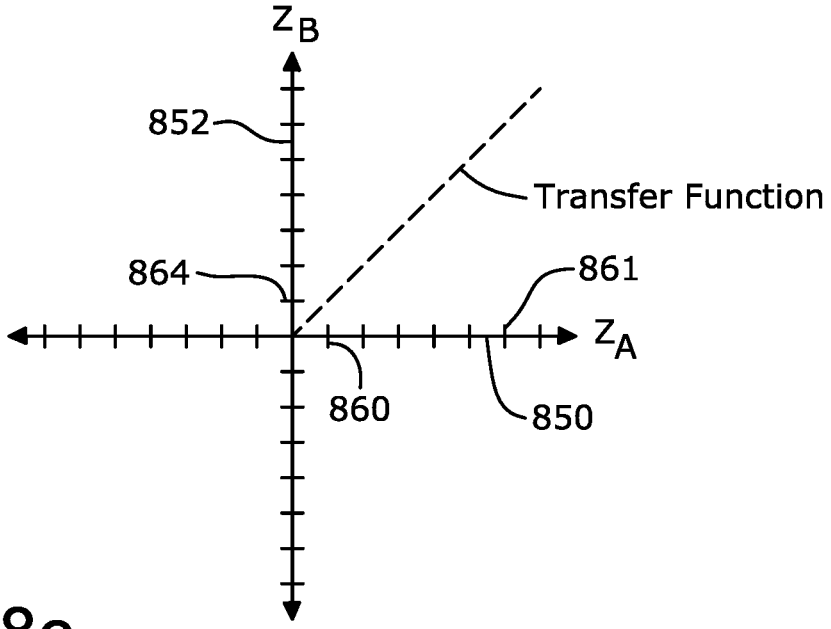
Z_B
852
Transfer Function
864
861
Z_A
860
850

FIG. 8c

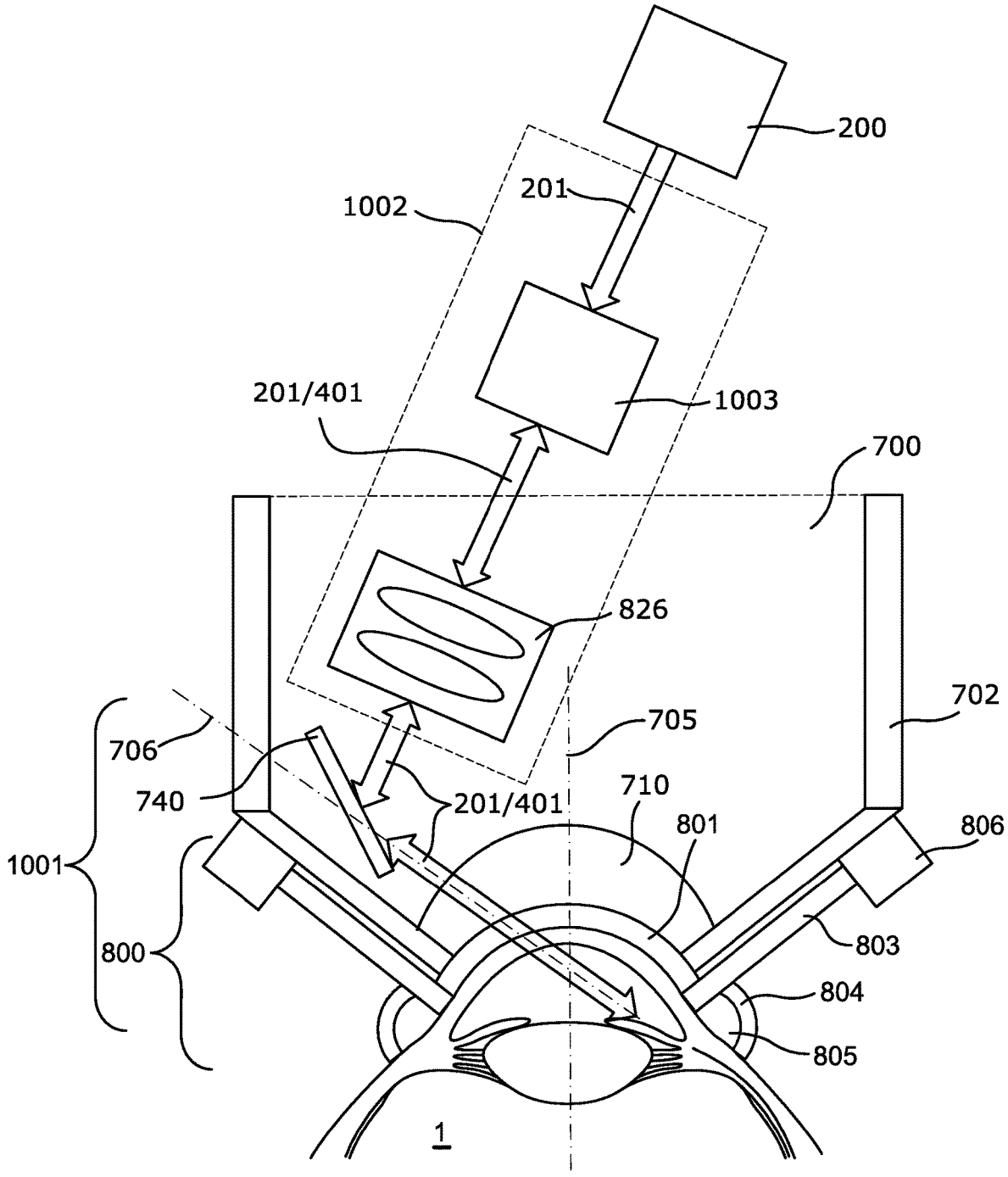
200
201
1002
201/401
1003
700
826
702
705
706
740
201/401
710
801
806
1001
803
800
804
805
1

FIG. 9a

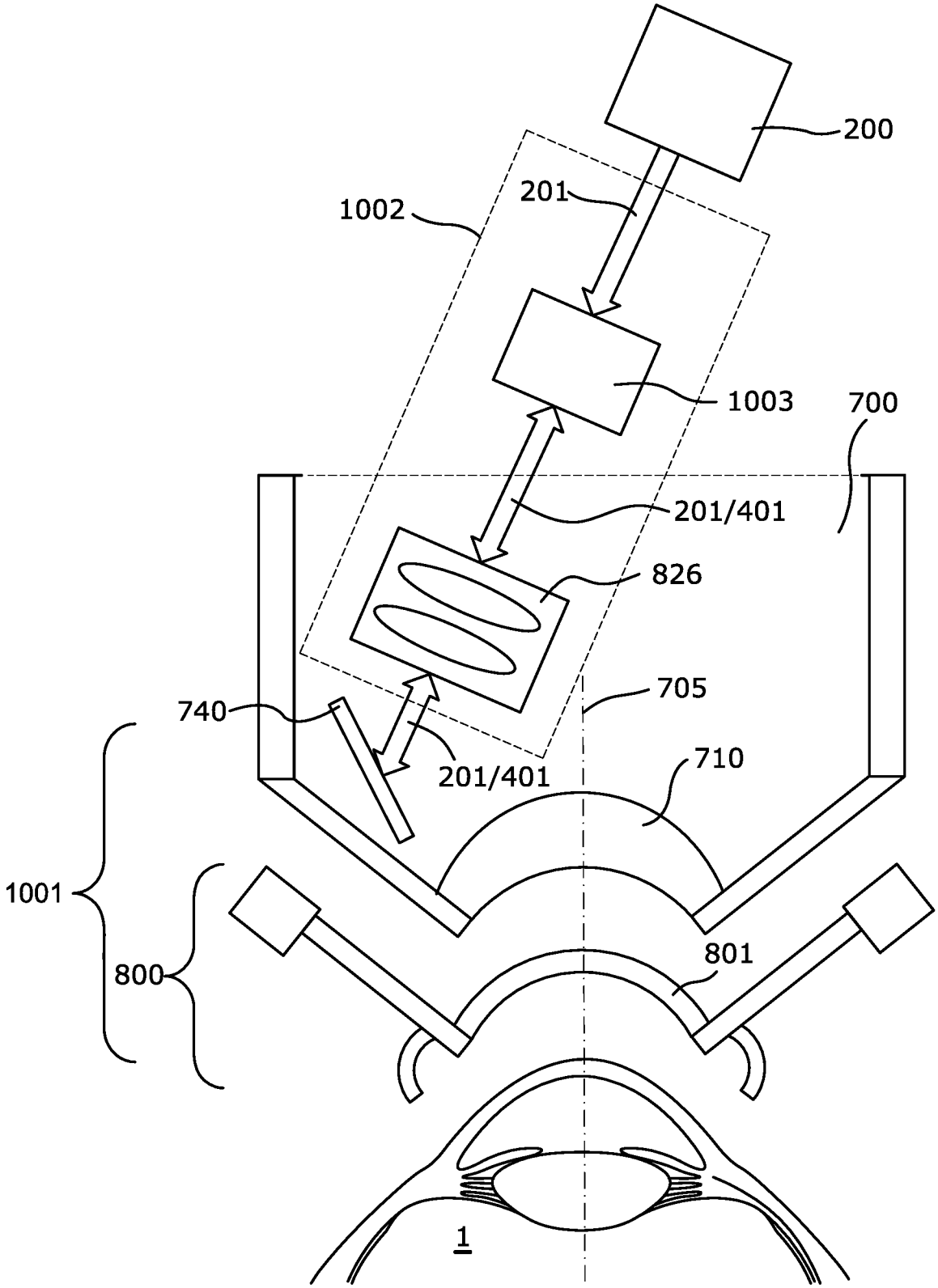
200
201
1002
1003
700
201/401
826
705
740
201/401
710
1001
800
801
1

FIG. 9b

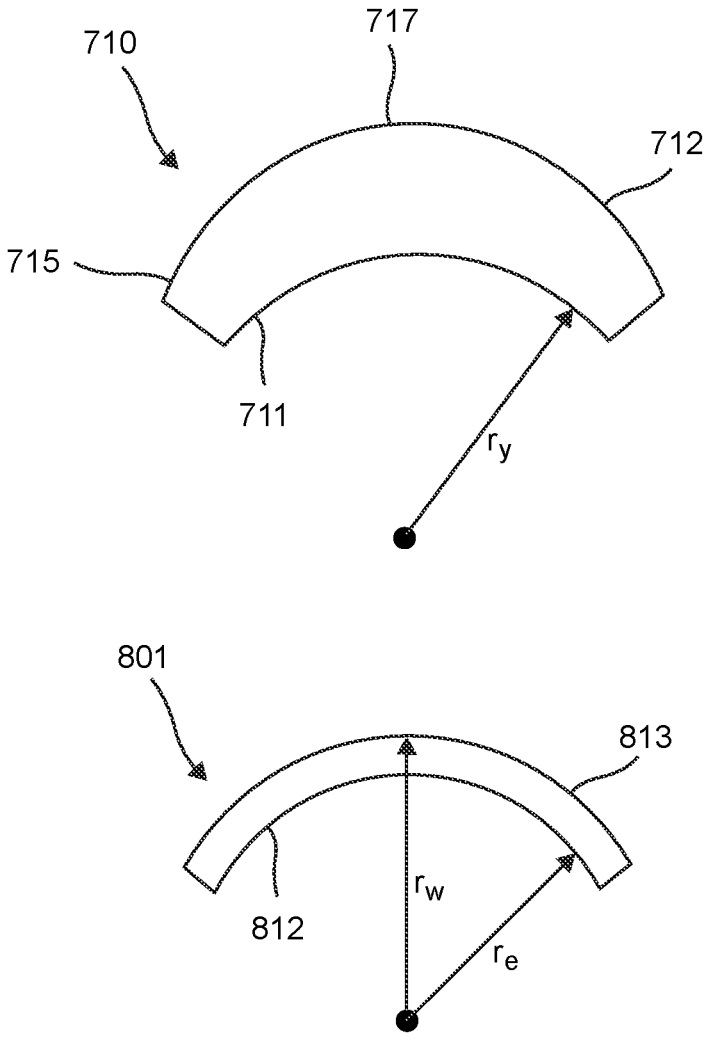

FIG. 9c

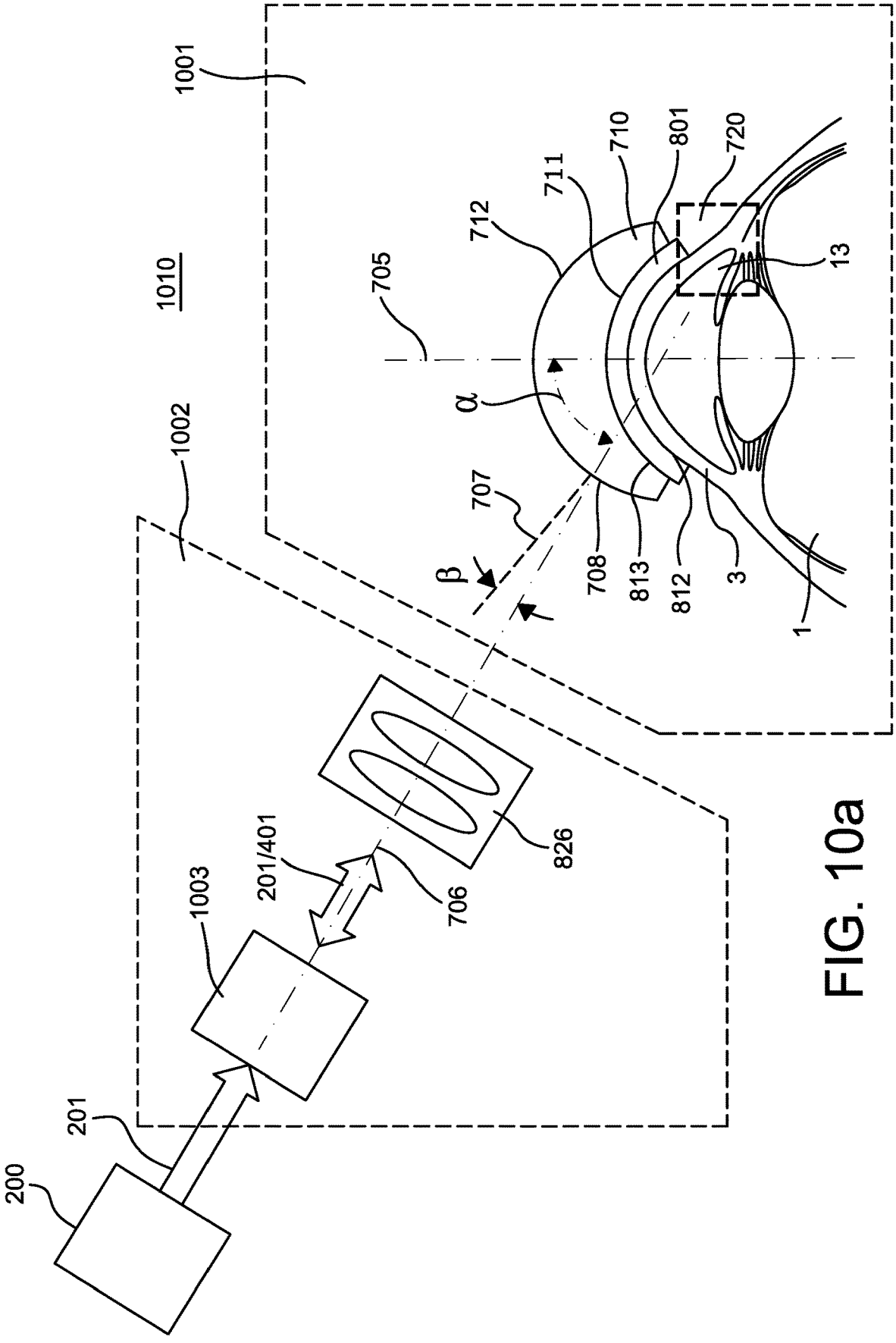
1001
1010
1002
1003
200
201
201/401
706
826
705
712
711
710
801
720
13
α
β
707
708
813
812
3
1

FIG. 10a

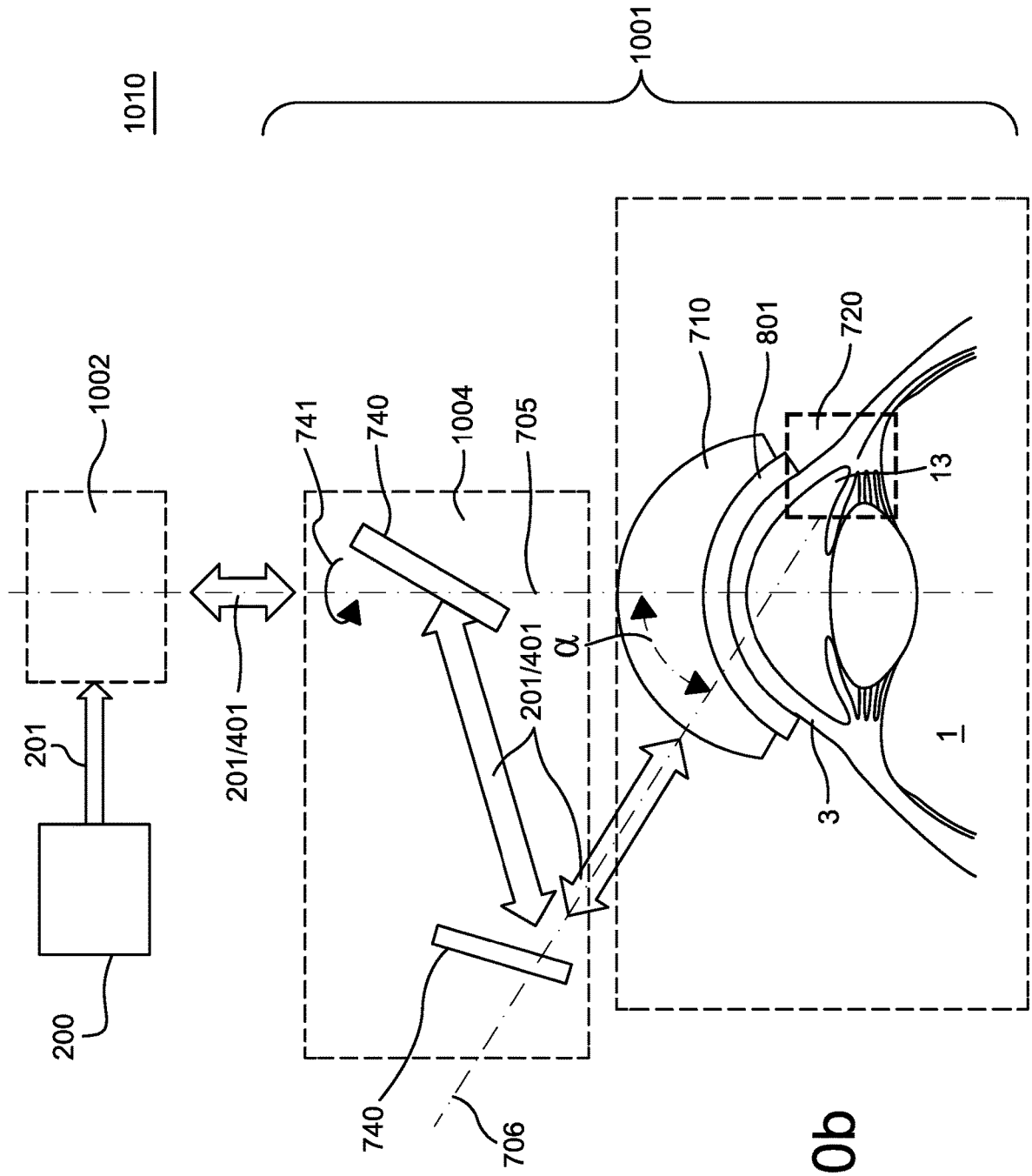
1010
1001
1002
741
740
1004
705
710
801
720
13
201
201/401
α
200
740
706
3
1

FIG. 10b

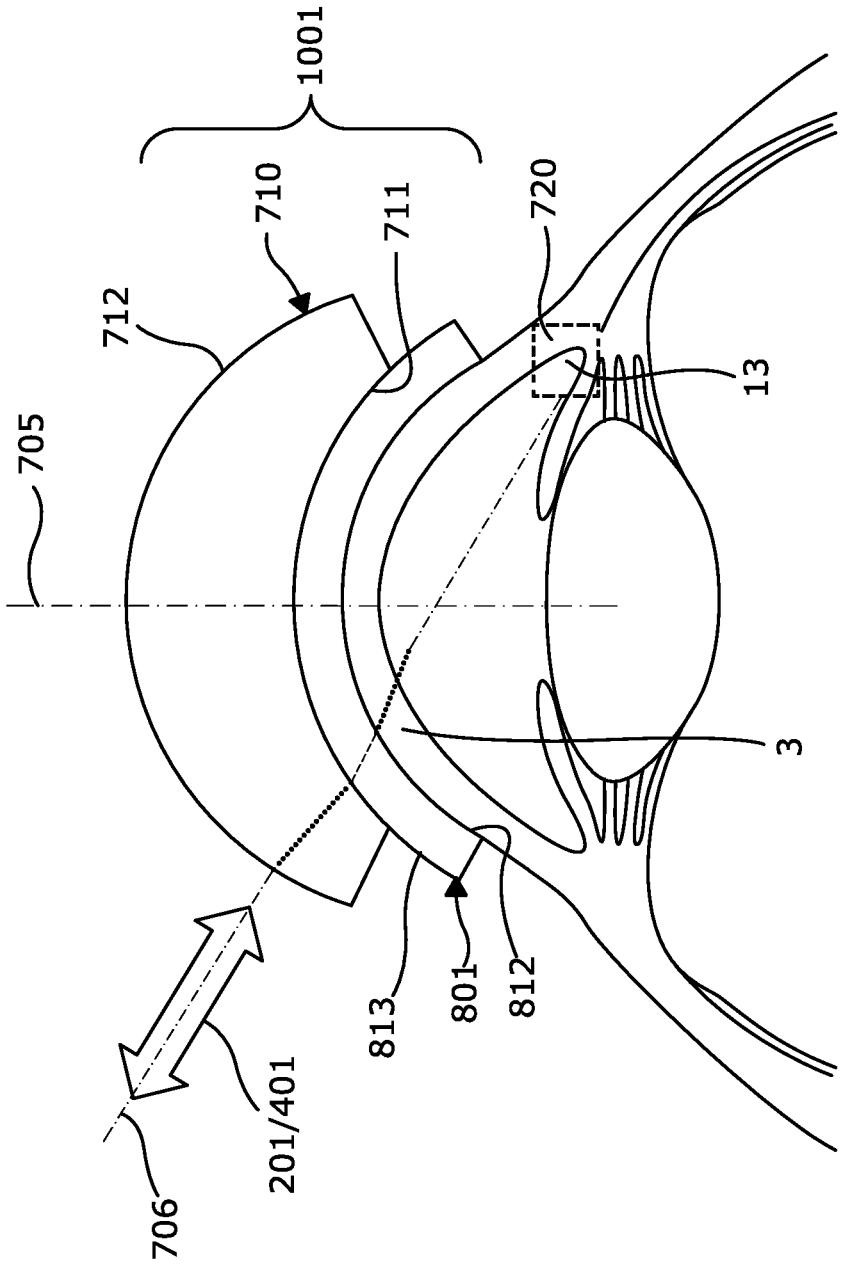

FIG. 10c

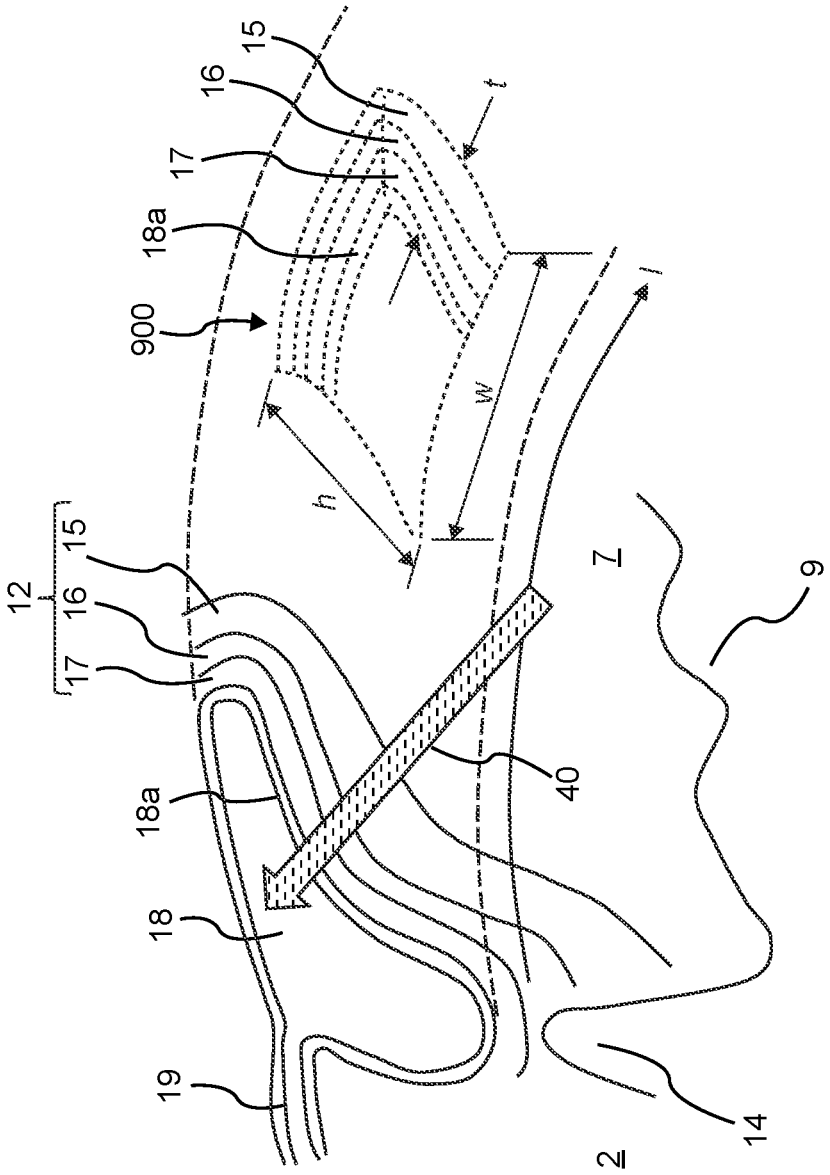

FIG. 11

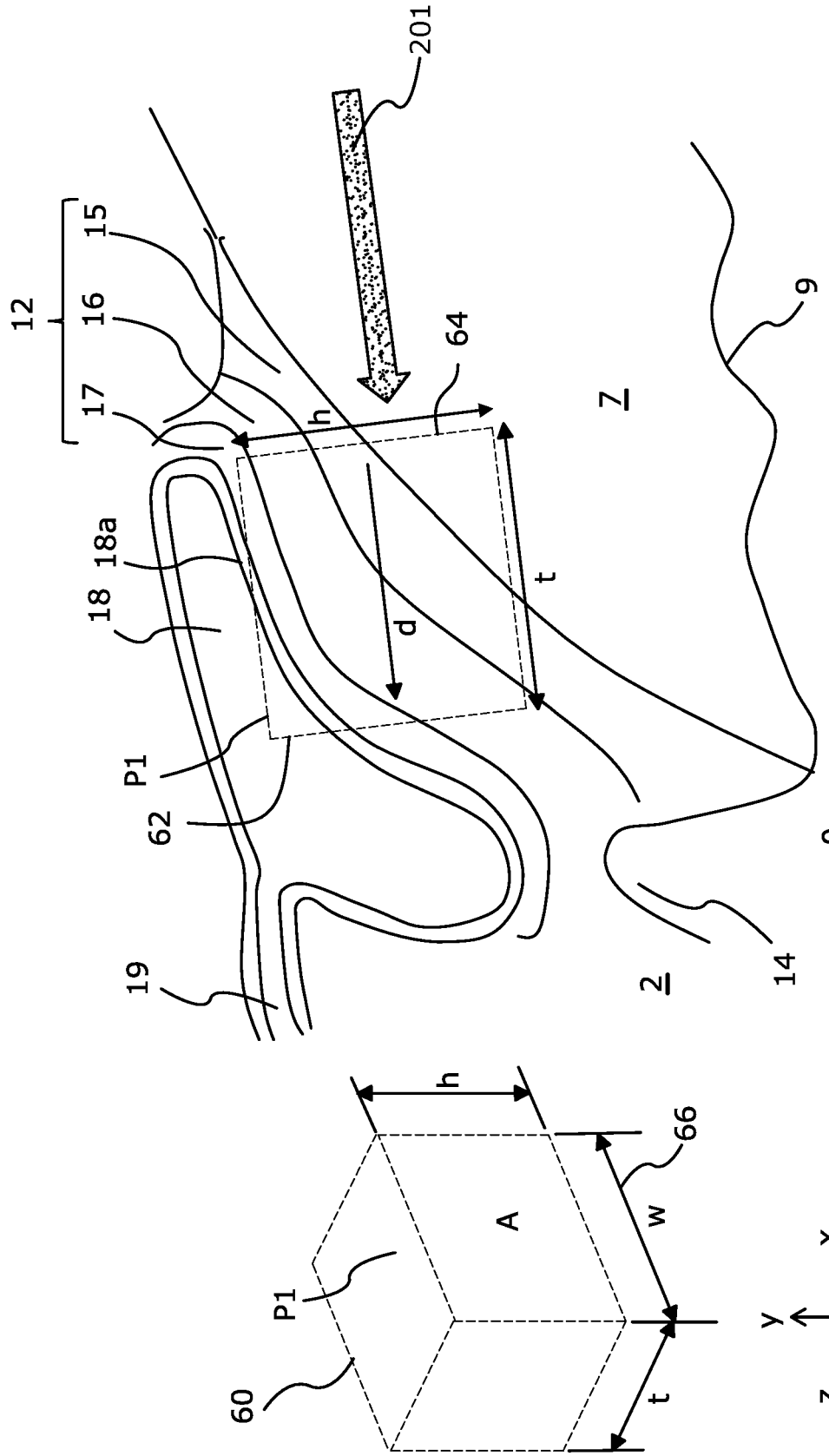

FIG. 12

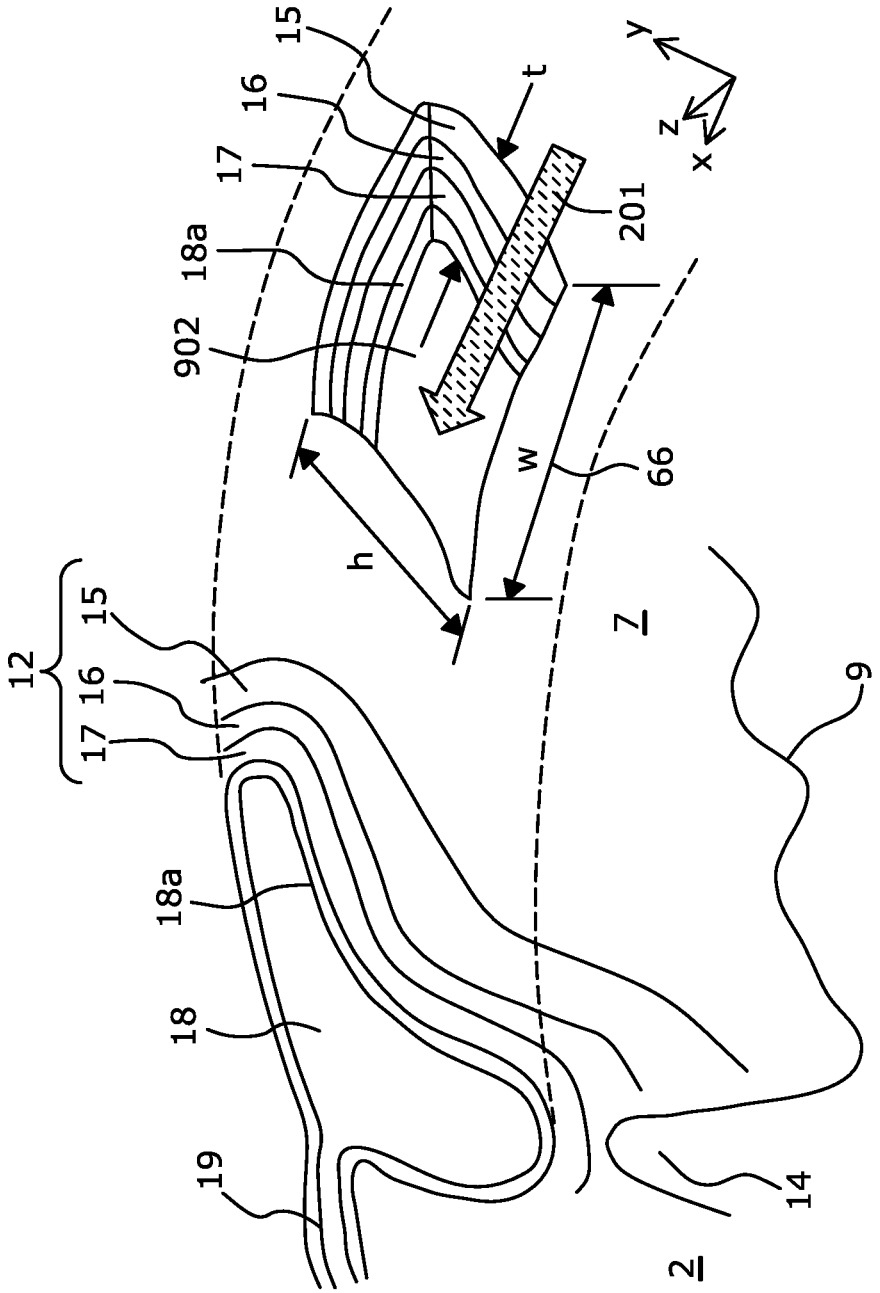

FIG. 13

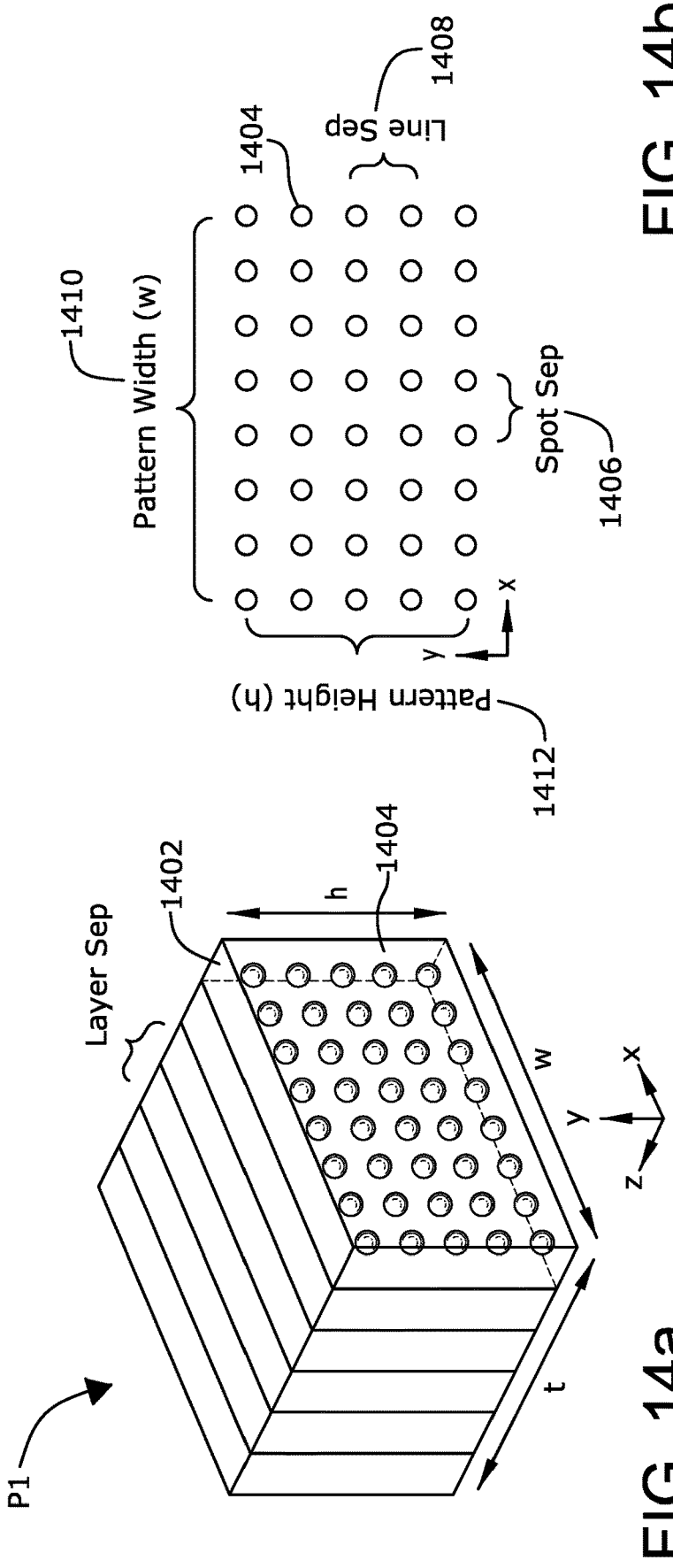

FIG. 14a

FIG. 14b

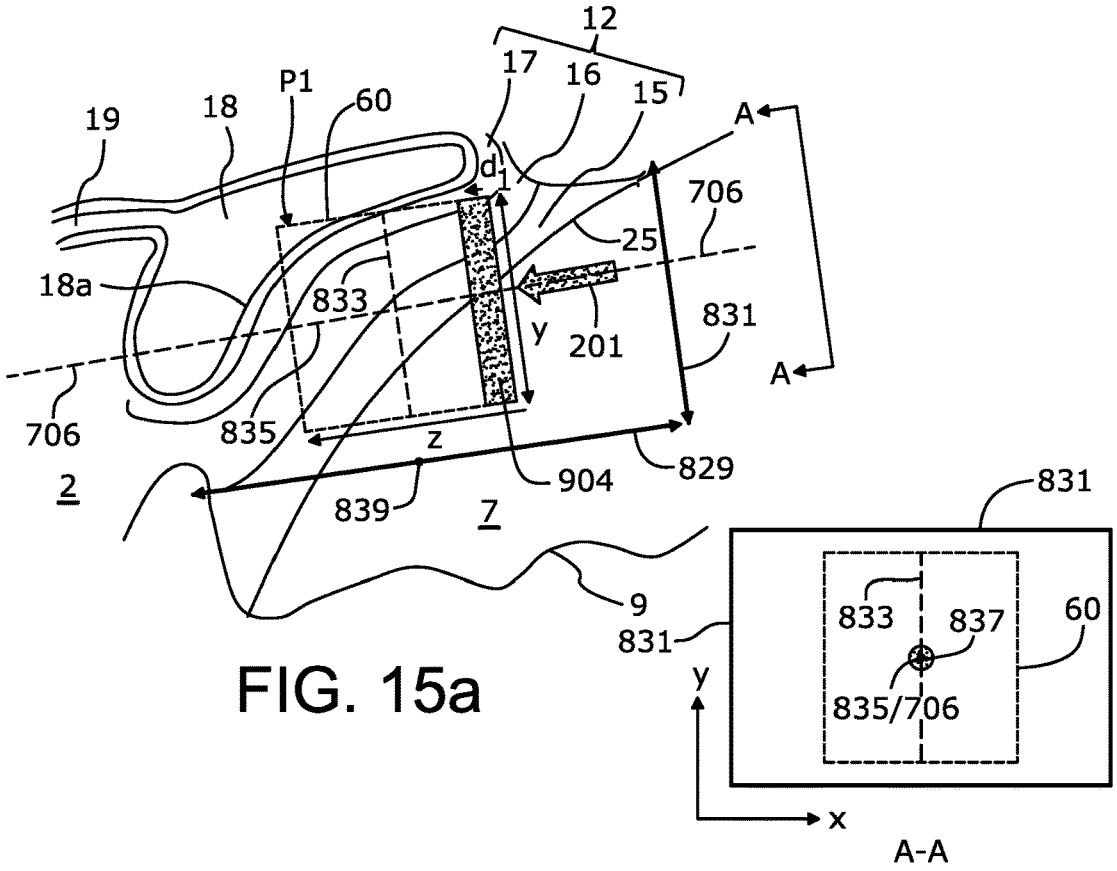

FIG. 15a

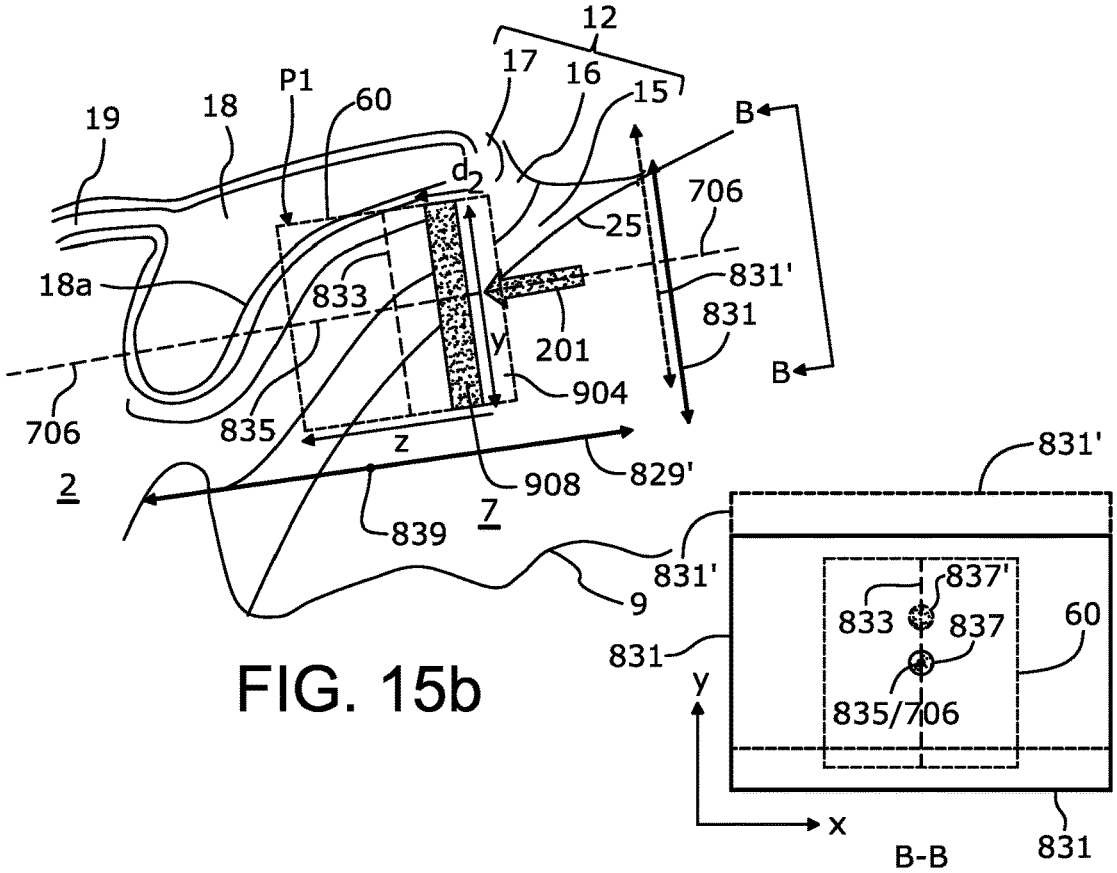

FIG. 15b

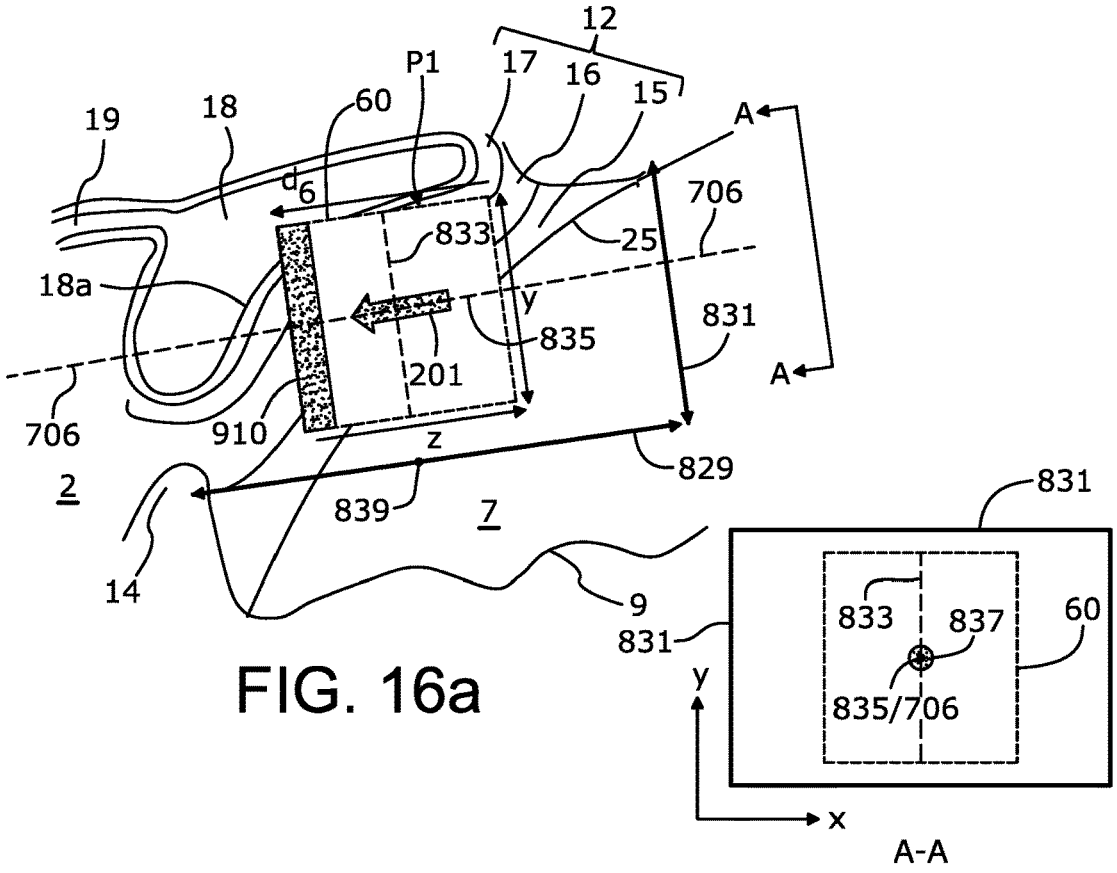

FIG. 16a

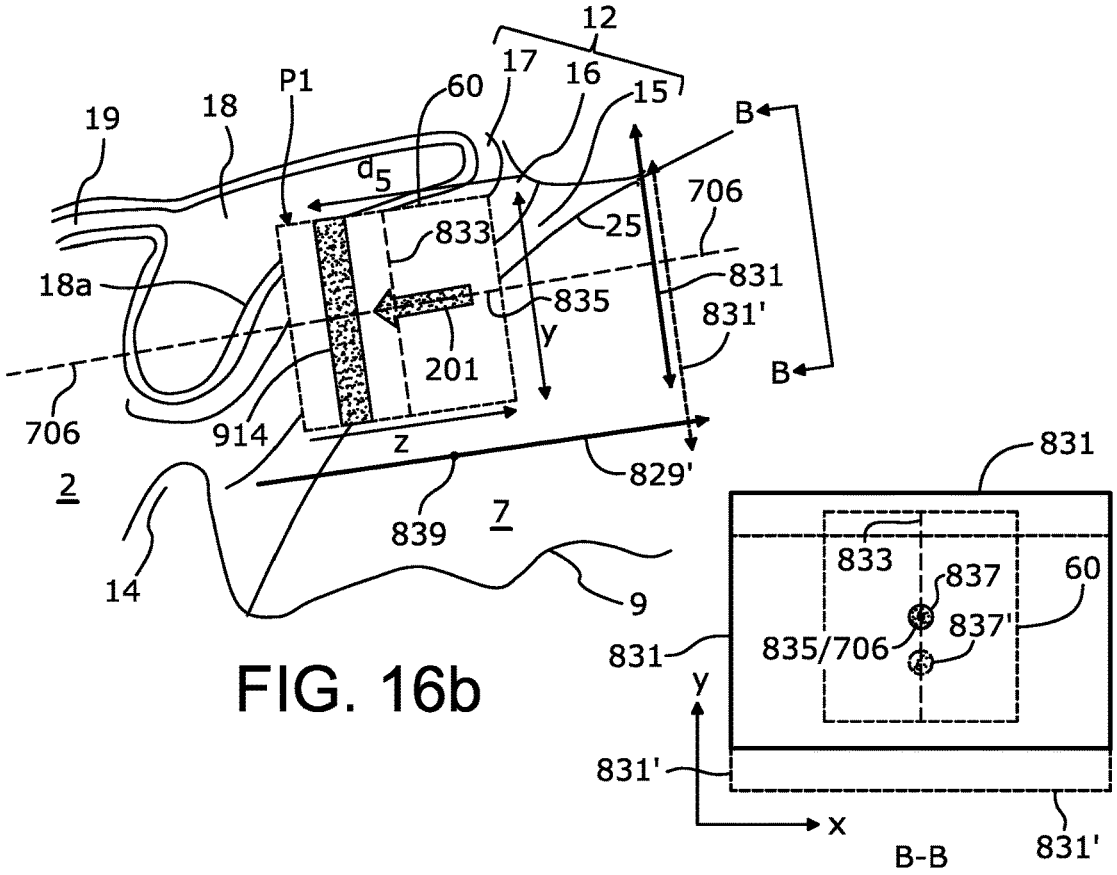

FIG. 16b

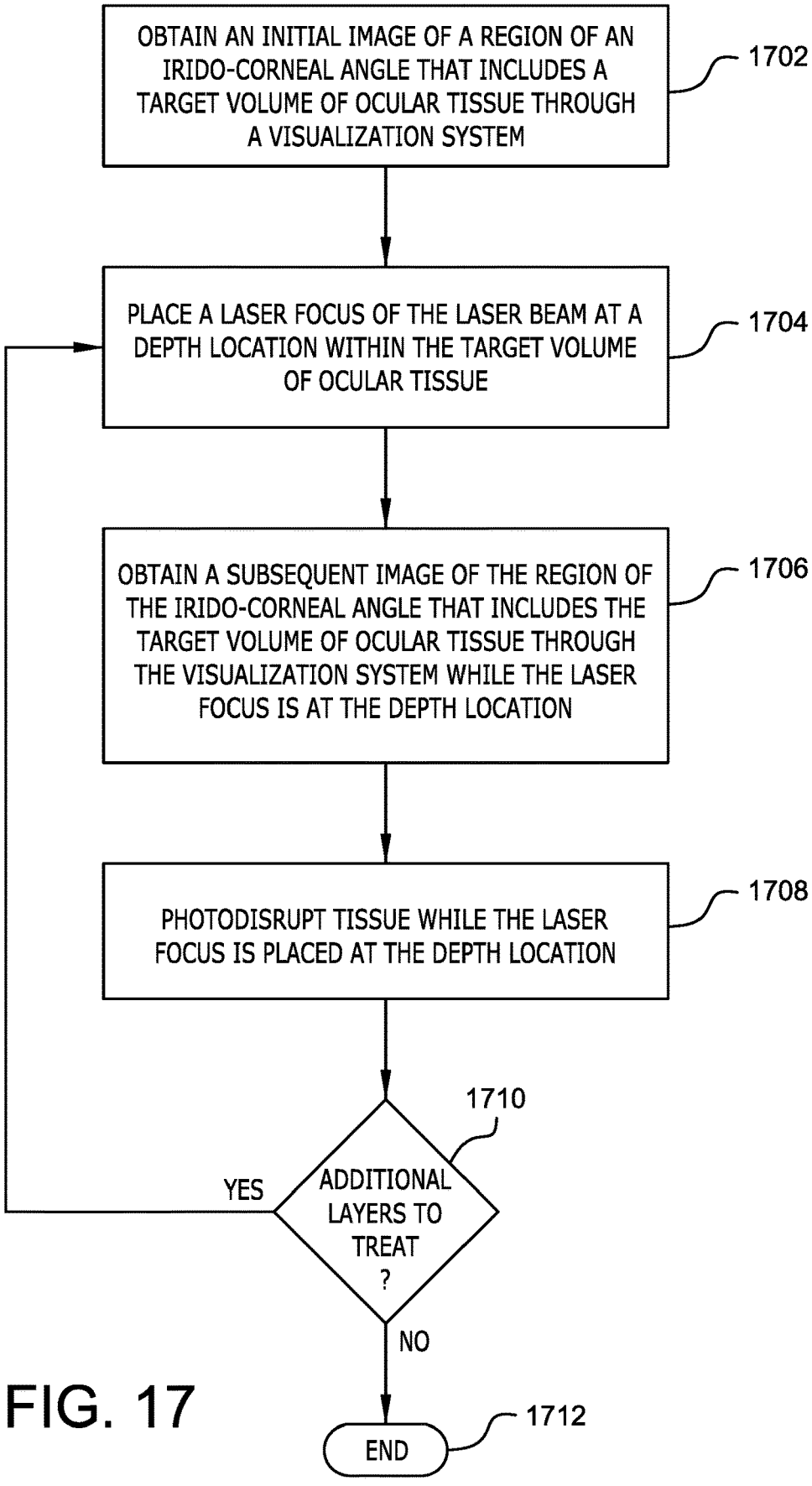
OBTAIN AN INITIAL IMAGE OF A REGION OF AN IRIDO-CORNEAL ANGLE THAT INCLUDES A TARGET VOLUME OF OCULAR TISSUE THROUGH A VISUALIZATION SYSTEM
1702
PLACE A LASER FOCUS OF THE LASER BEAM AT A DEPTH LOCATION WITHIN THE TARGET VOLUME OF OCULAR TISSUE
1704
OBTAIN A SUBSEQUENT IMAGE OF THE REGION OF THE IRIDO-CORNEAL ANGLE THAT INCLUDES THE TARGET VOLUME OF OCULAR TISSUE THROUGH THE VISUALIZATION SYSTEM WHILE THE LASER FOCUS IS AT THE DEPTH LOCATION
1706
PHOTODISRUPT TISSUE WHILE THE LASER FOCUS IS PLACED AT THE DEPTH LOCATION
1708
1710
ADDITIONAL LAYERS TO TREAT ?
YES
NO
END
1712

FIG. 17

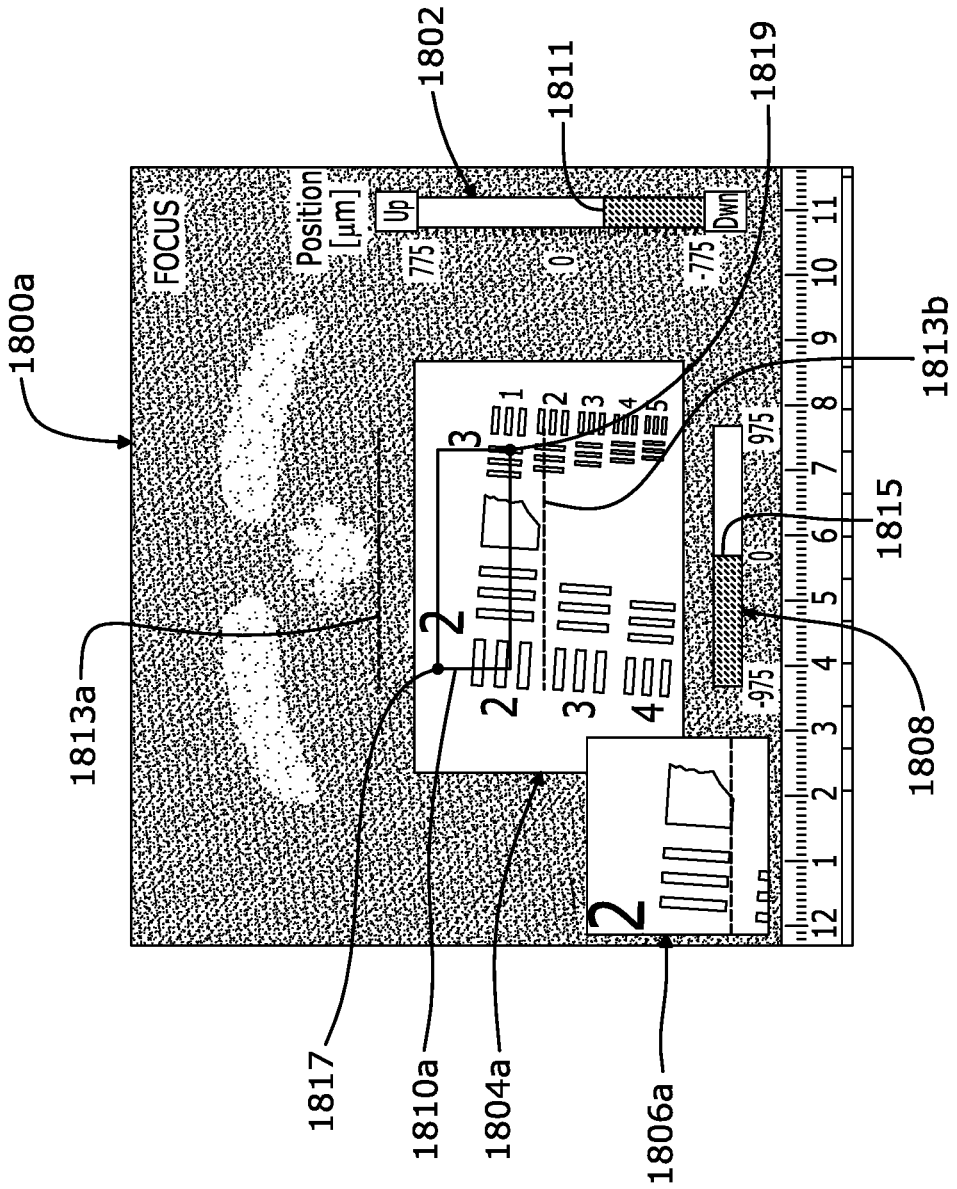
1800a
1802
1811
1819
1813b
1815
1813a
1808
1817
1810a
1804a
1806a
FOCUS
Position [µm]
Up
Dwn
775
0
-775
975
-975

FIG. 18a

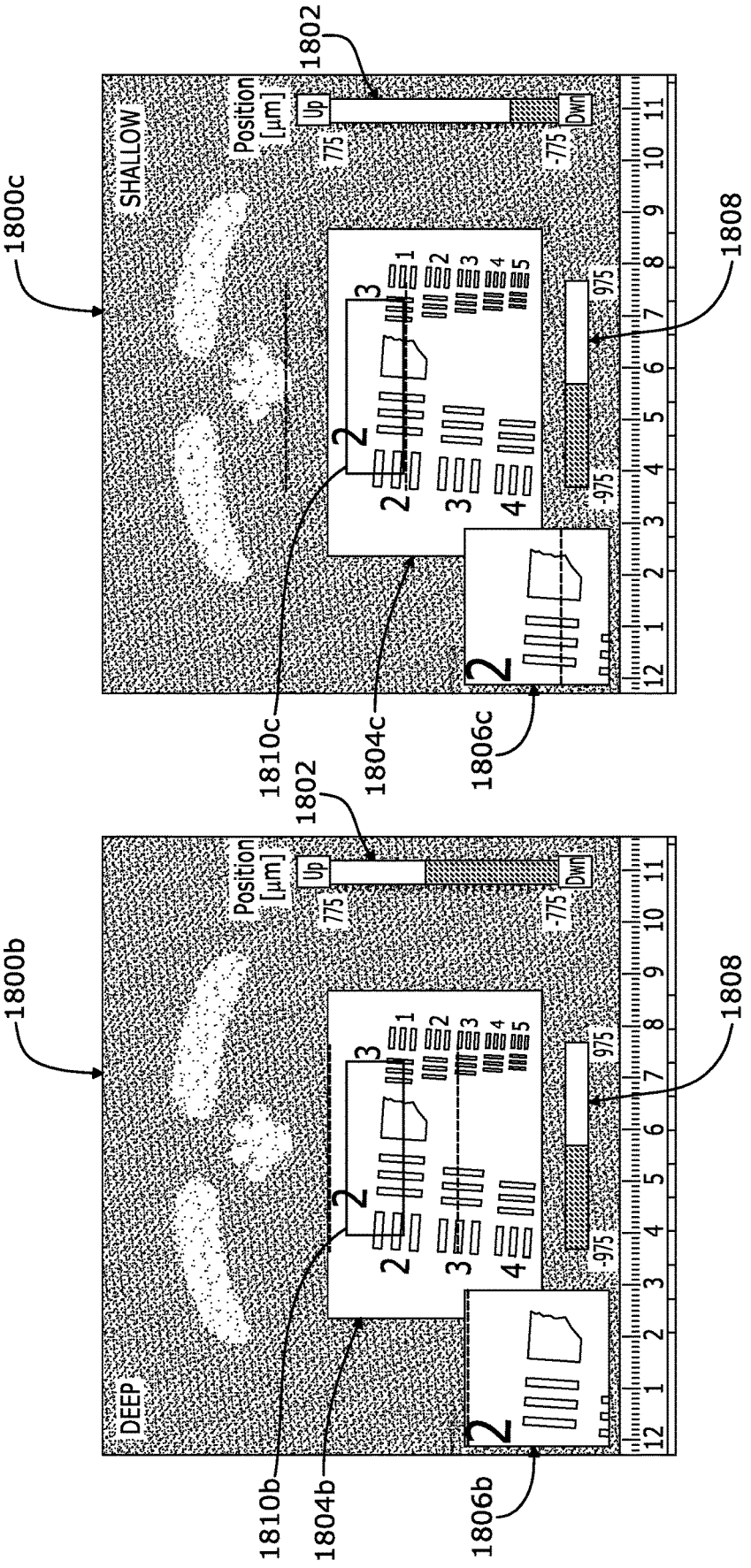

FIG. 18c

FIG. 18b

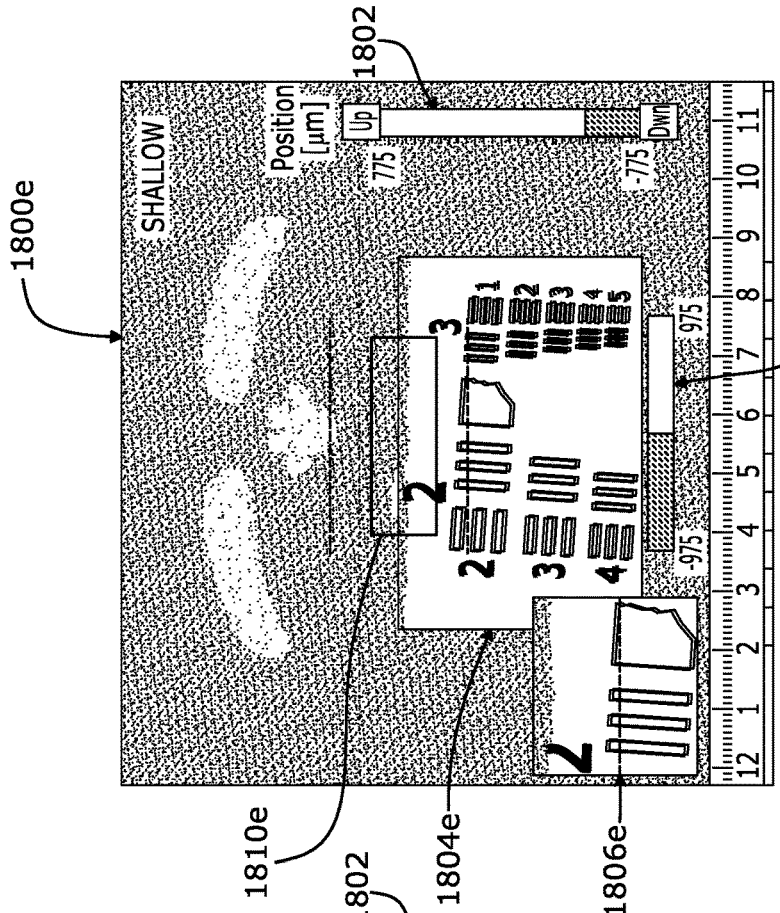

FIG. 18e

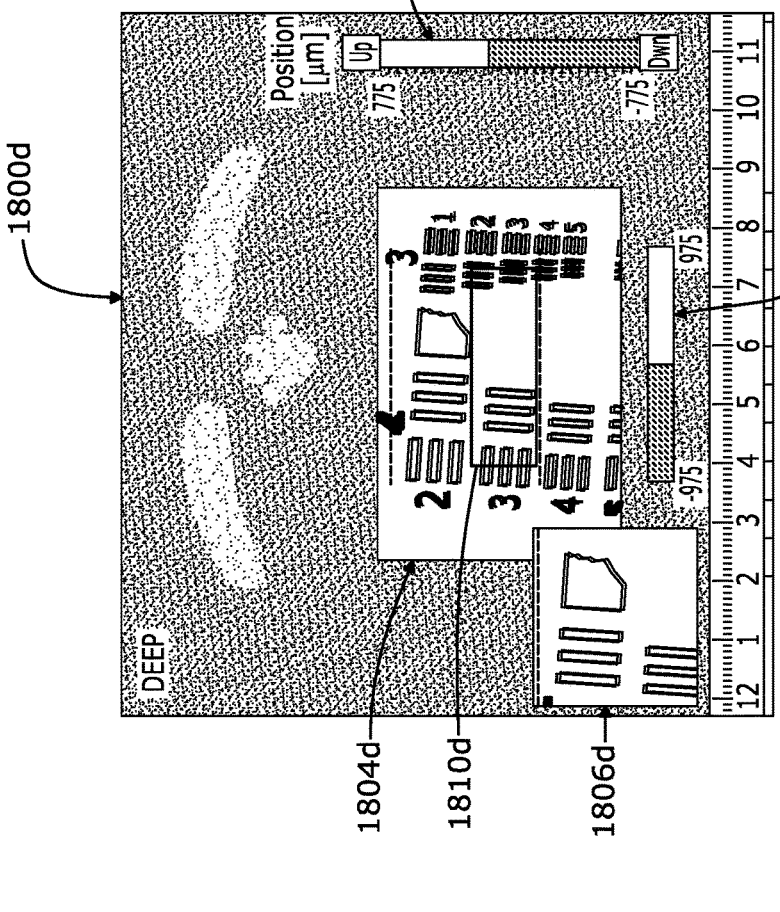

FIG. 18d

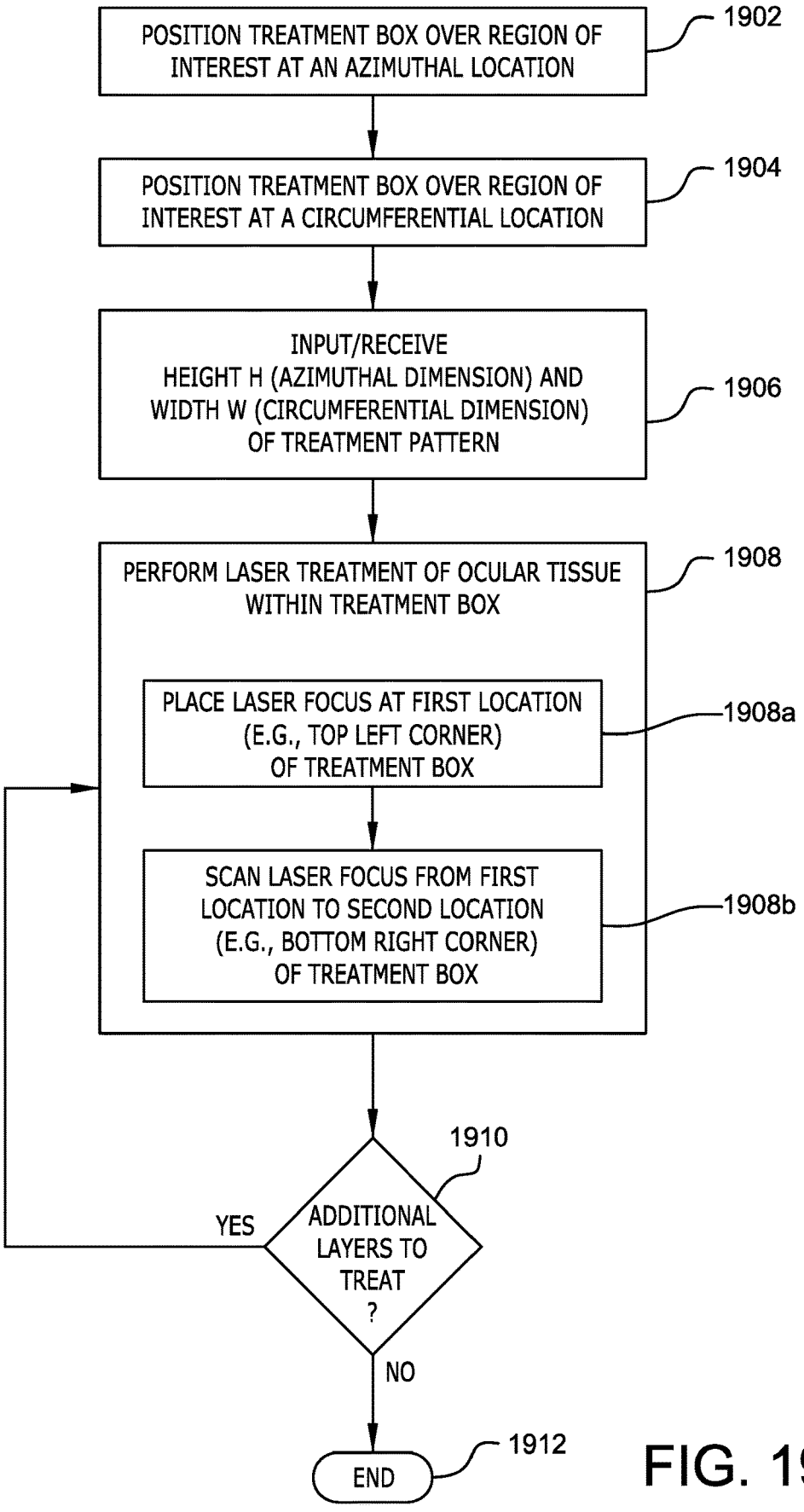
POSITION TREATMENT BOX OVER REGION OF INTEREST AT AN AZIMUTHAL LOCATION
1902
POSITION TREATMENT BOX OVER REGION OF INTEREST AT A CIRCUMFERENTIAL LOCATION
1904
INPUT/RECEIVE HEIGHT H (AZIMUTHAL DIMENSION) AND WIDTH W (CIRCUMFERENTIAL DIMENSION) OF TREATMENT PATTERN
1906
PERFORM LASER TREATMENT OF OCULAR TISSUE WITHIN TREATMENT BOX
1908
PLACE LASER FOCUS AT FIRST LOCATION (E.G., TOP LEFT CORNER) OF TREATMENT BOX
1908a
SCAN LASER FOCUS FROM FIRST LOCATION TO SECOND LOCATION (E.G., BOTTOM RIGHT CORNER) OF TREATMENT BOX
1908b
1910
ADDITIONAL LAYERS TO TREAT ?
YES
NO
END
1912

FIG. 19

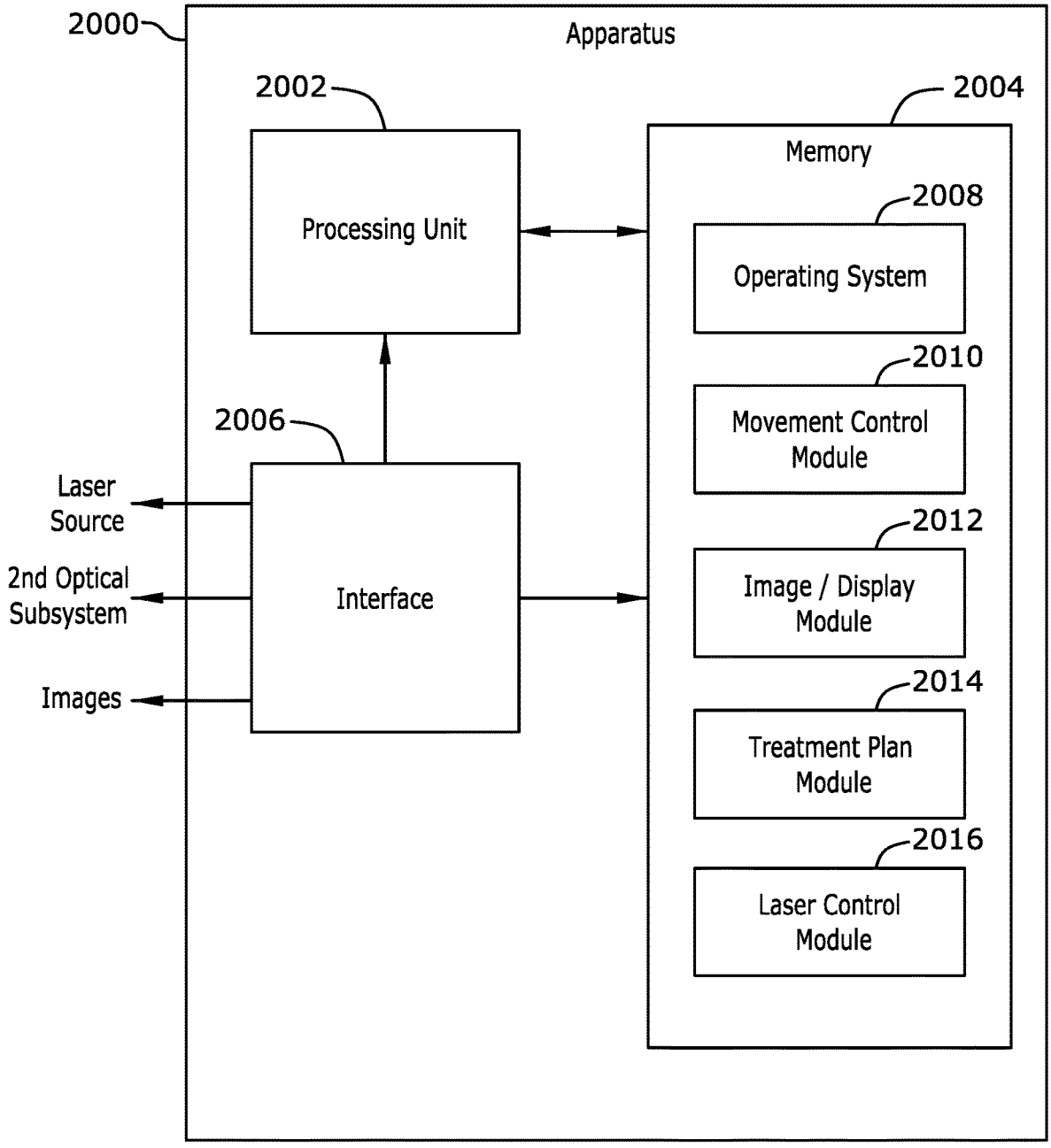
2000
Apparatus
2002
Processing Unit
2004
Memory
2008
Operating System
2010
Movement Control Module
2012
Image / Display Module
2014
Treatment Plan Module
2016
Laser Control Module
2006
Interface
Laser Source
2nd Optical Subsystem
Images

FIG. 20

SYSTEM AND METHOD FOR EYE REGION VISUALIZATION IN A LASER SURGICAL SYSTEM

TECHNICAL FIELD

[0001] The present disclosure relates generally to the field of medical devices and treatment of diseases in ophthalmology including glaucoma, and more particularly to systems and methods for visualization of a region of the eye in a laser surgical system.

BACKGROUND

[0002] Before describing the different types of glaucoma and current diagnosis and treatments options, a brief overview of the anatomy of the eye is provided.

[0003] Anatomy of the Eye

[0004] With reference to FIGS. **1-3**, the outer tissue layer of the eye **1** includes a sclera **2** that provides the structure of the eye's shape. In front of the sclera **2** is a cornea **3** that is comprised of transparent layers of tissue that allow light to enter the interior of the eye. Inside the eye **1** is a crystalline lens **4** that is connected to the eye by fiber zonules **5**, which are connected to the ciliary body **6**. Between the crystalline lens **4** and the cornea **3** is an anterior chamber **7** that contains a flowing clear liquid called aqueous humor **8**. Encircling the perimeter of the crystalline lens **4** is an iris **9** which forms a pupil around the approximate center of the crystalline lens. As shown in FIG. **2**, a posterior chamber **23** is an annular volume behind the iris **9** and bounded by the ciliary body **6**, fiber zonules **5**, and the crystalline lens **4**. The vitreous humor **10** is located between the crystalline lens **4** and the retina **11**. Light entering the eye is optically focused through the cornea **3** and crystalline lens.

[0005] With reference to FIG. **2**, the corneoscleral junction of the eye is the portion of the anterior chamber **7** at the intersection of the iris **9**, the sclera **2**, and the cornea **3**. The anatomy of the eye **1** at the corneoscleral junction includes a trabecular meshwork **12**. The trabecular meshwork **12** is a fibrous network of tissue that encircles the iris **9** within the eye **1**. In simplified, general terms the tissues of the corneoscleral junction are arranged as follows: the iris **9** meets the ciliary body **6**, the ciliary body meets with the underside of the scleral spur **14**, the top of the scleral spur serves as an attachment point for the bottom of the trabecular meshwork **12**. The ciliary body is present mainly in the posterior chamber, but also extends into the very corner of the anterior chamber **7**. The network of tissue layers that make up the trabecular meshwork **12** are porous and thus present a pathway for the egress of aqueous humor **8** flowing from the anterior chamber **7**. This pathway may be referred to herein as an aqueous humor outflow pathway, an aqueous outflow pathway, or simply an outflow pathway.

[0006] Referring to FIG. **3**, the pathway formed by the pores in the trabecular meshwork **12** connect to a set of thin, porous tissue layers called the uveal **15**, the corneoscleral meshwork **16**, and the juxtacanalicular tissue **17**. The juxtacanalicular tissue **17**, in turn, abuts a structure called Schlemm's canal **18**. The Schlemm's canal **18** carries a mixture of aqueous humor **8** and blood from the surrounding tissue to drain into the venous system though a system of collector channels **19**. As shown in FIG. **2**, the vascular layer of the eye, referred to as the choroid **20**, is next to the sclera **2**. A space, called the suprachoroidal space **21**, may be present between the choroid **20** and the sclera **2**. The general region near the periphery of the wedge between the cornea **3** and the iris **9**, running circumferentially is called the irido-corneal angle **13**. The irido-corneal angle **13** may also be referred to as the corneal angle of the eye or simply the angle of the eye. The ocular tissues illustrated in FIG. **3** are all considered to be within the irido-corneal angle **13**.

[0007] With reference to FIG. **4**, two possible outflow pathways for the movement of aqueous humor **8** include a trabecular outflow pathway **40** and a uveoscleral outflow pathway **42**. With additional reference to FIG. **2**, aqueous humor **8**, which is produced by the ciliary body **6**, flows from the posterior chamber **23** through the pupil into the anterior chamber **7**, and then exits the eye through one or more of the two different outflow pathways **40**, **42**. Approximately 90% of the aqueous humor **8** leaves via the trabecular outflow pathway **40** by passing through the trabecular meshwork **12**, into the Schlemm's canal **18** and through one or more plexus of collector channels **19** before draining through a drain path **41** into the venous system. Any remaining aqueous humor **8** leaves primarily through the uveoscleral outflow pathway **42**. The uveoscleral outflow pathway **42** passes through the ciliary body **6** face and iris root into the suprachoroidal space **21** (shown in FIG. **2**). Aqueous humor **8** drains from the suprachoroidal space **21**, from which it can be drained through the sclera **2**.

[0008] The intra-ocular pressure of the eye depends on the aqueous humor **8** outflow through the trabecular outflow pathway **40** and the resistance to outflow of aqueous humor through the trabecular outflow pathway. The intra-ocular pressure of the eye is largely independent of the aqueous humor **8** outflow through the uveoscleral outflow pathway **42**. Resistance to the outflow of aqueous humor **8** through the trabecular outflow pathway **40** may lead to elevated intra-ocular pressure of the eye, which is a widely recognized risk factor for glaucoma. Resistance through the trabecular outflow pathway **40** may increase due to a collapsed or malfunctioning Schlemm's canal **18** and trabecular meshwork **12**.

[0009] Referring to FIG. **5**, as an optical system, the eye **1** is represented by an optical model described by idealized centered and rotationally symmetrical surfaces, entrance and exit pupils, and six cardinal points: object and image space focal points, first and second principal planes, and first and second nodal points. Angular directions relative to the human eye are often defined with respect to an optical axis **24**, a visual axis **26**, a pupillary axis **28** and a line of sight **29** of the eye. The optical axis **24** is the symmetry axis, the line connecting the vertices of the idealized surfaces of the eye. The visual axis **26** connects the foveal center **22** with the first and second nodal points to the object. The line of sight **29** connects the fovea through the exit and entrance pupils to the object. The pupillary axis **28** is normal to the anterior surface of the cornea **3** and is directed to the center of the entrance pupil. These axes of the eye differ from one another only by a few degrees and fall within a range of what is generally referred to as the direction of view.

[0010] Glaucoma

[0011] Glaucoma is a group of diseases that can harm the optic nerve and cause vision loss or blindness. It is the leading cause of irreversible blindness. Approximately 80 million people are estimated to have glaucoma worldwide and of these, approximately 6.7 million are bilaterally blind.

More than 2.7 million Americans over age 40 have glaucoma. Symptoms start with loss of peripheral vision and can progress to blindness.

[0012] There are two forms of glaucoma, one is referred to as closed-angle glaucoma, the other as open-angled glaucoma. With reference to FIGS. **1-4**, in closed-angle glaucoma, the iris **9** in a collapsed anterior chamber **7** may obstruct and close off the flow of aqueous humor **8**. In open-angle glaucoma, which is the more common form of glaucoma, the permeability of ocular tissue may be affected by irregularities in the juxtacanalicular tissue **17** and inner wall of Schlemm's canal **18***a*, and blockage of tissue in the irido-corneal angle **13** along the trabecular outflow pathway **40**.

[0013] As previously stated, elevated intra-ocular pressure (TOP) of the eye, which damages the optic nerve, is a widely recognized risk factor for glaucoma. However, not every person with increased eye pressure will develop glaucoma, and glaucoma can develop without increased eye pressure. Nonetheless, it is desirable to reduce elevated TOP of the eye to reduce the risk of glaucoma.

[0014] Methods of diagnosing conditions of the eye of a patient with glaucoma include visual acuity tests and visual field tests, dilated eye exams, tonometry, i.e., measuring the intra-ocular pressure of the eye, and pachymetry, i.e., measuring the thickness of the cornea. Deterioration of vision starts with the narrowing of the visual field and progresses to total blindness. Imaging methods include slit lamp examination, observation of the irido-corneal angle with a gonioscopic lens and optical coherence tomography (OCT) imaging of the anterior chamber and the retina.

[0015] Once diagnosed, some clinically proven treatments are available to control or lower the intra-ocular pressure of the eye to slow or stop the progress of glaucoma. The most common treatments include: 1) medications, such as eye drops or pills, 2) laser surgery, and 3) traditional surgery. Treatment usually begins with medication. However, the efficacy of medication is often hindered by patient non-compliance. When medication does not work for a patient, laser surgery is typically the next treatment to be tried. Traditional surgery is invasive, more high risk than medication and laser surgery, and has a limited time window of effectiveness. Traditional surgery is thus usually reserved as a last option for patients whose eye pressure cannot be controlled with medication or laser surgery.

[0016] Laser Surgery

[0017] With reference to FIG. **2**, laser surgery for glaucoma targets the trabecular meshwork **12** to decrease aqueous humor **8** flow resistance. Common laser treatments include Argon Laser Trabeculoplasty (ALT), Selective Laser Trabeculoplasty (SLT) and Excimer Laser Trabeculectomy (ELT).

[0018] ALT was the first laser trabeculoplasty procedure. During the procedure, an argon laser of 514 nm wavelength is applied to the trabecular meshwork **12** around 180 degrees of the circumference of the irido-corneal angle **13**. The argon laser induces a thermal interaction with the ocular tissue that produces openings in the trabecular meshwork **12**. ALT, however, causes scarring of the ocular tissue, followed by inflammatory responses and tissue healing that may ultimately close the opening through the trabecular meshwork **12** formed by the ALT treatment, thus reducing the efficacy of the treatment. Furthermore, because of this scarring, ALT therapy is typically not repeatable.

[0019] SLT is designed to lower the scarring effect by selectively targeting pigments in the trabecular meshwork **12** and reducing the amount of heat delivered to surrounding ocular tissue. During the procedure, a solid-state laser of 532 nm wavelength is applied to the trabecular meshwork **12** between 180 to 360 degrees around the circumference of the irido-corneal angle **13** to remove the pigmented cells lining the trabeculae which comprise the trabecular meshwork. The collagen ultrastructure of the trabecular meshwork is preserved during SLT. **12**. SLT treatment can be repeated, but subsequent treatments have lower effects on TOP reduction.

[0020] ELT uses a 308 nm wavelength ultraviolet (UV) excimer laser and non-thermal interaction with ocular tissue to treat the trabecular meshwork **12** and inner wall of Schlemm's canal **18***a* in a manner that does not invoke a healing response. Therefore, the TOP lowering effect lasts longer. However, because the UV light of the laser cannot penetrate deep into the eye, the laser light is delivered to the trabecular meshwork **12** via an optical fiber inserted into the eye **1** through an opening and the fiber is brought into contact with the trabecular meshwork. The procedure is highly invasive and is generally practiced simultaneously with cataract procedures when the eye is already surgically open. Like ALT and SLT, ELT also lacks control over the amount of TOP reduction.

[0021] Visualization of the trabecular meshwork **12** and surrounding anatomy is a critical component of laser surgery for glaucoma. To adjust laser energy for patient anatomy or pigmentation, direct visualization of the trabecular meshwork **12** and surrounding anatomy is vital. However, in existing laser surgery systems, visualization systems for visualizing the trabecular meshwork **12** and surrounding anatomy are coupled to a laser objective that scans a laser pattern during treatment. This coupling of the visualization system to the laser objective tends to degrade the image quality of the visualization system during treatment and may adversely affect the functionality and usability of the laser surgery system.

[0022] Due to this degradation in image quality, what is needed are systems, apparatuses, and methods for laser surgery treatment of the eye that provide imaging of the trabecular meshwork **12** and surrounding anatomy during laser scanning that has a stable, consistent field of view and quality visual characteristics, e.g., focus, resolution, magnification, etc.

SUMMARY

[0023] The present disclosure relates to a system for imaging a region of an eye having a target volume of ocular tissue. The system includes a laser source configured to output a laser beam; a first optical subsystem configured to be coupled to the eye; a focusing objective optically coupled with the first optical subsystem and the laser source; a visualization system having a depth of field and a field of view, the visualization system optically coupled to the focusing objective and to the first optical subsystem through the focusing objective; a movement subsystem configured to move the focusing objective and the visualization system; and a control system. The control system is configured to control the movement subsystem and the visualization system to: place the depth of field and the field of view of the visualization system at respective positions relative to the target volume of ocular tissue so the target volume is within

the depth of field and within the field of view, obtain an image of the region of the eye with the visualization system, and maintain the position of the field of view of the visualization system relative to the target volume of ocular tissue during movement of a laser focus of the laser beam to a depth location within the target volume of ocular tissue.

[0024] The present disclosure also relates to a method of imaging a region of an eye including a target volume of ocular tissue. The method includes placing a depth of field and a field of view of a visualization system at respective positions relative to the target volume of ocular tissue and obtaining an image of the region of the eye with the visualization system. The method further includes maintaining the position of the field of view of the visualization system relative to the target volume of ocular tissue during a movement of a focus of a laser beam to a depth location within the target volume of ocular tissue; and repeating the maintaining for each of a plurality of movements of the focus of the laser beam to different depth locations within the target volume of ocular tissue.

[0025] The present disclosure further relates to a system for imaging a region of an eye including a target volume of ocular tissue. The system includes a laser source configured to output a laser beam; a first optical subsystem configured to be coupled to the eye; a second optical subsystem optically coupled to the first optical subsystem, and a control system. The second optical subsystem includes: a) a focusing objective that is optically coupled to obtain the laser beam from the laser source, b) a visualization system that is optically coupled to the focusing objective, c) a first movement mechanism arranged to move the focusing objective and the visualization system, and d) a second movement mechanism arranged to move the visualization system. The control system is coupled to the second optical subsystem and configured to control the visualization system, the first movement mechanism, and the second movement mechanism to: move a visualization system to place a field of view of the visualization system at a location relative to the region of the eye; move the focusing objective to place a laser focus of a laser beam at a depth location within the target volume of ocular tissue; and move the visualization system without moving the focusing objective to keep the field of view of the visualization system at the location relative to the region of the eye.

[0026] The present disclosure further relates to a method of imaging a region of an eye including a target volume of ocular tissue. The method includes moving a visualization system to place a field of view of the visualization system at a location relative to the region of the eye; moving a focusing objective to place a laser focus of a laser beam at a depth location within the target volume of ocular tissue; and moving the visualization system without moving the focusing objective to keep the field of view of the visualization system at the location relative to the region of the eye.

[0027] It is understood that other aspects of apparatuses and methods will become apparent to those skilled in the art from the following detailed description, wherein various aspects of apparatuses and methods are shown and described by way of illustration. As will be realized, these aspects may be implemented in other and different forms and its several details are capable of modification in various other respects. Accordingly, the drawings and detailed description are to be regarded as illustrative in nature and not as restrictive.

BRIEF DESCRIPTION OF THE DRAWINGS

[0028] Various aspects of systems, apparatuses, and methods will now be presented in the detailed description by way of example, and not by way of limitation, with reference to the accompanying drawings, wherein:

[0029] FIG. **1** is a sectional schematic illustration of a human eye and its interior anatomical structures.

[0030] FIG. **2** is a sectional schematic illustration of the irido-corneal angle of the eye of FIG. **1**.

[0031] FIG. **3** is a sectional schematic illustration detailing anatomical structures in the irido-corneal angle of FIG. **2**, including the trabecular meshwork, Schlemm's canal, and one or more collector channels branching from the Schlemm's canal.

[0032] FIG. **4** is a sectional schematic illustration of various outflow pathways for aqueous humor through the trabecular meshwork, Schlemm's canal, and collector channels of FIG. **3**.

[0033] FIG. **5** is a sectional schematic illustration of a human eye showing various axes associated with the eye.

[0034] FIG. **6** is a sectional schematic illustration of an angled beam path along which one or more light beams may access the irido-corneal angle of the eye.

[0035] FIG. **7** is a block diagram of an integrated surgical system for non-invasive glaucoma surgery including a control system, a laser source, a visual observation apparatus, an optional OCT imaging apparatus, beam conditioners, scanners, and combiners, a focusing objective head, and a patient interface.

[0036] FIG. **8***a* is a detailed block diagram of an embodiment of the integrated surgical system of FIG. **7**.

[0037] FIGS. **8***b* and **8***c* are detailed block diagrams of an embodiment of the integrated surgical system of FIG. **7** having a first optical subsystem that includes optical components of the focusing objective head and the patient interface, and a second optical subsystem that includes the visual observation apparatus, beam conditioners, scanners, and combiners, and a focusing objective of the focusing objective head.

[0038] FIGS. **9***a* and **9***b* are schematic illustrations of the focusing objective head of the integrated surgical system of FIG. **8***b* coupled to (FIG. **9***a*) and decoupled from (FIG. **9***b*) the patient interface of the integrated surgical system.

[0039] FIG. **9***c* is a schematic illustration of components of the focusing objective head and the patient interface included in FIGS. **9***a* and **9***b*.

[0040] FIGS. **10***a* and **10***b* are schematic illustrations of components of the integrated surgical system of FIGS. **7** and **8***b* functionally arranged to form a first optical system and a second optical subsystem that enable access to the irido-corneal angle along the angled beam path of FIG. **6**.

[0041] FIG. **10***c* is a schematic illustration of a beam passing through the first optical subsystem of FIGS. **10***a* and **10***b* and into the eye.

[0042] FIG. **11** is a three-dimensional schematic illustration of anatomical structures in the irido-corneal angle, including the trabecular meshwork, Schlemm's canal, a collector channel branching from the Schlemm's canal, and a surgical volume of ocular tissue to be treated by the integrated surgical system of FIG. **7**.

[0043] FIG. **12** is a two-dimensional schematic illustrations of anatomical structures in the irido-corneal angle and a three-dimensional laser treatment pattern to be applied by the integrated surgical system of FIG. **7** to affect a surgical

volume of ocular tissue between the Schlemm's canal and the anterior chamber as shown in FIG. **11**.

[0044] FIG. **13** is a three-dimensional schematic illustration of FIG. **11** subsequent to treatment of the surgical volume of ocular tissue by a laser based on the laser treatment pattern of FIG. **12** that forms an opening between the Schlemm's canal and the anterior chamber.

[0045] FIG. **14***a* is a schematic illustration of a three-dimensional laser treatment pattern formed by a number of stacked two-dimensional treatment planes or layers.

[0046] FIG. **14***b* is a schematic illustration of a two-dimensional treatment layer defined by an array of spots.

[0047] FIGS. **15***a* and **15***b* are schematic illustrations of two layers of a laser scanning process based on the treatment pattern of FIGS. **12**, where the scanning begins at a shallow depth adjacent the anterior chamber and proceeds toward the Schlemm's canal.

[0048] FIGS. **16***a* and **16***b* are schematic illustrations of two layers of a laser scanning process based on the treatment pattern of FIGS. **12**, where the scanning begins at a deep depth adjacent the Schlemm's canal and proceeds toward the anterior chamber.

[0049] FIG. **17** is a flowchart of a method imaging a region of an irido-corneal angle of an eye including a volume of ocular tissue targeted for laser treatment.

[0050] FIG. **18***a* is a schematic representation of a starting image obtained by the integrated surgical system of FIG. **8***b* while the focusing objective and visual observation apparatus are at a focus position.

[0051] FIGS. **18***b* and **18***c* are a schematic representations of subsequent images captured by the integrated surgical system of FIG. **8***b* after movement of the focusing objective and the visual observation apparatus in accordance with one or more aspects of this disclosure.

[0052] FIGS. **18***d* and **18***e* are a schematic representations of subsequent images captured by the integrated surgical system of FIG. **8***b* in the absence of movement of the focusing objective and the visual observation apparatus in accordance with one or more aspects of this disclosure.

[0053] FIG. **19** is a flowchart of the workflow of surgical steps enabled by the integrated surgical system of FIG. **8***b* to complete a laser cut in a region of interest.

[0054] FIG. **20** is a schematic block diagram of the control system of FIGS. **7** and **8***b*.

DETAILED DESCRIPTION

[0055] Disclosed herein are systems and methods for imaging a region of an eye during laser treatment of a target volume of ocular tissue of the eye. The region of the eye may be, for example, the irido-corneal angle. The system includes a laser source configured to output a laser beam, a first optical subsystem configured to be coupled to the eye, a second optical subsystem optically coupled to the first optical subsystem, and a control system coupled to the second optical subsystem. The laser source may be a femtosecond laser source or a picosecond laser source. Such lasers provide non-thermal photo-disruption interaction with ocular tissue.

[0056] The second optical subsystem includes: a) a focusing objective that is optically coupled to obtain the laser beam from the laser source, b) a visualization system optically coupled to the focusing objective, c) a first movement mechanism arranged to move the focusing objective and the visualization system along a first axis, and d) a second movement mechanism arranged to move the visualization system along a second axis. In some embodiments, the first movement mechanism may include a first structure with which the focusing objective and the visualization system are associated, and a first motor configured to move the structure. In one configuration, the first structure is a plate, the focusing objective and the visualization system are mounted to the plate, and the first motor is a stepper motor that moves the plate (and thus the focusing objective and the visualization system) in incremental units associated with a scanning of the laser through the target volume of ocular tissue.

[0057] Similarly, the second movement mechanism may include a second structure with which the only visualization system is associated, and a second motor configured to move the second structure. In one configuration, the second structure is a plate, the visualization system is mounted to the plate, and the second motor is a stepper motor that moves the plate (and thus the visualization system) in incremental units associated with a scanning of the laser through the target volume of ocular tissue. Other mechanical arrangements for moving the focusing objective and the visualization system are contemplated. For example, the focusing objective may itself be associated with a motorized structure configured to move the objective only along the first axis, while the visualization system may itself be associated with a different motorized structure configured to move the visualization system along both the first axis and the second axis.

[0058] The control system is configured to control the visualization system, the first movement mechanism, and the second movement mechanism to: obtain a starting image of a region of an eye through the visualization system, place a laser focus of the laser beam at a depth location within the target volume of ocular tissue, and capture a subsequent image of the region of the eye through the visualization system while the laser focus is at the depth location. The visualization system is moved by the second movement mechanism such the subsequent image has a one or more image characteristics consistent with one or more corresponding characteristics of the starting image. These image characteristics may include, for example, field of view and one or more visual characteristics, such as quality of focus, magnification, resolution, contrast, and other quality factors (e.g., such as distortion and optical aberrations).

[0059] Femtosecond Laser Source

[0060] A surgical component of the integrated surgical system disclosed herein is a femtosecond laser. A femtosecond laser provides highly localized, non-thermal photo-disruptive laser-tissue interaction with minimal collateral damage to surrounding ocular tissue. Photo-disruptive interaction of the laser is utilized in optically transparent tissue. The principal mechanism of laser energy deposition into the ocular tissue is not by absorption but by a highly nonlinear multiphoton process. This process is effective only at the focus of the pulsed laser where the peak intensity is high. Regions where the beam is traversed but not at the focus are not affected by the laser. Therefore, the interaction region with the ocular tissue is highly localized both transversally and axially along the laser beam. The process can also be used in weakly absorbing or weakly scattering tissue. While femtosecond lasers with photo-disruptive interactions have been successfully used in ophthalmic surgical systems and

commercialized in other ophthalmic laser procedures, none have been used in an integrated surgical system that accesses the irido-corneal angle.

[0061] In known refractive procedures, femtosecond lasers are used to create corneal flaps, pockets, tunnels, arcuate incisions, lenticule shaped incisions, partial or fully penetrating corneal incisions for keratoplasty. For cataract procedures the laser creates a circular cut on the capsular bag of the eye for capsulotomy and incisions of various patterns in the lens for breaking up the interior of the crystalline lens to smaller fragments to facilitate extraction. Entry incisions through the cornea opens the eye for access with manual surgical devices and for insertions of phacoemulsification devices and intra-ocular lens insertion devices. Several companies have commercialized such surgical systems, among them the IntraLase system now available from Johnson & Johnson Vision, Santa Ana, Calif., The LenSx and WaveLight systems from Alcon, Fort Worth, Tex., other surgical systems from Bausch and Lomb, Rochester, N.Y., Carl Zeiss Meditec AG, Germany, Ziemer, Port, Switzerland, and LENSAR, Orlando, Fla.

[0062] These existing systems are developed for their specific applications, for surgery in the cornea, and the crystalline lens and its capsular bag and are not capable of performing surgery in the irido-corneal angle **13** for several reasons. First, the irido-corneal angle **13** is not accessible with these surgical laser systems because the irido-corneal angle is too far out in the periphery and is outside of surgical range of these systems. Second, the angle of the laser beam from these systems, which is along the optical axis **24** to the eye **1**, is not appropriate for reaching the irido-corneal angle **13**, where there is significant scattering and optical distortion at the applied wavelength. Third, any imaging capabilities these systems may have do not have the accessibility, penetration depth and resolution to image the tissue along the trabecular outflow pathway **40** with sufficient detail and contrast.

[0063] In accordance with the integrated surgical system disclosed herein, clear access to the irido-corneal angle **13** is provided along the angled beam path **30**. The tissue, e.g., cornea **3** and the aqueous humor **8** in the anterior chamber **7**, along this angled beam path **30** is transparent for wavelengths from approximately 400 nm to 2500 nm and femtosecond lasers operating in this region can be used. Such mode locked lasers work at their fundamental wavelength with Titanium, Neodymium or Ytterbium active material. Non-linear frequency conversion techniques known in the art, frequency doubling, tripling, sum and difference frequency mixing techniques, optical parametric conversion can convert the fundamental wavelength of these lasers to practically any wavelength in the above-mentioned transparent wavelength range of the cornea.

[0064] Existing ophthalmic surgical systems apply lasers with pulse durations longer than 1 ns have higher photo-disruption threshold energy, require higher pulse energy and the dimension of the photo-disruptive interaction region is larger, resulting in loss of precision of the surgical treatment. When treating the irido-corneal angle **13**, however, higher surgical precision is required. To this end, the integrated surgical system may be configured to apply lasers with pulse durations from 10 femtosecond (fs) to 1 nanosecond (ns) for generating photo-disruptive interaction of the laser beam with ocular tissue in the irido-corneal angle **13**. While lasers with pulse durations shorter than 10 fs are available, such laser sources are more complex and more expensive. Lasers with the described desirable characteristics, e.g., pulse durations from 10 femtosecond (fs) to 1 nanosecond (ns), are commercially available from multiple vendors, such as Newport, Irvine, Calif., Coherent, Santa Clara, Calif., Amplitude Systems, Pessac, France, NKT Photonics, Birkerod, Denmark, and other vendors.

[0065] Visual Observation Apparatus

[0066] An imaging component of the integrated surgical system disclosed herein is a visual observation apparatus, also referred to herein as a visualization system. The visual observation apparatus may include, for example, a video camera, a telescope, and one or more illumination sources. The camera may be a digital camera fitted with a goniolens to provide gonioscopic images of the eye. The illumination sources are positioned for optimal irradiance of the object of interested, e.g., the irido-corneal angle of the eye including in particular, the trabecular meshwork. Illumination sources may be LEDs or light delivered via fiber optic cables. Illumination schemes are numerous: refractive ballistic schemes where the sources are placed in air and light refracts through the optics to reach the trabecular meshwork; transmissive ballistic schemes where illumination sources are inserted into pre-drilled holes or features inside lenses and adhered using index-matched epoxy; or reflective schemes where light from illumination sources strikes the trabecular meshwork after reflecting off designed reflective surfaces on lenses close to the eye.

[0067] OCT Imaging

[0068] An optional imaging component of the integrated surgical system disclosed herein is an OCT imaging apparatus. OCT technology may be used to diagnose, locate, and guide laser surgery directed to the irido-corneal angle of the eye. For example, with reference to FIGS. **1-3**, OCT imaging may be used to determine the structural and geometrical conditions of the anterior chamber **7**, to assess possible obstruction of the trabecular outflow pathway **40** and to determine the accessibility of the ocular tissue for treatment. As previously described, the iris **9** in a collapsed anterior chamber **7** may obstruct and close off the flow of aqueous humor **8**, resulting in closed-angle glaucoma. In open-angle glaucoma, where the macroscopic geometry of the angle is normal, the permeability of ocular tissue may be affected, by blockage of tissue along the trabecular outflow pathway **40** or by the collapse of the Schlemm's canal **18** or collector channels **19**.

[0069] OCT imaging can provide the necessary spatial resolution, tissue penetration and contrast to resolve microscopic details of ocular tissue. When scanned, OCT imaging can provide two-dimensional (2D) cross-sectional images of the ocular tissue. As another aspect of the integrated surgical system, 2D cross-sectional images may be processed and analyzed to determine the size, shape, and location of structures in the eye for surgical targeting. It is also possible to reconstruct three-dimensional (3D) images from a multitude of 2D cross-sectional images but often it is not necessary. Acquiring, analyzing, and displaying 2D images is faster and can still provide all information necessary for precise surgical targeting.

[0070] OCT is an imaging modality capable of providing high resolution images of materials and tissue. Imaging is based on reconstructing spatial information of the sample from spectral information of scattered light from within the sample. Spectral information is extracted by using an inter-

ferometric method to compare the spectrum of light entering the sample with the spectrum of light scattered from the sample. Spectral information along the direction that light is propagating within the sample is then converted to spatial information along the same axis via the Fourier transform. Information lateral to the OCT beam propagation is usually collected by scanning the beam laterally and repeated axial probing during the scan. 2D and 3D images of the samples can be acquired this way. Image acquisition is faster when the interferometer is not mechanically scanned in a time domain OCT, but interference from a broad spectrum of light is recorded simultaneously. This implementation is called a spectral domain OCT. Faster image acquisition may also be obtained by scanning the wavelength of light rapidly from a wavelength scanning laser in an arrangement called a swept-source OCT.

[0071] The axial spatial resolution limit of the OCT is inversely proportional to the bandwidth of the probing light used. Both spectral domain and swept source OCTs are capable of axial spatial resolution below 5 micrometers (m) with sufficiently broad bandwidth of 100 nanometers (nm) or more. In the spectral domain OCT, the spectral interference pattern is recorded simultaneously on a multichannel detector, such as a charge coupled device (CCD) or complementary metal oxide semiconductor (CMOS) camera, while in the swept source OCT the interference pattern is recorded in sequential time steps with a fast optical detector and electronic digitizer. There is some acquisition speed advantage of the swept source OCT but both types of systems are evolving and improving rapidly, and resolution and speed is sufficient for purposes of the integrated surgical system disclosed herein. Stand-alone OCT systems and OEM components are now commercially available from multiple vendors, such as Optovue Inc., Fremont, Calif., Topcon Medical Systems, Oakland, N.J., Carl Zeiss Meditec AG, Germany, Nidek, Aichi, Japan, Thorlabs, Newton, N.J., Santec, Aichi, Japan, Axsun, Billercia, Mass., and other vendors.

[0072] Accessing the Irido-Corneal Angle

[0073] An important feature afforded by the integrated surgical system is access to the targeted ocular tissue in the irido-corneal angle **13**. With reference to FIG. **6**, the irido-corneal angle **13** of the eye may be accessed via the integrated surgical system along an angled beam path **30** passing through the cornea **3** and through the aqueous humor **8** in the anterior chamber **7**. For example, one or more of an imaging beam, e.g., an OCT beam and/or a visual observation beam, and a laser beam may access the irido-corneal angle **13** of the eye along the angled beam path **30**.

[0074] An optical system disclosed herein is configured to direct a light beam to an irido-corneal angle **13** of an eye along an angled beam path **30**. The optical system includes a first optical subsystem and a second optical subsystem. The first optical subsystem includes a window formed of a material with a refractive index n_w and has opposed concave and convex surfaces. The first optical subsystem also includes an exit lens formed of a material having a refractive index n_x. The exit lens also has opposed concave and convex surfaces. The concave surface of the exit lens is configured to couple to the convex surface of the window to define a first optical axis extending through the window and the exit lens. The concave surface of the window is configured to detachably couple to a cornea of the eye with a refractive index n_c such that, when coupled to the eye, the first optical axis is generally aligned with the direction of view of the eye.

[0075] The second optical subsystem is configured to output a light beam, e.g., an OCT beam or a laser beam. The optical system is configured so that the light beam is directed to be incident at the convex surface of the exit lens along a second optical axis at an angle α that is offset from the first optical axis. The respective geometries and respective refractive indices n_x, and n_w of the exit lens and window are configured to compensate for refraction and distortion of the light beam by bending the light beam so that it is directed through the cornea **3** of the eye toward the irido-corneal angle **13**. More specifically, the first optical system bends the light beam to that the light beam exits the first optical subsystem and enters the cornea **3** at an appropriate angle so that the light beam progresses through the cornea and the aqueous humor **8** in a direction along the angled beam path **30** toward the irido-corneal angle **13**.

[0076] Accessing the irido-corneal angle **13** along the angled beam path **30** provides several advantages. An advantage of this angled beam path **30** to the irido-corneal angle **13** is that the OCT beam and laser beam passes through mostly clear tissue, e.g., the cornea **3** and the aqueous humor **8** in the anterior chamber **7**. Thus, scattering of these beams by tissue is not significant. With respect to OCT imaging, this enables the use of shorter wavelength, less than approximately 1 micrometer, for the OCT to achieve higher spatial resolution. An additional advantage of the angled beam path **30** to the irido-corneal angle **13** through the cornea **3** and the anterior chamber **7** is the avoidance of direct laser beam or OCT beam light illuminating the retina **11**. As a result, higher average power laser light and OCT light can be used for imaging and surgery, resulting in faster procedures and less tissue movement during the procedure.

[0077] Another important feature provided by the integrated surgical system is access to the targeted ocular tissue in the irido-corneal angle **13** in a way that reduces beam discontinuity. To this end, the window and exit lens components of the first optical subsystem are configured to reduce the discontinuity of the optical refractive index between the cornea **3** and the neighboring material and facilitate entering light through the cornea at a steep angle.

[0078] Having thus generally described the integrated surgical system and some of its features and advantages, a more detailed description of the system and its component parts follows.

[0079] Integrated Surgical System

[0080] In the following description, the term "beam" may—depending on the context—refer to one of a laser beam, an OCT beam, an illumination beam, an observation beam, an illumination/observation beam, or a visual beam. The term "colinear beams" refers to two or more different beams that are combined by optics of the integrated surgical system **1000** to share a same path to a same target location of the eye as they enter the eye. The term "non-colinear beams" refers to two or more different beams that have different paths into the eye. The term "co-targeted beams" refers to two or more different beams that have different paths into the eye but that target a same location of the eye. In colinear beams, the different beams may be combined to share a same path into the eye by dichroic or polarization beam splitters and delivered along a same optical path

through a multiplexed delivery of the different beams. In non-colinear beams, the different beams are delivered into the eye along different optical paths that are separated spatially or by an angle between them. In the description to follow, any of the foregoing beams or combined beams may be generically referred to as a light beam. The terms distal and proximal may be used to designate the direction of travel of a beam, or the physical location of components relative to each other within the integrated surgical system. The distal direction refers to a direction toward the eye; thus, an OCT beam output by the OCT imaging apparatus moves in the distal direction toward the eye. The proximal direction refers to a direction away from the eye; thus, an OCT return beam from the eye moves in the proximal direction toward the OCT imaging apparatus.

[0081] With reference to FIG. **7**, an example integrated surgical system **1000** for non-invasive glaucoma surgery includes a control system **100**, a surgical component **200**, an optional first imaging component **300** and a second imaging component **400**. In the embodiment of FIG. **7**, the surgical component **200** is a femtosecond laser source, the optional first imaging component **300** is an OCT imaging apparatus, and the second imaging component **400** is a visual observation apparatus, e.g., a microscopic video camera, for direct viewing of anatomy of the eye. Other components of the integrated surgical system **1000** include beam conditioners, scanners, and combiners **500**, beam combiners **600**, a focusing objective head **700**, and a patient interface **800**.

[0082] The control system **100** may be a single computer or and plurality of interconnected computers configured to control the hardware and software components of the other components of the integrated surgical system **1000**. A user interface **110** of the control system **100** accepts instructions from a user and displays information for observation by the user. Input information and commands from the user include but are not limited to system commands, motion controls for docking the patient's eye to the system, selection of pre-programmed or live generated surgical plans, navigating through menu choices, setting of surgical parameters, responses to system messages, determining and acceptance of surgical plans and commands to execute the surgical plan. Outputs from the system towards the user includes but are not limited to display of system parameters and messages, display of images of the eye, graphical, numerical, and textual display of the surgical plan and the progress of the surgery.

[0083] The control system **100** is connected to the other components **200**, **300**, **400**, **500** of the integrated surgical system **1000**. Control signals from the control system **100** to the femtosecond laser source **200** function to control internal and external operation parameters of the laser source, including for example, power, repetition rate and beam shutter. Control signals from the control system **100** to the optional OCT imaging apparatus **300** function to control OCT beam scanning parameters, and the acquiring, analyzing, and displaying of OCT images.

[0084] Laser beams **201** from the femtosecond laser source **200** and OCT beams **301** from the optional OCT imaging apparatus **300** are directed towards beam conditioners, scanners, and combiners **500**. Beam conditioners set the basic beam parameters, beam size, divergence. Beam conditioners may also include additional functions, setting the beam power or pulse energy and shutter the beam to turn it on or off. Different kind of scanners can be used for the purpose of scanning the laser beam **201** and the OCT beam **301**. For scanning transversal to a beam **201**, **301**, angular scanning galvanometer scanners are available for example from Cambridge Technology, Bedford, Mass., Scanlab, Munich, Germany.

[0085] To optimize scanning speed, the scanner mirrors are typically sized to the smallest size, which still support the required scanning angles and numerical apertures of the beams at the target locations. The ideal beam size at the scanners is typically different from the beam size of the laser beam **201** or the OCT beam **301**, and different from what may be needed at an optical entrance of the focusing objective head **700**. Therefore, beam conditioners may be applied before, after, or in between individual scanners. The beam conditioners, scanners, and combiners **500** includes scanners for scanning the beam transversally and axially. Axial scanning changes the depth of the focus at the target region. Axial scanning can be performed by moving a lens axially in the beam path with a servo or stepper motor.

[0086] Beam combiners, such as dichroic, polarization or other kind of beam combiners, collinearly combine the laser beam **201** and the OCT beam **301**. In some embodiments, the laser beam **201** and the OCT beam **301** may be combined and then scanned using a common scanner. In other embodiments, the laser beam **201** and the OCT beam **301** beams may be scanned using separate scanners and then collinearly combined. In either case, a combined laser/OCT beam **550** is collinearly combined with an illumination beam **401** of the visual observation apparatus **400** with dichroic, polarization or other kind of beam combiners **600**. The beam combiner **600** uses dichroic or polarization beam splitters to split and recombine light with different wavelength and/or polarization. The beam combiner **600** may also include optics to change certain parameters of the individual beams **201**, **301**, **401** such as beam size, beam angle and divergence. The combined laser/OCT/visual beam **701** is passed through optics of the focusing objective head **700** and optics of the patient interface **800** to reach a common target volume or surgical volume in the eye **1**.

[0087] To resolve ocular tissue structures of the eye in sufficient detail, the imaging components **300**, **400** of the integrated surgical system **1000** may provide an OCT beam **301** and a visual observation beam **401** having a spatial resolution of several micrometers. The resolution of the OCT beam **301** is the spatial dimension of the smallest feature that can be recognized in the OCT image. It is determined mostly by the wavelength and the spectral bandwidth of the OCT source, the quality of the optics delivering the OCT beam **301** to the target location in the eye, the numerical aperture of the OCT beam and the spatial resolution of the OCT imaging apparatus at the target location. In one embodiment, the OCT beam **301** of the integrated surgical system **1000** has a resolution of no more than 5 μm.

[0088] Likewise, the surgical laser beam **201** provided by the femtosecond laser source **200** may be delivered to targeted locations with several micrometer accuracy. The resolution of the laser beam **201** is the spatial dimension of the smallest feature at the target location that can be modified by the laser beam without significantly affecting surrounding ocular tissue. It is determined mostly by the wavelength of the laser beam **201**, the quality of the optics delivering the laser beam to target location in the eye, the numerical aperture of the laser beam, the energy of the laser

pulses in the laser beam and the spatial resolution of the laser scanning system at the target location. In addition, to minimize the threshold energy of the laser for photo-disruptive interaction, the size of the laser spot should be no more than approximately 5 μm.

[0089] It should be noted that, while the visual observation beam **401** is acquired by the visual observation apparatus **400** using fixed, non-scanning optics, the OCT beam **301** of the OCT imaging apparatus **300** is scanned laterally in two transversal directions. The laser beam **201** of the femtosecond laser source **200** is scanned in two lateral dimensions and the depth of the focus is scanned axially.

[0090] For practical embodiments, beam conditioning, scanning, and combining the optical paths are certain functions performed on the laser, OCT, and visual observation optical beams. Implementation of those functions may happen in a different order than what is indicated in FIG. **7**. Specific optical hardware that manipulates the beams to implement those functions can have multiple arrangements with regards to how the optical hardware is arranged. They can be arranged in a way that they manipulate individual optical beams separately, in another embodiment one component may combine functions and manipulates different beams. For example, a single set of scanners can scan both the laser beam **201** and the OCT beam **301**. In this case, separate beam conditioners set the beam parameters for the laser beam **201** and the OCT beam **301**, then a beam combiner combines the two beams for a single set of scanners to scan the beams. While many combinations of optical hardware arrangements are possible for the integrated surgical system, the following section describes in detail an example arrangement.

[0091] Referring to FIG. **8***a*, in some embodiments an integrated surgical system **1000** includes optical subsystems configured together to deliver each of a laser beam **201**, an OCT beam **301**, and an illumination beam **401** in the distal direction toward an eye **1**, and receive each of an OCT return beam and an observation beam **401** back from the eye **1**.

[0092] Regarding the delivery of a laser beam, a laser beam **201** output by the femtosecond laser source **200** passes through a beam conditioner **510** where the basic beam parameters, beam size, divergence are set. The beam conditioner **510** may also include additional functions, setting the beam power or pulse energy and shutter the beam to turn it on or off. After existing the beam conditioner **510**, the laser beam **210** enters an axial scanning lens **520**. The axial scanning lens **520**, which may include a single lens or a group of lenses, is movable in the axial direction **522** by a servo motor, stepper motor or other control mechanism. Movement of the axial scanning lens **520** in the axial direction **522** changes the axial distance of the focus of the laser beam **210** at a focal point.

[0093] In accordance with a particular embodiment of the integrated surgical system **1000**, an intermediate focal point **722** is set to fall within, and is scannable in, the conjugate surgical volume **721**, which is an image conjugate of the surgical volume **720**, determined by optics of the focusing objective head **700**. The surgical volume **720** is the spatial extent of the region of interest within the eye where imaging and surgery is performed. For glaucoma surgery, the surgical volume **720** is the vicinity of the irido-corneal angle **13** of the eye **1**.

[0094] A pair of transverse scanning mirrors **530**, **532** rotated by a galvanometer scanner scan the laser beam **201** in two essentially orthogonal transversal directions, e.g., in the x and y directions. Then the laser beam **201** is directed towards a dichroic or polarization beam splitter **540** where it is reflected toward a beam combining mirror **601** configured to combine the laser beam **201** with an OCT beam **301**.

[0095] Regarding delivery of an OCT beam, an OCT beam **301** output by the OCT imaging apparatus **300** passes through a beam conditioner **511**, an axially moveable focusing lens **521** and a transversal scanner with scanning mirrors **531** and **533**. The focusing lens **521** is used set the focal position of the OCT beam in the conjugate surgical volume **721** and the real surgical volume **720**. The focusing lens **521** is not scanned for obtaining an OCT axial scan. Axial spatial information of the OCT image is obtained by Fourier transforming the spectrum of the interferometrically recombined OCT return beam **301** and reference beams **302**. However, the focusing lens **521** can be used to re-adjust the focus when the surgical volume **720** is divided into several axial segments. This way the optimal imaging spatial resolution of the OCT image can be extended beyond the Rayleigh range of the OCT beam **301**, at the expense of time spent on scanning at multiple ranges.

[0096] Proceeding in the distal direction toward the eye **1**, after the scanning mirrors **531** and **533**, the OCT beam **301** is combined with the laser beam **201** by the beam combiner mirror **601**. The OCT beam **301** and laser beam **201** components of the combined laser/OCT beam **550** are multiplexed and travel in the same direction to be focused at an intermediate focal point **722** within the conjugate surgical volume **721**. After having been focused in the conjugate surgical volume **721**, the combined laser/OCT beam **550** propagates to a second beam combining mirror **602** where it is combined with a visual observation beam **401** to form a combined laser/OCT/visual beam **701**.

[0097] The combined laser/OCT/visual beam **701** traveling in the distal direction then passes through a relay lens **750** included in the focusing objective head **700**, is reflected by a reflecting surface **740**, which may be a planar beam-folding mirror or a facet inside an optic, and then passes through an exit lens **710** of the focusing objective head and a window **801** of a patient interface, where the intermediate focal point **722** of the laser beam within the conjugate surgical volume **721** is re-imaged into a focal point in the surgical volume **720**. The optics of the focusing objective head **700** re-images the intermediate focal point **722**, through the window **801** of the patient interface, into the ocular tissue within the surgical volume **720**. In one configuration, the reflecting surface **740** in the form of a facet inside an optic may have a specialized coating for broadband reflection (visible, OCT and femtosecond) and low difference between s and p polarization group delay dispersion (GDD).

[0098] A scattered OCT return beam **301** from the ocular tissue travels in the proximal direction to return to the OCT imaging apparatus **300** along the same paths just described, in reverse order. The reference beam **302** of the OCT imaging apparatus **300**, passes through a reference delay optical path and return to the OCT imaging apparatus from a moveable mirror **330**. The reference beam **302** is combined interferometrically with the OCT return beam **301** on its return within the OCT imaging apparatus **300**. The amount of delay in the reference delay optical path is adjustable by moving the moveable mirror **330** to equalize the optical paths of the OCT return beam **301** and the reference beam

302. For best axial OCT resolution, the OCT return beam **301** and the reference beam **302** are also dispersion compensated to equalize the group velocity dispersion within the two arms of the OCT interferometer.

[0099] When the combined laser/OCT/visual beam **701** is delivered through the cornea **3** and the anterior chamber **7**, the combined beam passes through posterior and anterior surface of the cornea at a steep angle, far from normal incidence. These surfaces in the path of the combined laser/OCT/visual beam **701** may create excessive astigmatism and coma aberrations that need to be compensated for.

[0100] Referring to FIG. **8***b*, in some embodiments disclosed herein an integrated surgical system **1000** for treating a target volume of ocular tissue includes a control system **100**, a laser source **200**, a first optical subsystem **1001**, and a second optical subsystem **1002**. These components are arranged and configured together to deliver a laser beam **201** and an illumination beam **401** in the distal direction toward a target volume of ocular tissue of an eye **1**, and receive an observation beam **401** back from the eye **1**. The delivered illumination beam and received observation beam may collectively be referred to herein as an illumination/observation beam **401**.

[0101] The first optical subsystem **1001** includes optics configured to establish a common optical axis **706** or common optical path through the cornea and the anterior chamber into the irido-corneal angle for a laser beam **201** and an illumination/observation beam **401**. The common optical axis **706** is offset from a first optical axis **705** within the direction of view. In one configuration, the first optical subsystem **1001** includes a reflecting surface **740** in the form of a beam-folding mirror, an exit lens **710**, and a window **801**. In another configuration, the first optical subsystem **1001** includes a facet inside an optic that has a specialized coating for broadband reflection (visible and femtosecond) and low difference between s and p polarization group delay dispersion (GDD), an exit lens **710** associated with the optic, and a window **801**.

[0102] The second optical subsystem **1002** includes a scanner component **830**, a focusing objective **826**, and a visualization system **828**. The scanner component **830** is arranged and configured to receive a laser beam **201** from the laser source **200** and to optically couple the laser beam with the focusing objective **826**. The scanner component **830** may include a pair of galvanometer scanning mirrors. In some embodiments the second optical subsystem **1002** is configured to rotate relative to the first optical axis **705**. This rotation enables optical access to the whole 360-degree circumference of the irido-corneal angle **13** of the eye **1**.

[0103] The focusing objective **826** is arranged and configured to receive the laser beam **201** from the scanner component **830** and to optically couple the laser beam with the first optical subsystem **1001**. To this end, the focusing objective **826** aligns the laser beam **201** with the reflecting surface **740**, which in turn aligns the laser beam along the common optical axis **706**. In some embodiments the focusing objective **826** includes focusing optics, e.g., a back-end objective **832** having two lenses (not shown) and a front-end objective **836** with a first objective lens **838***a* and a second objective lens **838***b*, and a dichroic mirror **834** located between the back-end objective **832** and the front-end objective **836**.

[0104] The focusing objective **826** is mounted on a first structure, e.g., a first plate **844**, that is instrumented with a first motor, e.g., an objective motor **845**, configured to move the focusing objective back and forth along a first mechanical axis **850** in the Z_A direction, to thereby adjust the position of the focus of the laser beam **201** along the common optical axis **706**. The first mechanical axis **850** may be aligned with, e.g., co-axial with or parallel to the central, optical axis of the focusing objective **826**.

[0105] The visualization system **828**, which in some embodiments includes a visual observation apparatus **400** and a telescope **842**, is arranged and configured to optically couple an illumination beam **401** with the focusing objective **826**. To this end, the visual observation apparatus **400** of the visualization system **828** may include an illumination source that provides the illumination beam **401**. In other configurations (not shown in FIG. **8***b*), the illumination source may be a component of the visualization system **828** that is separate from the visual observation apparatus **400**. In either case, the optical output of the visualization system **828** is aligned with the dichroic mirror **834** of the focusing objective **826**, and thereby couples the illumination beam **401** with the dichroic mirror. The dichroic mirror **834** may collinearly combine the laser beam **201** and the illumination beam **401**. The dichroic mirror **834** aligns the collinearly combined laser/illumination beam **201**/**401** with the reflecting surface **740** of the first optical subsystem **1001**, which in turn aligns the laser/illumination beam along the common optical axis **706**.

[0106] The visualization system **828** is mounted on a second structure, e.g., a second plate **846**, that is instrumented with a second motor, e.g., a camera motor **847**, configured to move the visualization system back and forth along a second mechanical axis **852** in the Z_B direction, to thereby adjust the position of the depth of field of the visualization system **828** along the common optical axis **706**. The second mechanical axis **852** may be aligned with, e.g., co-axial with or parallel to the central, optical axis of the visualization system **828**. The second plate **846** is also mounted on the first plate **844**. Accordingly, the visualization system **828** moves together with the focusing objective **826** in the Z_A direction upon movement of the first plate **844**. This movement maintains the alignment of the visualization system **828** with the dichroic mirror **834** of the focusing objective **826**, and thereby maintains optical coupling between the visualization system and the focusing objective.

[0107] Additionally, through its association with the second plate **846**, the visualization system **828** may also move in the Z_B direction without any corresponding movement by the focusing objective **826**. As will be described further below, the combination of: 1) movement of the visualization system **828** and movement of the focusing objective **826** along the first mechanical axis **850** in the Z_A direction, and 2) movement of the visualization system by itself along the second mechanical axis **852** in the Z_B direction without corresponding movement of the focusing objective, provides for fixed, stable, real-time imaging of the target volume of ocular tissue during laser scanning, wherein the field of view and depth of field of the image are consistent.

[0108] In the integrated surgical system **1000** of FIG. **8***b*, the focusing objective **826** and the visualization system **828** are arranged such that the first mechanical axis **850** (or corresponding optical axis) of the focusing objective is orthogonal with the second mechanical axis **852** (or corresponding optical axis) of the visualization system. This arrangement, also referred to herein as the "geometry," of

the optical axes of the focusing objective **826** and the visualization system **828** is merely one example geometry. Numerous other geometries are possible. For example, the focusing objective **826** and the visualization system **828** may be arranged such that the first mechanical axis **850** and the second mechanical axis **852** are at any angle relative to each other, are parallel to each other, or are co-axial (i.e., they share the same mechanical axis).

[0109] Continuing with reference to FIG. **8***b*, the laser source **200** is configured to emit a laser beam **201** of femtosecond light pulses through a control shutter **820** and into an articulated arm **822**. The articulated arm **822** transmits the laser beam **201** onto a turning mirror **824**. The fixed turning mirror **824** is separate from the second optical subsystem **1002** and is arranged relative to the laser source **200** and the second optical subsystem to direct a laser beam **201** into the scanner component **830** of the second optical subsystem. The scanner component **830**, in turn directs the laser beam **201** into the back-end objective **832** of the focusing objective **826**.

[0110] The back-end objective **832** functions as an expanding telescope that increases the diameter of the laser beam **201** that, together with other components and aspects of the optical design, pre-compensates for aberrations, e.g., astigmatism, coma, spherical aberration, which will be introduced by the human cornea. The expanded laser beam **201** is then incident onto the dichroic mirror **834**. The dichroic mirror **834** is configured to transmit the laser wavelength, e.g., 1030 nm in the case of a femtosecond laser, and to not reflect the laser wavelength. The expanded laser beam is then incident into the first objective lens **838***a* included in the front-end objective **836** of the focusing objective **826**. The laser beam **201** continues to diverge as it passes through the first objective lens **838***a*. The laser beam **201** is then incident into the second objective lens **838***b*. The laser beam **201** exits the second objective lens **838***b* and enters the first optical subsystem **1001**.

[0111] Once in the first optical subsystem **1001**, the laser beam **201** is directed into a reflective surface **740** in the form of a beam-folding mirror, through the exit lens **710** and the window **801**, and into the irido-corneal angle. In the case of a reflective surface **740** in the form of a facet in an optic that has a specialized coating for broadband reflection (visible and femtosecond) and low difference between s and p polarization GDD, the laser beam **201** refracts through a convex surface of the optic, strikes the facet and internally reflects through the optic and then exits through a concave surface corresponding to the exit lens **710**. The laser beam **201** then passes through the window **801**, the cornea, and the anterior chamber, and to a spot **840** in the irido-corneal angle at a predetermined distance from the exit surface of the second objective lens **838***b*.

[0112] Regarding the diameter of the expanded laser beam **201**, the diameter of the beam when it enters the first objective lens **838***a* in the front-end objective **836** determines the final numerical aperture of the laser beam. The larger the diameter of the expanded laser beam **201**, the greater the numerical aperture. In general, laser beams **201** with greater numerical apertures are focused onto smaller spots **840**. The beam diameter and the numerical aperture are design choices that depend on the intended use of the device. In the integrated surgical system **1000**, the diameter of the expanded laser beam is about 6 mm.

[0113] Continuing with reference to FIG. **8***b*, the visualization system **828** enables visualization of anatomy of the eye **1**, including the circumferential angle. As previously mentioned, the visualization system **828** may include a visual observation apparatus **400** and a telescope **842**. In one configuration, the visual observation apparatus **400** includes an illumination source and a gonioscopic video camera. The illumination source component of the visual observation apparatus **400** shines an illumination beam **401** through the telescope **842** and onto the dichroic mirror **834**. The illumination beam **401** reflects from the dichroic mirror **834** into the first objective lens **838***a* included in the front-end objective **836**. The illumination beam **401** passes through the first objective lens **838***a* and into the second objective lens **838***b*. The second objective lens **838***b* focuses visible light from the illumination beam **401** to illuminate an area within the circumferential angle. The illumination beam **401** exits the second objective lens **838***b* and enters the first optical subsystem **1001**.

[0114] Once in the first optical subsystem **1001**, the illumination beam **401** may be directed into the reflective surface **740**, through the exit lens **710** and the window **801**, and into the irido-corneal angle. The illumination beam **401** diffuses or scatters inside the target volume of ocular tissue and back-scattered light exits the tissue as a returning observation beam. The returning observation beam **401** reflects off the reflective surface **740** and returns to the second optical subsystem **1002** through the front-end objective **836** and onto the second dichroic mirror **834**. The returning observation beam **401** of light enters the visualization system **828** where it is focused by the telescope **842** onto the video camera component of the visual observation apparatus **400** where the observation beam **401** impinges a sensor to form an image of the circumferential angle.

[0115] In accordance with embodiments disclosed herein, the visualization system **828** is positioned during laser scanning such that the depth of field of the visualization system is fixed relative to an image object, e.g., the surface of the trabecular meshwork where a target volume of ocular tissue is located. As such, the image resulting from impingement of the observation beam **401** on the sensor of the visualization system **828** is fixed. In other words, the mapping between the points of the image object and the points on the sensor of the visualization system **828** are fixed during scanning. Accordingly, the field of view of the captured image is fixed and image quality is consistent.

[0116] As disclosed further below, the visualization system **828** has a depth of field greater than the thickness of the target volume of ocular tissue. For example, in some embodiments, the depth of field is in the range of 1.5 mm to 3.0 mm in tissue. This design feature of the visualization system **828** maintains image quality during scanning. Other optical specifications of the visualization system **828** include: 1) a resolution capable of resolving features of a certain size, e.g., less than 10 μm, 2) illumination uniformity, meaning illumination coverage is uniform and does not have hot spots or uneven light intensity, and 3) a field of view (FOV) greater that 60 degrees so that a surgeon can see enough of the relevant anatomy.

[0117] Although not shown in FIG. **8***b*, the second optical subsystem **1002** may include an OCT imaging apparatus similar to that describe with reference to FIG. **8***a*. In such a configuration, an OCT beam output by an OCT imaging apparatus may be optically, collinearly combined with the

laser beam **201** by additional optics (not shown) of the second optical subsystem **1002**. An example of a second optical subsystem configured as such is disclosed in U.S. Patent Application Publication No. US 2020/0352785, the entire disclosure of which is hereby incorporated by reference.

[0118] The second optical subsystem **1002** may also include a dual beam apparatus for use in detecting a surface of ocular tissue in the target volume of ocular tissue. In such a configuration, dual aiming beams output by a dual beam apparatus may be optically, collinearly combined with the laser beam **201** by additional optics (not shown) of the second optical subsystem **1002**. An example of a second optical subsystem configured as such is also disclosed in U.S. Patent Application Publication No. US 2020/0352785.

[0119] With reference to FIGS. **9***a* and **9***b*, considering further the embodiment of the integrated surgical system **1000** described with reference to FIG. **8***b*, components of the first optical subsystem **1001** and the second optical subsystem **1002** may be included in one or more of the focusing objective head **700** and the patient interface **800** of the integrated surgical system. For example, as shown in FIGS. **9***a* and **9***b*, the window **801** of the first optical subsystem **1001** may be included in the patient interface **800**, while the exit lens **710** and the reflecting surface **740** of the first optical subsystem and the focusing objective **826** of the second optical subsystem **1002** may be included in the focusing objective head **700**. FIG. **9***a* shows the eye **1**, the patient interface **800** and the focusing objective head **700** coupled together. FIG. **9***b* shows the eye **1**, the patient interface **800** and the focusing objective head **700** detached from one another.

[0120] The patient interface **800** optically and physically couples the eye **1** to the focusing objective head **700**, which in turn optically couples with other optic components of the integrated surgical system **1000**. The patient interface **800** serves multiple functions. It immobilizes the eye relative to components of the integrated surgical system; creates a sterile barrier between the components and the patient; and provides optical access between the eye and the instrument. The patient interface **800** is a sterile, single use disposable device and it is coupled detachably to the eye **1** and to the focusing objective head **700** of the integrated surgical system **1000**.

[0121] The patient interface **800** includes the window **801** of the first optical subsystem **1001**. The window **801** has an eye-facing, concave surface **812** and an objective-facing, convex surface **813** opposite the concave surface. The window **801** thus has a meniscus form. With reference to FIG. **9***c*, the concave surface **812** is characterized by a radius of curvature re, while the convex surface **813** is characterized by a radius of curvature r_w. The concave surface **812** is configured to couple to the eye, either through a direct contact or through index matching material, liquid, or gel, placed in between the concave surface **812** and the eye **1**.

[0122] The window **801** may be formed of glass and has a refractive index n_w. In one embodiment, the window **801** is formed of fused silica and has a refractive index n_w of 1.45. Fused silica has the lowest index from common inexpensive glasses. Fluoropolymers such as the Teflon AF are another class of low index materials that have refractive indices lower than fused silica, but their optical quality is inferior to glasses, and they are relatively expensive for high volume production. In another embodiment the window **801** is formed of the common glass BK7 and has a refractive index n_w of 1.50. A radiation resistant version of this glass, BK7G18 from Schott AG, Mainz, Germany, allows gamma sterilization of the patient interface **800** without the gamma radiation altering the optical properties of the window **801**.

[0123] Returning to FIGS. **9***a* and **9***b*, the window **801** is surrounded by a wall **803** of the patient interface **800** and an immobilization device, such as a suction ring **804**. When the suction ring **804** is in contact with the eye **1**, an annular cavity **805** is formed between the suction ring and the eye. When vacuum applied to the suction ring **804** and the cavity via a vacuum tube a vacuum pump (not shown in FIGS. **9***a* and **9***b*), vacuum forces between the eye and the suction ring attach the eye to the patient interface **800** during surgery. Removing the vacuum releases or detach the eye **1**.

[0124] The end of the patient interface **800** opposite the eye **1** includes an attachment interface **806** configured to attach to the housing **702** of the focusing objective head **700** to thereby affix the position of the eye relative to the other components of the integrated surgical system **1000**. The attachment interface **806** can work with mechanical, vacuum, magnetic or other principles and it is also detachable from the integrated surgical system.

[0125] The focusing objective head **700** includes the exit lens **710** of the first optical subsystem **1001**. The exit lens **710** may also be referred to herein as the superdome. In one configuration, the exit lens **710** is an aspheric lens having an eye-facing, concave surface **711** and a convex surface **712** opposite the concave surface. The exit lens **710** thus has a meniscus form. While the exit lens **710** shown in FIGS. **9***a* and **9***b* is an aspheric lens giving more design freedom, in other configurations the exit lens may be a spherical lens. Alternatively, constructing the exit lens **710** as a compound lens, as opposed to a singlet, allows more design freedom to optimize the optics while preserving the main characteristics of the optical system as presented here.

[0126] With reference to FIG. **9***c*, the concave surface **711** of the exit lens **710** is characterized by a radius of curvature r_y, while the convex surface **712** is characterized by an aspheric shape. The aspheric convex surface **712** in combination with the spherical concave surface **711** result in an exit lens **710** having varying thickness, with the outer perimeter edges **715** of the lens being thinner than the central, apex region **717** of the lens. The concave surface **711** is configured to couple to the convex surface **813** of the window **801**. In one embodiment, the exit lens **710** is formed of fused silica and has a refractive index n_x of 1.45.

[0127] FIGS. **10***a* and **10***b* are schematic illustrations of different configurations of an optical system **1010** of the integrated surgical system **1000** of FIG. **8***b*. Each configuration of an optical system **1010** includes the first optical subsystem **1001** and the second optical subsystem **1002** of FIG. **8***b*. FIG. **10***c* is a schematic illustration of a laser/visual beam **201/401** passing through the first optical subsystem **1001** of FIGS. **10***a* and **10***b*. For simplicity of illustration, all components of the first optical subsystem **1001** and the second optical subsystem **1002** are not included in FIGS. **10***a* and **10***b*. Also, for additional simplicity in FIG. **10***a*, the reflecting surface **740** of the first optical subsystem **1001** is not included and the combined laser/visual beam **201/401** shown in FIG. **9***a* is unfolded or straightened out. It is understood by those skilled in the art that adding or removing planar beam folding mirrors does not alter the principal

working of the optical system **1010** formed by the first optical subsystem **1001** and the second optical subsystem **1002**.

[0128] With reference to FIG. **10***a*, the first optical subsystem **1001** of the integrated surgical system **1000** includes the exit lens **710** of a focusing objective head **700** and the window **801** of a patient interface **800**. The exit lens **710** and the window **801** are arranged relative to each other to define a first optical axis **705**. The first optical subsystem **1001** is configured to receive a beam, e.g., a combined laser/visual beam **201**/**401**, incident at the convex surface **712** of the exit lens **710** along a second optical axis **706**, and to direct the beam toward a surgical volume **720** in the irido-corneal angle **13** of the eye.

[0129] During a surgical procedure, all, or a portion of the first optical subsystem **1001** may be assembled by interfacing the convex surface **813** of the window **801** with the concave surface **711** of the exit lens **710**. To this end, a focusing objective head **700** is docked together with a patient interface **800**. As a result, the concave surface **711** of the exit lens **710** is coupled to the convex surface **813** of the window **801**. The coupling may be by direct contact or through a layer of index matching fluid. For example, when docking the patient interface **800** to the focusing objective head **700**, a drop of index matching fluid can be applied between the contacting surfaces to eliminate any air gap that may be between the two surfaces **711**, **813** to thereby help pass the laser/visual beam **201**/**401** through the gap with minimal Fresnel reflection and distortion.

[0130] In order to direct the beam toward a surgical volume **720** of ocular tissue in the irido-corneal angle **13** of the eye, the first optical subsystem **1001** is designed to account for refraction of the beam **201**/**401** as it passes through the exit lens **710**, the window **801** and the cornea **3**. To this end, and with reference to FIG. **10***c*, the refractive index n_x of the exit lens **710** and the refractive index n_w of the window **801** are selected in view of the refractive index n_c of the cornea **3** to cause appropriate beam bending through the first optical subsystem **1001** so that when the laser/visual beam **201**/**401** exits the subsystem and passes through the cornea **3**, the beam path is generally aligned to fall within the irido-corneal angle **13**.

[0131] Continuing with reference to FIG. **10***c* and beginning with the interface between the window **801** and the cornea **3**. Too steep of an angle of incidence at the interface where the laser/visual beam **201**/**401** exits the window **801** and enters the cornea **3**, i.e., at the interface between the concave surface **812** of the window and the convex surface of the cornea **3**, can create excessive refraction and distortion. To minimize refraction and distortion at this interface, in one embodiment of the first optical subsystem **1001**, the refractive index of the window **801** is closely matched to the index of the cornea **3**. For example, as describe above with reference to FIGS. **9***a* and **9***b*, the window **801** may have a refractive index lower than 1.42 to closely match the cornea **3**, which has a refractive index of 1.36.

[0132] Excessive refraction and distortion at the interface where the combined laser/visual beam **201**/**401** exits the window **801** and enters the cornea **3** may be further compensated for by controlling the bending of the beam as it passed through the exit lens **710** and the window **801**. To this end, in one embodiment of the first optical subsystem **1001** the index of refraction n_w of the window **801** is larger than each of the index of refraction n_x of the exit lens **710** and the index of refraction n_c of the cornea **3**. As a result, at the interface where the combined laser/visual beam **201**/**401** exits the exit lens **710** and enters the window **801**, i.e., interface between the concave surface **711** of the exit lens and the convex surface **813** of the window, the beam passes through a refractive index change from high to low that cause the beam to bend in a first direction. Then, at the interface where the combined laser/visual beam **201**/**401** exits the window **801** and enters the cornea **3**, i.e., interface between the concave surface **812** of the exit lens and the convex surface of the cornea, the beam passes through a refractive index change from low to high that cause the beam to bend in a second direction opposite the first direction.

[0133] The shape of the window **801** is chosen to be a meniscus lens. As such, the incidence angle of light has similar values on both surfaces **812**, **813** of the window **801**. The overall effect is that at the convex surface **813** the light bends away from the surface normal and at the concave surface **812** the light bends towards the surface normal. The effect is like when light passes through a plan parallel plate. Refraction on one surface of the plate is compensated by refraction on the other surface a light passing through the plate does not change its direction. Refraction at the entering, convex surface **712** of the exit lens **710** distal to the eye is minimized by setting the curvature of the entering surface such that angle of incidence β of light **201**/**401** at the entering surface is close to a surface normal **707** to the entering surface at the intersection point **708**.

[0134] Here, the exit lens **710**, the window **801**, and the eye **1** are arranged as an axially symmetric system with a first optical axis **705**. In practice, axial symmetry is an approximation because of manufacturing and alignment inaccuracies of the optical components, the natural deviation from symmetry of the eye and the inaccuracy of the alignment of the eye relative to the window **801** and the exit lens **710** in a clinical setting. But, for design and practical purposes the eye **1**, the window **801**, and the exit lens **710** are considered as an axially symmetric first optical subsystem **1001**.

[0135] With continued reference to FIG. **10***a*, the second optical subsystem **1002** of the optical system **1010** is optically coupled to the first optical subsystem **1001** at an angle α relative to the first optical axis **705** of the first optical subsystem **1001**. The advantage of this arrangement is that both optical subsystems **1001**, **1002** can be designed at a much lower numerical aperture compared to a system where all optical components are designed on axis with a common optical axis.

[0136] The second optical subsystem **1002** includes the focusing objective **826** and various other components collectively indicated as an optical subsystem step **1003**. Referring to FIG. **8***b*, these other components may include the scanner component **830** that optically couples with the laser source **200**, and the visualization system **828**, which may include a visual observation apparatus **400** and a telescope **842**.

[0137] Returning to FIG. **10***a*, as previously described, the second optical subsystem **1002** includes mechanical parts (not shown) including a motorized first plate **844** and a motorized second plate **846** for moving one or more of the focusing objective **826** and the visualization system **828**. The second optical subsystem **1002** may further include mechanical parts (not shown) configured to rotate the entire second optical subsystem around the first optical axis **705** of

the first optical subsystem **1001**. This allows optical access to the whole 360-degree circumference of the irido-corneal angle **13** of the eye **1**.

[0138] With reference to FIG. **10***b*, flexibility in arranging the first and second optical subsystems **1001**, **1002**, relative to each other may be provided by an optical interface **1004** interposed between the optical output of the second optical subsystem **1002** and the optical input of the first optical subsystem **1001**. In one embodiment, the optical interface **1004** may include one or more reflecting surfaces **740**, prisms (not shown) or optical gratings (not shown) configured to receive the optical output, e.g., combined laser/visual beam **201**/**401**, of the second optical subsystem **1002**, change or adjust the direction of the combined laser/visual beam, and direct the beam to the optical input of the first optical subsystem **1001** while preserving the angle α between the first optical axis **705** and the second optical axis **706**.

[0139] In another configuration, the optical interface **1004** further includes mechanical parts (not shown) configured to rotate **741** the optical interface of reflecting surfaces **740** around the first optical axis **705** of the first optical subsystem **1001**, while keeping the second optical subsystem **1002** stationary. Accordingly, the second optical axis **706** of the second optical subsystem **1002** can be rotated around the first optical axis **705** of the first optical subsystem **1001**. This allows optical access to the whole 360-degree circumference of the irido-corneal angle **13** of the eye **1**.

[0140] With considerations described above with reference to FIGS. **9***a*, **9***b* and **9***c*, the design of the first optical subsystem **1001** is optimized for angled optical access at an angle α relative to the first optical axis **705** of the first optical subsystem **1001**. Optical access at the angle α compensates for optical aberrations of the first optical subsystem **1001**. Table 1 shows the result of the optimization at access angle α=72 degrees with Zemax optical design software package. This design is a practical embodiment for image guided femtosecond glaucoma surgery.

TABLE 1

Surface	Structure and Material	Refractive index	Radius [mm]	Center Thickness [mm]
concave surface 711, convex surface 712	exit lens 710 of focusing objective head 700. fused silica	1.45	−10	4.5
concave surface 812, convex surface 813	window 801 of patient interface 800. BK7G18	1.50	−10.9	1.0
3	cornea	1.36	−7.83	0.54
8	aqueous humor	1.32	−6.53	3.5
target	ophthalmic tissue	1.38	N/A	0 to 1 mm

[0141] This design produces diffraction limited focusing of 1030 nm wavelength laser beams with numerical aperture (NA) up to 0.2. In one design, the optical aberrations of the first optical subsystem **1001** are compensated to a degree that the Strehl ratio of the first optical subsystem for a laser beam **201** with numerical aperture larger than 0.15 at the irido-corneal angle is larger than 0.9. In another design, the optical aberrations of the first optical subsystem **1001** are partially compensated, the remaining uncompensated aberrations of the first optical system are compensated by optical elements of the second optical subsystem **1002** to a degree that the Strehl ratio of the combined first and second optical subsystem for laser beam **201** with numerical aperture larger than 0.15 at the irido-corneal angle is larger than 0.9.

[0142] Surgical Treatments Overview

[0143] FIG. **11** is a three-dimensional schematic illustration of anatomical structures of the eye relevant to the surgical treatment enabled by the integrated surgical system **1000**. To reduce the IOP, laser treatment targets ocular tissues that affect the trabecular outflow pathway **40**. These ocular tissues may include the trabecular meshwork **12**, the scleral spur **14**, the Schlemm's canal **18**, and the collector channels **19**. The trabecular meshwork **12** has three layers, the uveal **15**, the corneoscleral meshwork **16**, and the juxtacanalicular tissue **17**. These layers are porous and permeable to aqueous, with the uveal **15** being the most porous and permeable, followed by the corneoscleral meshwork **16**. The least porous and least permeable layer of the trabecular meshwork **12** is the juxtacanalicular tissue **17**. The inner wall **18***a* of the Schlemm's canal **18**, which is also porous and permeable to aqueous, has characteristics similar to the juxtacanalicular tissue **17**.

[0144] FIG. **12** includes three-dimensional illustrations of a treatment pattern P**1** to be applied by the integrated surgical system **1000** to affect the surgical volume **900** of ocular tissue shown in FIG. **11**, and a two-dimensional schematic illustration of the treatment pattern P**1** overlaying anatomical structures to be treated. FIG. **13** is a three-dimensional schematic illustration of the anatomical structures of the eye including an opening **902** through the trabecular meshwork **12** that results from the application of the laser treatment pattern of FIG. **12**. The opening **902** may also be referred to as a channel or aperture. The opening **902** provides and outflow pathway **40** that reduces the flow resistance in the ocular tissue to increase aqueous flow from the anterior chamber **7** into the Schlemm's canal **18** and thereby reduce the IOP of the eye.

[0145] Surgical treatments reduce outflow pathway resistance while minimizing ocular tissue modification through design and selection of laser treatment patterns. A treatment pattern is considered to define a collection of a laser-tissue interaction volumes, referred to herein as cells. The size of a cell is determined by the extent of the influence of the laser-tissue interaction. When the laser spots, or cells, are spaced close along a line, the laser creates a narrow, microscopic channel. A wider channel can be created by closely spacing a multitude of laser spots within the cross section of the channel. The arrangement of the cells may resemble the arrangement of atoms in a crystal structure.

[0146] With reference to FIG. **12**, a treatment pattern P**1** may be in the form of a cubic structure that encompasses individual cells arranged in regularly spaced rows, columns and sheets or layers. The treatment pattern P**1** may be characterized by x, y, z dimensions, with x, y, z coordinates of the cells being calculated sequentially from neighbor to neighbor in the order of a column location (x coordinate), a row location (y coordinate), and a layer location (z coordinate). A treatment pattern P**1** as such, defines a three-dimensional model of ocular tissue to be modified by a laser or a three-dimensional model of ocular fluid to be affected by a laser.

[0147] A treatment pattern P**1** is typically defined by a set of surgical parameters. The surgical parameters may include one or more of a treatment area A that represents a surface area or layer of ocular tissue through which the laser will travel. The treatment area A is determined by the treatment height, h, and the lateral extent of the treatment, w. A treatment thickness t that represents the level to which the laser will cut into the ocular tissue from the distal extent or border of the treatment volume at or near Schlemm's canal **18** to the proximal extent or border at or near the surface of the trabecular meshwork **12**. Thus, a laser applied in accordance with a treatment pattern may affect or produce a surgical volume that resembles the three-dimensional model of the treatment pattern or may affect fluid located in an interior of an eye structure resembled by the three-dimensional model.

[0148] Additional surgical parameters define the placement of the surgical volume or affected volume within the eye. For example, with reference to FIGS. **11** and **12**, placement parameters may include one or more of a location l that represents where the treatment is to occur relative to the circumferential angle of the eye, and a treatment depth d that represents a position of the three-dimensional model of ocular tissue or ocular fluid within the eye relative to a reference eye structure. In the following, the treatment depth d is shown and described relative to the region where the anterior chamber **7** meets the trabecular meshwork **12**. Together, the treatment pattern and the placement parameters define a treatment plan.

[0149] A femtosecond laser provides highly localized, non-thermal photo-disruptive laser-tissue interaction with minimal collateral damage to surrounding ocular tissue. Photo-disruptive interaction of the laser is utilized in optically transparent tissue. The principal mechanism of laser energy deposition into the ocular tissue is not by absorption but by a highly nonlinear multiphoton process. This process is effective only at the focus of the pulsed laser where the peak intensity is high. Regions where the beam is traversed but not at the focus are not affected by the laser. Therefore, the interaction region with the ocular tissue is highly localized both transversally and axially along the laser beam.

[0150] With reference to FIGS. **11** and **12**, a surgical volume **900** of ocular tissue to be treated is identified by the integrated surgical system **1000** and a treatment pattern P**1** corresponding to the surgical volume is designed by the integrated surgical system. Alternatively, the treatment pattern P**1** may be designed first, and then an appropriate surgical volume **900** for applying the treatment pattern may be identified. The surgical volume **900** of ocular tissue may comprise portions of the trabecular meshwork **12** and the Schlemm's canal **18**. For example, the surgical volume **900** of ocular tissue shown in FIG. **11** includes portions of the uveal **15**, the corneoscleral meshwork **16**, the juxtacanalicular tissue **17**, and the inner wall **18***a* of the Schlemm's canal **18**. The treatment pattern P**1** defines a laser scanning procedure whereby a laser is focused at different depth locations in ocular tissue and then scanned in multiple directions to affect a three-dimensional volume of tissue comprising multiple sheets or layers of affected tissue.

[0151] With reference to FIGS. **12** and **13**, during a laser treatment procedure, a surgical laser **201** may scan ocular tissue in accordance with the treatment pattern P**1** to form an opening **902** that extends from the anterior chamber **7**, through each of the uveal **15**, the corneoscleral meshwork **16**, the juxtacanalicular tissue **17** of the trabecular meshwork **12**, and the inner wall **18***a* of the Schlemm's canal **18**. While the example opening **902** in FIG. **13** is depicted as a continuous, single lumen defining a fluid pathway, the opening may be defined an arrangement of adjacent pores forming a sponge like structure defining a fluid pathway or a combination thereof. While the example opening **902** in FIG. **13** is in the shape of a cube, the opening may have other geometric shapes.

[0152] The movement of the laser as it scans to affect the surgical volume **900** follows the treatment pattern P**1**, which is defined by a set of surgical parameters that include a treatment area A and a thickness t. The treatment area A is defined by a width w and a height h. The width may be defined in terms of a measure around the circumferential angle. For example, the width w may be defined in terms of an angle, e.g., 90 degrees, around the circumferential angle.

[0153] Referring to FIGS. **11** and **12**, an initial placement of the laser focus within the eye is defined by a set of placement parameters, including a depth d and a location l. The location l defines a point around the circumferential angle of the eye at which laser treatment will begin, while the depth d defines a point between the anterior chamber **7** and the Schlemm's canal **18** where the laser treatment begins or ends. The depth d is measured relative to the region where the anterior chamber **7** meets the trabecular meshwork **12**. Thus, a first point that is closer to the Schlemm's canal **18** side of the trabecular meshwork **12** may be described as being deeper than a second point that is closer to the anterior chamber **7** side of the trabecular meshwork **12**. Alternatively, the second point may be described as being shallower than the first point.

[0154] With reference to FIG. **13**, the opening **902** resulting from laser application of the treatment pattern P**1** resembles the surgical volume **900** and is characterized by an area A and thickness t similar to those of the surgical volume and the treatment pattern. The thickness t of the resulting opening **902** extends from the anterior chamber **7** and through the inner wall **18***a* of the Schlemm's canal **18**, while the area A defines the cross-section size of the opening **902**.

[0155] During a laser treatment procedure, a laser focus is moved to different depths d in ocular tissue and then scanned in two lateral dimensions or directions as defined by a treatment pattern P**1** to affect a three-dimensional surgical volume **900** of ocular tissue comprising multiple sheets or layers of affected tissue. The two lateral dimensions are generally orthogonal to the axis of movement of the laser focus. With reference to FIG. **13**, the movement of a laser focus during laser scanning is described herein with reference to x, y, and z directions or axes, wherein: 1) movement of the laser focus to different depths d through the thickness t of treatment pattern P**1** or the surgical volume **900** of tissue corresponds to movement of the focus along the z axis, 2) movement of the laser focus in two dimensions or directions orthogonal to the z axis corresponds to movement of the laser focus along the width w of the treatment pattern P**1** or the surgical volume **900** of tissue in the x direction, and movement of the laser focus along the height h of the treatment pattern P**1** or the surgical volume **900** of tissue in the y direction.

[0156] As used herein scanning of the laser focus generally corresponds to a raster type movement of the laser focus in the x direction, the y direction, and the z direction. The

laser focus may be located at a point in the z direction and then raster scanned in two dimensions or directions, in the x direction and the y direction. The focal point of the laser in the z direction may be referred to as a depth d within the treatment pattern P**1** or the surgical volume **900** of tissue. The two-direction raster scanning of the laser focus defines a layer of laser scanning, which in turn produces a layer of laser-affected tissue.

[0157] During laser scanning, pulse shots of a laser are delivered to tissue within the volume of ocular tissue corresponding to the treatment pattern P**1**. Because the laser interaction volume is small, on the order of a few micrometers (m), the interaction of ocular tissue with each laser shot of a repetitive laser breaks down ocular tissue locally at the focus of the laser. Pulse duration of the laser for photodisruptive interaction in ocular tissue can range from several femtoseconds to several nanoseconds and pulse energies from several nanojoules to tens of microjoules. The laser pulses at the focus, through multiphoton processes, breaks down chemical bonds in the molecules, locally photodissociate tissue material and create gas bubbles in wet tissue. The breakdown of tissue material and mechanical stress from bubble formation fragments the tissue and create clean continuous cuts when the laser pulses are laid down in proximity to one another along geometrical lines and surfaces.

[0158] Table 2 includes examples of treatment pattern parameters and surgical laser parameters for treating tissue. The range of the parameter set is limited by practical ranges for the repetition rate of the laser and the scanning speed of the scanners.

TABLE 2

Tissue treated	Treatment pattern dimensions w[mm], h[mm], t[mm]	Opening cross section A [mm^2]	Cell size w[μm], h[μm], t[μm]	Laser average power [W]	Laser repetition rate [kHz]	Laser pulse energy [μJ]	Procedure time [s]
Trabecular meshwork	1.5, 0.2, 0.2	0.3	3, 3, 3	0.9	300	3	7.4
Trabecular meshwork	2, 0.2, 0.2	0.4	4, 4, 4	1	200	5	6.3
Trabecular meshwork	0.5, 0.2, 0.5	0.1	5, 5, 5	0.75	50	15	8.0
Trabecular meshwork	0.5, 0.2, 0.5	0.1	5, 5, 5	0.14	10	14	40.0
Trabecular meshwork	0.5, 0.2, 1.0	0.1	10, 10, 10	0.35	10	35	10.0
Trabecular meshwork	0.75, 0.25, 0.35	0.1875	10, 10, 10	0.7	20	35	3.3

[0159] With reference to FIGS. **14***a* and **14***b*, a 3D treatment pattern P**1** may be defined by a number of 2D treatment layers **1402** or treatment planes that are stacked to form a 3D treatment pattern characterized by a width w, height h, and depth or thickness t. Each individual treatment layer **1402** is in turn characterized by a pattern height h (equal to the height h of the 3D treatment pattern P**1**) and a pattern width w (equal to the width w of the 3D treatment pattern P**1**) and comprises an array of spots **1404** spaced apart to establish or fit within the height and width. The pattern width w corresponds to a distance along the circumference of the corneal angle parallel to the trabecular meshwork. This direction is also known as the circumferential direction. The pattern height h corresponds to a distance transverse to the circumference of the corneal angle perpendicular to the trabecular meshwork. This direction is also known as the azimuthal direction.

[0160] Each spot **1404** in the treatment pattern P**1** corresponds to a site within a target volume of ocular tissue where optical energy is applied at a laser focus to create a microphotodisruption site. With reference to FIG. **14***b*, each spot **1404** in a treatment layer **1402** is separated from a neighboring spot by programmable distances called spot separation (Spot Sep **1406**) and a line separation (Line Sep **1408**). A treatment layer **1402** is completed with the programmed pattern width w **1410** and pattern height h **1412** is achieved. Each treatment layer **1402** in the 3D treatment pattern P**1** is separated from a neighboring layer by a layer separation (Layer Sep).

[0161] A treatment pattern P**1** may be defined by a set of programmable parameters, such as shown in Table 3.

TABLE 3

Parameter	Minimum	Maximum
width w	10 μm	2000 μm
height h	10 μm	2000 μm
depth/thickness t	10 μm	4000 μm
Spot Sep	2 μm	40 μm
Line Sep	2 μm	40 μm
Layer Sep	2 μm	200 μm
pulse energy	0 μJ	35 μJ

[0162] Other, non-rectangular and more irregular treatment patterns can also be programmed and created in the tissue. These irregular patterns can still be decomposed to spots, lines, and layers and their extent characterized by width, height, and depth. Examples of irregular treatment patterns are described in U.S. patent application Ser. No. 16/838,858, entitled Method, System, and Apparatus for Generating Three-Dimensional Treatment Patterns for Laser Surgery of Glaucoma, the disclosure of which is hereby incorporated by reference.

[0163] In one example treatment pattern P**1**, the parameters are:

[0164] width=750 μm

[0165] height=250 μm

[0166] depth=350 μm

[0167] spot separation=10 μm

[0168] line separation=10 μm

[0169] layer separation=10 μm

[0170] During laser treatment, each treatment layer **1402** is individually created by scanning the laser focus in two dimensions, e.g., width and height, or z and y, to the various spots **1404** defining the layer, while the focus is fixed at the third dimension, e.g., depth or Z. Once a treatment layer **1402** is created, the focus is moved in the depth or z direction and the next treatment layer in the stack is created. This process is repeated until all treatment layers **1402** in the 3D treatment pattern P**1** are created.

[0171] Laser Treatment Procedures with Fixed Image of Treatment Site

[0172] In accordance with embodiments disclosed herein, a fixed image of a treatment site is obtained and displayed by an integrated surgical system **1000** while scanning a focus of a laser beam at different depths of a treatment pattern. Following are descriptions of some laser treatment procedures that provide such fixed imaging.

[0173] With reference to FIGS. **15***a* and **15***b*, in one type of laser treatment procedure the laser scanning of treatment layers begins at a shallow depth at the end of the treatment pattern P**1** adjacent the anterior chamber **7** and proceeds, layer-by-layer, in a direction that generally corresponds to the direction of propagation of the laser beam **201**. More specifically, and with reference to FIG. **15***a*, the laser scanning of treatment layers proceeds in the z direction (the depth direction) toward an anatomical structure, e.g., the Schlemm's canal **18**, while the direction of propagation of the laser beam **201** also proceeds toward the same anatomical structure, e.g., the Schlemm's canal **18**.

[0174] With reference to FIGS. **15***a* and **15***b*, in one type of laser treatment procedure the laser scanning of treatment layers begins at a shallow depth at the end of the treatment pattern P**1** adjacent the anterior chamber **7** and proceeds, layer-by-layer, in a direction that generally corresponds to the direction of propagation of the laser beam **201**. More specifically, and with reference to FIG. **15***a*, the laser scanning of treatment layers proceeds in the z direction (the depth direction) toward an anatomical structure, e.g., the Schlemm's canal **18**, while the direction of propagation of the laser beam **201** also proceeds toward the same anatomical structure, e.g., the Schlemm's canal **18**.

[0175] In FIG. **15***a*, the focus of the laser beam **201** may be initially located at a depth d_1 within a target volume **60** of ocular tissue. With reference to FIG. **8***b*, location of the focus of the laser beam **201** (also referred to herein at times, as the laser focus) at the depth d_1 may be accomplished through movement of the first plate **844** in a Z_A direction. Movement of the first plate **844** results in a corresponding movement of the focusing objective **826** and the focus of the laser beam **201** along the common optical axis **706** in the z direction of FIG. **15***a*. The depth d_1 places the laser focus in an initial layer **904** of tissue.

[0176] Continuing with FIG. **15***a*, an image of a treatment site **25** that includes the target volume **60** of ocular tissue is obtained by placing the depth of field **829** and the field of view **831** of the visualization system **828** at respective positions relative to the target volume of ocular tissue so that the target volume is within the depth of field and within the field of view. Placement of the depth of field **829** and the field of view **831** as such provides an initial or starting image of the treatment site **25** including the target volume **60** of ocular tissue.

[0177] The depth of field **829** of the visualization system **828** may be placed so a first axis **833** associated with the target volume **60** of ocular tissue is within the depth of field. The first axis **833** of the target volume **60** of ocular tissue may correspond to an axis that passes through an x-z plane of the target volume and extends along the height of the target volume in the y direction of FIG. **15***a*. In some embodiments, the first axis **833** passes through the center of the x-z plane and the depth of field **829** is placed so that the first axis **833** aligns with the center **839** of the depth of field.

[0178] The field of view **831** of the visualization system **828** may be placed so a point **837** of the field of view and a second axis **835** associated with the target volume **60** of ocular tissue are aligned with the common optical axis **706** of the first optical subsystem **1001**. The point **837** of the field of view **831** may correspond to the center point of the x-y plane of the field of view. The second axis **835** of the target volume **60** of ocular tissue may correspond to an axis that passes through the center of the x-y plane of the target volume and extends along the length of the target volume in the z direction of FIG. **15***a*.

[0179] With the depth of field **829** and the field of view **831** placed as such, the visualization system **828** may obtain an initial image like the image shown in FIG. **18***a*. With reference to FIG. **8***b*, initial placement of the depth of field **829** and the field of view **831** may be accomplished through movement of one or both of the first plate **844** along the first mechanical axis **850** in a Z_A direction and the second plate **846** along the second mechanical axis **852** in the Z_B direction. Movement of these plates **844**, **846** results in corresponding movements of the visualization system **828** and the focusing objective **826** and thus movements of the depth of field **829** and the field of view **831** relative to the target volume **60** of ocular tissue.

[0180] Continuing with FIG. **15***a*, with the depth of field **829** and the field of view **831** of visualization system **828** placed to capture an image of the treatment site **25** and the laser focus positioned at the initial depth d_1, the laser focus is scanned in multiple directions while being maintained at the initial depth. With reference to FIG. **14***a*, the multiple directions are the x direction (or circumferential direction) and the y direction (or azimuthal direction), where the x direction is into the plane of FIG. **15***a*.

[0181] With reference to FIG. **15***b*, the scanning of the laser focus of the laser beam **201** in the multiple directions results in the photodisruption of the initial layer **904** of tissue. The laser focus of the laser beam **201** is then moved along the common optical axis **706** in the z direction toward the Schlemm's canal **18** to another depth d_2. With reference to FIG. **8***b*, movement of the laser focus of the laser beam **201** is accomplished by movement of the first plate **844** along the first mechanical axis **850** in a Z_A direction which results in a corresponding movement of the focusing objective **826** and the focus of the laser beam **201** in the z direction of FIG. **15***b*. This depth d_2 places the laser focus at a subsequent layer **908** of tissue deeper than the initial layer **904**. Once the laser focus is positioned at the subsequent layer **908**, the laser focus is scanned in multiple directions while being maintained at that depth.

[0182] Typically, movement of the first plate **844** in a Z_A direction as just described also results in a corresponding

movement of the visualization system **828** in a Z_A direction and corresponding movements or shifts of the depth of field **829** and the field of view **831** of the visualization system relative to the target volume **60** of ocular tissue. In FIG. **15***b*, the shifted depth of field due to this movement is indicated by callout **829'**, while the shifted field of view is indicated by **831'**. Regarding the position of the shifted depth of field **829'**, it is shifted in the z direction relative to the first axis **833** associated with the target volume **60** of ocular tissue such that the first axis is not aligned with the center **839** of the shifted depth of field. This shift, however, does not affect the quality, e.g., focus, of the image captured by the visualization system **828** because the entirety of the target volume **60** along its depth in the z direction is still within the shifted depth of field **829'** of the visualization system.

[0183] Regarding the position of the shifted field of view **831'**, it is offset in the y direction relative to the second axis **835** associated with the target volume **60** of ocular tissue. This shift results in a shifted center **837'** of the field of view that is not aligned with the second axis **835** of the target volume **60** (unlike that shown in FIG. **15***a*). This position of the shifted field of view **831'** relative to the target volume **60** of ocular tissue produces a corresponding shift in the field of view of the image captured by the visualization system **828**. As described later below with reference to FIGS. **18***a*-**18***e*, left unaccounted for, such movement of the field of view **831'** relative to the target volume **60** of ocular tissue causes the visualization system **828** to capture an image of the treatment site that has a different field of view relative to the initial image.

[0184] To avoid shifting and movement of the field of view during laser scanning, in accordance with embodiments disclosed herein, the field of view **831** of the visualization system **828** is maintained at its initial position relative to the target volume **60** of ocular tissue through independent movement of the visualization system **828**. In one configuration, the independent movement of the visualization system **828** is in a direction opposite the z direction shown in FIG. **15***b*. For example, with reference to FIG. **8***b*, such independent movement of the visualization system **828** is accomplished by movement of the second plate **846** along the second mechanical axis **852** in a Z_B direction opposite the direction of movement of the first plate **844**.

[0185] This movement of the second plate **846** results in a corresponding movement of the field of view of the visualization system **828** in the y direction shown in FIG. **15***b* and maintains the position of the field of view **831** relative to the target volume **60** of ocular tissue at its initial position. In FIG. **15***b*, maintenance of the position of the field of view **831** resulting from this movement of the visualization system **828** shows the field of view at a location corresponding to the initial location shown in FIG. **15***a*. Movement of the visualization system **828** as such maintains the position of the field of view relative to the target volume **60** of ocular tissue such that the point **837** of the field of view remains aligned with the second axis **835** of the target volume.

[0186] Returning to FIG. **15***b*, after scanning of the subsequent layer **908**, the focus of the laser beam **201** is moved in the z direction toward the Schlemm's canal **18** to additional depths and scanned through additional treatment layers until all layers of the target volume **60** of ocular tissue have been treated. Each movement of the laser focus along the common optical axis **706** in the z direction is accompanied by a corresponding movement of the visualization system **828** as described above. As such, the position of the field of view **831** of the visualization system **828** is maintained at its initial position relative to the target volume **60** of ocular tissue and the field of view of the image of the treatment site **25** captured by the visualization system is maintained consistent with the initial or starting image of the treatment site.

[0187] With reference to FIGS. **16***a* and **16***b*, in an alternative laser treatment procedure the laser scanning of treatment layers begins at a deep depth at the end of the treatment pattern P**1** adjacent the Schlemm's canal **18** and proceeds, layer-by-layer, in a direction generally opposite to or against the direction of propagation of the laser beam **201**. More specifically, and with reference to FIG. **16***a*, the laser scanning of treatment layers starts near an anatomical structure, e.g., the Schlemm's canal **18**, and proceeds away from that structure in the z direction (the depth direction) toward the anterior chamber **7**, while the direction of propagation of the laser beam **201** proceeds toward the structure.

[0188] In FIG. **16***a*, the focus of the laser beam **201** may be initially located at a depth d_6 within a target volume **60** of ocular tissue. With reference to FIG. **8***b*, location of the focus of the laser beam **201** (also referred to herein at times, as the laser focus) at the depth d_6 may be accomplished through movement of the first plate **844** in a Z_A direction. Movement of the first plate **844** results in a corresponding movement of the focusing objective **826** and the focus of the laser beam **201** along the common optical axis **706** in the z direction of FIG. **16***a*. The depth d_6 places the laser focus in an initial layer **910** of tissue.

[0189] Continuing with FIG. **16***a*, an image of a treatment site **25** that includes the target volume **60** of ocular tissue is obtained by placing the depth of field **829** and the field of view **831** of the visualization system **828** at respective positions relative to the target volume of ocular tissue so that the target volume is within the depth of field and within the field of view. Placement of the depth of field **829** and the field of view **831** as such provides an initial or starting image of the treatment site **25** including the target volume **60** of ocular tissue.

[0190] The depth of field **829** of the visualization system **828** may be placed so a first axis **833** associated with the target volume **60** of ocular tissue is within the depth of field. The first axis **833** of the target volume **60** of ocular tissue may correspond to an axis that passes through an x-z plane of the target volume and extends along the height of the target volume in the y direction of FIG. **16***a*. In some embodiments, the first axis **833** passes through the center of the x-z plane and the depth of field **829** is placed so that the first axis **833** aligns with the center **839** of the depth of field.

[0191] The field of view **831** of the visualization system **828** may be placed so a point **837** of the field of view and a second axis **835** associated with the target volume **60** of ocular tissue are aligned with the common optical axis **706** of the first optical subsystem **1001**. The point **837** of the field of view **831** may correspond to the center point of the x-y plane of the field of view. The second axis **835** of the target volume **60** of ocular tissue may correspond to an axis that passes through the center of the x-y plane of the target volume and extends along the length of the target volume in the z direction of FIG. **16***a*.

[0192] With the depth of field **829** and the field of view **831** placed as such, the visualization system **828** may obtain an initial image like the image shown in FIG. **18***a*. With

reference to FIG. **8***b*, initial placement of the depth of field **829** and the field of view **831** may be accomplished through movement of one or both of the first plate **844** along the first mechanical axis **850** in a Z_A direction and the second plate **846** along the second mechanical axis **852** in the Z_B direction. Movement of these plates **844**, **846** results in corresponding movements of the visualization system **828** and the focusing objective **826** and thus movements of the depth of field **829** and the field of view **831** relative to the target volume **60** of ocular tissue.

[0193] Continuing with FIG. **16***a*, with the depth of field **829** and the field of view **831** of visualization system **828** placed to capture an image of the treatment site **25** and the laser focus positioned at the initial depth d_6, the laser focus is scanned in multiple directions while being maintained at the initial depth. With reference to FIG. **14***a*, the multiple directions are the x direction (or circumferential direction) and the y direction (or azimuthal direction), where the x direction is into the plane of FIG. **16***a*.

[0194] With reference to FIG. **16***b*, the scanning of the laser focus of the laser beam **201** in the multiple directions results in the photodisruption of the initial layer **910** of tissue. The laser focus of the laser beam **201** is then moved along the common optical axis **706** in the z direction toward the anterior chamber **7** to another depth d_5. With reference to FIG. **8***b*, movement of the laser focus of the laser beam **201** is accomplished by movement of the first plate **844** along the first mechanical axis **850** in a Z_A direction which results in a corresponding movement of the focusing objective **826** and the focus of the laser beam **201** in the z direction of FIG. **16***b*. This depth d_5 places the laser focus at a subsequent layer **914** of tissue deeper than the initial layer **904**. Once the laser focus is positioned at the subsequent layer **914**, the laser focus is scanned in multiple directions while being maintained at that depth.

[0195] Typically, movement of the first plate **844** in a Z_A direction as just described also results in a corresponding movement of the visualization system **828** in a Z_A direction and corresponding movements or shifts of the depth of field **829** and the field of view **831** of the visualization system relative to the target volume **60** of ocular tissue. In FIG. **16***b*, the shifted depth of field due to this movement is indicated by callout **829'**, while the shifted field of view is indicated by **831'**. Regarding the position of the shifted depth of field **829'**, it is shifted in the z direction relative to the first axis **833** associated with the target volume **60** of ocular tissue such that the first axis is not aligned with the center **839** of the shifted depth of field. This shift, however, does not affect the quality, e.g., focus, of the image captured by the visualization system **828** because the entirety of the target volume **60** along its depth in the z direction is still within the shifted depth of field **829'** of the visualization system.

[0196] Regarding the position of the shifted field of view **831'**, it is offset in the y direction relative to the second axis **835** associated with the target volume **60** of ocular tissue. This shift results in a shifted center **837'** of the field of view that is not aligned with the second axis **835** of the target volume **60** (unlike that shown in FIG. **16***a*). This position of the shifted field of view **831'** relative to the target volume **60** of ocular tissue produces a corresponding shift in the field of view of the image captured by the visualization system **828**. As described later below with reference to FIGS. **18***a*-**18***e*, left unaccounted for, such movement of the field of view **831'** relative to the target volume **60** of ocular tissue causes the visualization system **828** to capture an image of the treatment site that has a different field of view relative to the initial image.

[0197] To avoid shifting and movement of the field of view during laser scanning, in accordance with embodiments disclosed herein, the field of view **831** of the visualization system **828** is maintained at its initial position relative to the target volume **60** of ocular tissue through independent movement of the visualization system **828**. In one configuration, the independent movement of the visualization system **828** is in a direction opposite the z direction shown in FIG. **16***b*. For example, with reference to FIG. **8***b*, such independent movement of the visualization system **828** is accomplished by movement of the second plate **846** along the second mechanical axis **852** in a Z_B direction opposite the direction of movement of the first plate **844**.

[0198] This movement of the second plate **846** results in a corresponding movement of the field of view of the visualization system **828** in the y direction shown in FIG. **16***b* and maintains the position of the field of view **831** relative to the target volume **60** of ocular tissue at its initial position. In FIG. **16***b*, maintenance of the position of the field of view **831** resulting from this movement of the visualization system **828** shows the field of view at a location corresponding to the initial location shown in FIG. **16***a*. Movement of the visualization system **828** as such maintains the position of the field of view relative to the target volume **60** of ocular tissue such that the point **837** of the field of view remains aligned with the second axis **835** of the target volume.

[0199] Returning to FIG. **16***b*, after scanning of the subsequent layer **914**, the focus of the laser beam **201** is moved in the z direction toward the anterior chamber **7** to additional depths and scanned through additional treatment layers until all layers of the target volume **60** of ocular tissue have been treated. Each movement of the laser focus along the common optical axis **706** in the z direction is accompanied by a corresponding movement of the visualization system **828** as described above. As such, the position of the field of view **831** of the visualization system **828** is maintained at its initial position relative to the target volume **60** of ocular tissue and the field of view of the image of the treatment site **25** captured by the visualization system is maintained consistent with the initial or starting image of the treatment site.

[0200] In another treatment, instead of creating a treatment pattern **P1** one treatment layer **1402** at a time, the focus of the laser beam **201** is scanned in three dimensions. For example, while the laser focus is being moved transversely through a height and/or width, e.g., in the x and/or y direction, the laser focus is also oscillated back and forth axially through a depth, e.g., in the z direction. The treatment pattern **P1** characterized by such scanning of the laser focus may be referred to as a "clearing pattern." Oscillation of the laser focus through the depth in the z direction occurs simultaneous with transverse movement of the laser focus in the x and y directions. An example of scanning a laser in accordance with a clearing pattern is disclosed in U.S. patent application Ser. No. 17/202,257, the entire disclosure of which is hereby incorporated by reference.

[0201] In accordance with embodiments disclosed herein, to maintain a consistent quality, fixed field-of-view image of the treatment site while scanning a focus of a laser beam **201** at different depths of a treatment pattern or clearing pattern, the field of view **831** of the visualization system **828** is kept or maintained at its initial location through counter or offset

movements of the visualization system. For example, for every movement of the focus of the laser beam **201** in a direction toward the Schlemm's canal **18** there is a corresponding movement of the visualization system **828** in the opposite direction toward the anterior chamber **7** that keeps or maintains the field of view **831** of the visualization system relative to the treatment site at its initial location. Likewise, for every movement of the focus of the laser beam **201** in a direction toward the anterior chamber **7** there is a corresponding movement of the focus of the visualization system **828** in the opposite direction toward the Schlemm's canal **18** that keeps or maintains the field of view **831** of the visualization system at its initial location.

[0202] While the foregoing descriptions of the imaging operation of the integrated surgical system **1000** may speak in terms of obtaining a starting or initial image and obtaining subsequent images, such terminology is used to aid in describing a sequential operation. In some embodiments, the visualization system **828** of the integrated surgical system **1000** is configured to obtain a continuous, real-time image of the relevant area of eye, and thus instead of there being a separate initial image followed by one or more subsequent images, there is one continuous image overtime. Furthermore, while the directions of movement among the physical structures, including the visualization system **828** and the focusing objective **826**, are described as being opposite each other, other relative movements are possible depending on the geometry, i.e., optical axis arrangement of these structures.

[0203] Method of Fixed Imaging During Laser Treatment

[0204] FIG. **17** is a flowchart of a method of imaging a region of an eye including a target volume of ocular tissue. The region of the eye may be, for example, the irido-corneal angle. The method may be performed during a laser treatment of the target volume to provide real-time imaging of the region of the eye. With reference to FIGS. **12**, the target volume **60** of ocular tissue is characterized by a distal extent **62**, a proximal extent **64**, and a lateral extent **66**. The distal extent **62** corresponds to the part or point of the target volume **60** that is most distal along the direction of propagation of the laser beam **201**. The proximal extent **64** corresponds to the part or point of the target volume **60** that is most proximal along the direction of propagation of the laser beam **201**. The lateral extent **66** corresponds to the distance or width w of the target volume **60** along the circumference angle.

[0205] The method, which may be performed by the integrated surgical system **1000** of FIG. **8***b*, begins at a point in a surgical procedure where the region of the eye, e.g., the irido-corneal angle, is accessible and the target volume **60** of ocular tissue has been identified for treatment. Systems and methods for accessing the irido-corneal angle are described in U.S. patent application Ser. No. 16/036,883, entitled Integrated Surgical System and Method for Treatment in the Irido-Corneal Angle of the Eye, the disclosure of which is hereby incorporated by reference. Systems and method for identifying volumes of ocular tissue for treatment and designing treatment patterns reference are described in U.S. patent application Ser. No. 16/125,588, entitled Non-Invasive and Minimally Invasive Laser Surgery for the Reduction of Intraocular Pressure in the Eye, the disclosure of which is hereby incorporated by reference.

[0206] With reference to FIG. **8***b*, the visualization system **828**, e.g., a gonioscopic video camera, is configured to provide a direct image of the irido-corneal angle **13** of the eye during a laser treatment procedure. The direct image may be provided by the visualization system **828** to the control system **100**, which in turn presents the image on a display **110** of the integrated surgical system. The control system **100** may be configured to add surgical guidance objects to the image to assist a surgeon in identifying and marking a treatable surgical area and a location of the target volume **60** of ocular tissue within the treatable surgical area.

[0207] FIGS. **18***a*-**18***c* are schematic representations of images that may be obtained and displayed by the integrated surgical system **1000** of FIG. **8***b* with the visualization system **828** configured in accordance with embodiments disclosed herein. FIGS. **18***d* and **18***e* are schematic representations of images that would otherwise be obtained by a surgical system that is not configured in accordance with embodiments disclosed herein. The image inside the respective bounding box of each of FIGS. **18***a*-**18***e* is a schematic representations of a gonioscopic image **1800***a*-**1800***e* obtained by a visualization system **828**. The gonioscopic image **1800***a*-**1800***e* is of the same region of the irido-corneal angle of an eye. A vertical scale **1802** in micrometers (μm) may represent the height of the treatment pattern in the y direction (or azimuthal direction). The major sub-box **1804***a*-**1804***e* corresponds to a region of the gonioscopic image **1800***a*-**1800***e*, wherein the region is shown as a focus chart. For purposes of clarity in illustrating differences among the images, focus charts are shown instead of schematic images of ocular tissue.

[0208] Continuing with FIGS. **18***a*-**18***e*, the minor sub-box **1806***a*-**1806***e* represents a magnified portion of the images within the major sub-boxes **1804***a*-**1804***e*. Changes in field of view and focus and other characteristics of the gonioscopic image **1800***a*-**1800***e* are more discernable in the minor sub-boxes **1806***a*-**1806***e*. A horizontal scale **1808** in micrometers (μm) represents the width of the treatment pattern along the circumferential angle and in the x direction (or circumferential direction). Also included in FIGS. **18***a*-**18***e* are surgical guidance objects including a treatment overlay **1810***a*-**1810***e* that represents a surgical treatment pattern, and a pair of horizontal bars that indicate a treatable surgical area of the laser surgical system. The treatment overlay **1810***a*-**1810***e*, also referred to herein as treatment box, physically represents the location and size of a laser cut. These guidance objects are software constructs generated by the control system **100** and are added to the display of the gonioscopic images **1800***a*-**1800***e*.

[0209] Returning to FIG. **17**, at block **1702**, and with additional reference to FIGS. **8***b*, **12**, and **18***a*, the integrated surgical system **1000** obtains an initial image in the direction of the second optical axis **706** of a region of an irido-corneal angle **13** that includes a target volume **60** of ocular tissue through a visualization system **828**. As shown in the embodiment of FIG. **8***b*, the visualization system **828** is optically coupled to a focusing objective **826** that, in turn is optically coupled to obtain a laser beam **201** from a laser source **200**. With reference to FIG. **12**, the initial image may be of the anterior chamber **7** and the trabecular meshwork **12** near the proximal extent **64** of the target volume **60** of ocular tissue. The initial image is displayed on the display **110** of the integrated surgical system **1000**. With reference to FIG. **18***a*, the initial image may correspond to the gonioscopic image **1800***a*.

[0210] With additional reference to FIGS. **8***b* and **15***a*, the initial image **1800***a* of a region of an irido-corneal angle may be obtained by placing the depth of field **829** and the field of view **831** of the visualization system **828** at initial positions relative to the target volume **60** of ocular tissue such that the target volume is within the depth of field and the field of view. Such initial placement of the depth of field **829** and the field of view **831** of the visualization system **828** is typically done at the start of a surgical procedure after the patient's eye is docked to a patient interface **800** and may be done by moving the visualization system **828** and the focusing objective **826** an initial distance in an initial direction along a first mechanical axis **850**. The first mechanical axis **850** is axially aligned with the front-end objective **836** of the focusing objective **826** and reflects off the reflecting mirror **740** to align with the second optical axis **706**. The initial direction may be in either of two opposite directions as represented by the Z_A double arrow in FIGS. **8***b* and **8***c*.

[0211] With reference to FIGS. **15***a*, **15***b*, **16***a*, and **16***b*, the depth of field **829** and field of view **831** of the visualization system **828** may be initially placed such that the first axis **833** through the target volume **60** of ocular tissue in the y direction is aligned with the center **839** of the depth of field, and the second axis **835** through the target volume in the z direction is aligned with the center of the field of view. The initial image **1800***a* obtained after such initial placement the depth of field **829** and field of view **831** of the visualization system **828** has one or more image characteristics. These image characteristics may include, for example, field of view and one or more visual characteristics, such as quality of focus, magnification, resolution, contrast, and other quality factors (e.g., such as distortion and optical aberrations). Focus may be characterized in terms of sharpness, clarity, etc. Field of view may be characterized as the portion of an image that falls within a boundary.

[0212] In some embodiments, during initial placement of the depth of field **829** and field of view **831** relative to the target volume **60**, the visualization system **828** and the focusing objective **826** are simultaneously or synchronously moved in the first direction along the first mechanical axis **850**. For example, in the configuration of FIG. **8***b* the visualization system **828** and the focusing objective **826** are associated with the same first movement mechanism, e.g., first plate **844** and first motor **845**. As such, movement of the first plate **844** results in a simultaneous or synchronous movement of the visualization system **828** and the focusing objective **826**. In other embodiments, the visualization system **828** and the focusing objective **826** may be separately or asynchronously moved in the first direction along the first mechanical axis **850**. For example, the visualization system **828** and the focusing objective **826** may be associated with independent movement mechanisms, each arranged to move its respective component the initial distance in the initial direction along the first mechanical axis **850**. In this embodiment, movement of the visualization system **828** and the focusing objective **826** may be synchronous or asynchronous.

[0213] At block **1704**, the integrated surgical system **1000** places a laser focus of the laser beam **201** at a depth location within the target volume of ocular tissue in accordance with the treatment pattern P**1**. To this end, the focusing objective **826** may be moved a first distance in a first direction along the first mechanical axis **850**. In the embodiment of FIGS. **8***b* and **8***c*, the first direction of movement of the focusing objective **826** may be in either of two opposite directions as represented by the Z_A double arrow. More specifically for purposes of example only, with reference to FIG. **8***c* the focusing objective **826** may be moved a first distance **860** in a first direction **862** along the first mechanical axis **850**.

[0214] With continued reference to FIG. **8***c* and additional reference to FIG. **15***a*, the focus of the laser beam **201** may be moved a first distance **860** to place it at an initial depth d_1 corresponding to the proximal extent **64** of the target volume **60** of ocular tissue. Alternatively, with continued reference to FIG. **8***c* and additional reference to FIG. **16***a*, the focus of the laser beam **201** may be moved a first distance **861** to place it at an initial depth d_6 corresponding to the distal extent **62** of the target volume **60** of ocular tissue. The first distance **860**, **861** may be an increment corresponding to the distance the focus of the laser beam **201** is moved in the z direction during a scanning. For example, as described above with reference to FIGS. **14***a* and **14***b*, a laser focus may move in the z direction a distance corresponding to a layer separation, which for example may be 10 μm.

[0215] At block **1706**, and with additional reference to FIGS. **8***b*, **18***b* and **18***c*, the integrated surgical system **1000** obtains a subsequent image **1800***b*, **1800***c* of the region of the irido-corneal angle through the visualization system **828** while the laser focus is at the depth location. The subsequent image is displayed on the display **110** of the integrated surgical system **1000**. The subsequent image may correspond to a gonioscopic image **1800***b*, **1800***c*. As shown in FIGS. **18***b* and **18***c*, the subsequent image **1800***b*, **1800***c* has a field of view consistent with the initial image **1800***a* of FIG. **18***a*, and visual characteristics, e.g., focus, consistent with the initial image **1800***a*.

[0216] Details on the configuration and operation of the integrated surgical system **1000** that enable the obtaining of subsequent images having consistent field of view and consistent focus are provided after the description of the method of FIG. **17**. Briefly for now and regarding field of view, the visualization system **828** is moved a second distance in a second direction along a second mechanical axis **852** to counter any movement of the visualization system **828** a first distance in a first direction along the first mechanical axis **850** that occurs during placement of the laser focus in block **1704**. This second movement keeps or maintains the field of view **831** of the visualization system **828** at its initial position relative to the target volume **60** of ocular tissue.

[0217] At block **1708**, the integrated surgical system **1000** may photodisrupt tissue while the focus of the laser beam **201** is placed at the depth location. For example, with reference to FIG. **15***a*, the integrated surgical system **1000** focuses light from a femtosecond laser **201** at a spot in the tissue at the shallow depth d_1 and applies optical energy to the tissue, which energy is at a level sufficient to photodisrupt the tissue. In another example, with reference to FIG. **16***a*, the integrated surgical system **1000** focuses light from a femtosecond laser **201** at a spot in the tissue at the deep depth d_6 and applies optical energy to the tissue, which energy is at a level sufficient to photodisrupt the tissue. In either case, optical energy is applied while scanning the laser beam **201** in multiple directions defining an initial layer **904** or treatment plane at the shallow depth d_1 (in FIG. **15***a*) or an initial layer **910** or treatment plane at the deep depth d_6 (in FIG. **16***a*) to thereby photodisrupt an initial layer of

tissue of the target volume of ocular tissue. With reference to FIG. **13**, the scanning may be in the form of a raster scan where the laser is scanned in a first direction along the lateral extent **66**, i.e., the x direction, and then slightly repositioned in a second direction. i.e., the y direction, and then scanned again along the lateral extent.

[0218] At block **1710**, the integrated surgical system **1000** determines if additional layers of the target volume **60** of ocular tissue are to be treated. If no additional layers are to be treated, the integrated surgical system ends the procedure at block **1712**.

[0219] Returning to block **1710**, if additional layers of the target volume **60** of ocular tissue are to be treated, the integrated surgical system **1000** repeats the placing (block **1704**) and the capturing (block **1706**) and the photodisrupting (block **1708**) for one or more different depth locations within the target volume of ocular tissue.

[0220] The foregoing description of the method of FIG. **17** is based on the arrangement of the visualization system **828** and the focusing objective **826** illustrated in FIG. **8***b*, where the direction of movement of the visualization system by itself along the second mechanical axis **852** is described as opposite the direction of movement of the visualization system together with the focusing objection along the first mechanical axis **850**. In a configuration where the visualization system **828** and the focusing objective **826** are not mechanically coupled together and instead move independently of each other, a way to describe relative movement of the visualization system **828** and the focusing objective **826** may be in terms of a common component, such as the dichroic mirror **834**. Under this convention, each of the visualization system **828** and the front-end objective **836** of the focusing objective **826** may be described as moving toward or away from the dichroic mirror **834**. However, it is entirely feasible that the relationship could be different, with both moving towards the dichroic. The nature of this relationship may depend upon the optical design of the system (e.g., number of lenses, magnification less than or greater than 1, the geometry of the design, etc.).

[0221] Fixed Field of View

[0222] As mentioned above, the integrated surgical system **1000** is configured to provide an image of the treatment site that has a consistent field of view during laser scanning. Consistent field of view means the portion of the subsequent image **1800***b*, **1800***c* that falls within the bounding box of FIG. **18***b* or **18***c* is the same as the portion of the initial image **1800***a* that falls within the bounding box of FIG. **18***a*. Perceptually, this means the image on the display **110** of the integrated surgical system **1000** appears still, without any shifting, during laser scanning.

[0223] In accordance with embodiments disclosed herein, images having a consistent field of view are obtained by moving the visualization system **828** in a way that keeps or maintains the field of view **831** of the visualization system at its initial position relative to the target volume **60** regardless of movement of the laser focus to different depths during laser scanning. In doing so, the field of view of the image of the target volume **60** obtained by the visualization system **828** and displayed by the integrated surgical system **1000** is fixed.

[0224] In one possible configuration, the field of view **831** is kept or maintained at its initial position relative to the target volume **60** by returning the field of view to its initial position after movement of the field of view. In this configuration, the visualization system **828** may first be moved together with the focusing objective **826** a first distance in a first direction along the first mechanical axis **850**, and then quickly moved a second distance in a second direction along a second mechanical axis **852** without corresponding movement by the focusing objective along the second mechanical axis. The first movement of the visualization system **828** moves the field of view **831** away from its initial position. The second movement, however, returns the field of view **831** of the visualization system **828** back to its initial position

[0225] In another possible configuration, the field of view **831** is kept or maintained at its initial position relative to the target volume **60** by preventing movement of the field of view in the first place. In this configuration, a movement of the visualization system a first distance in a first direction along the first mechanical axis **850** that would move the field of view from its initial position is countered by a simultaneous movement of the visualization system a second distance in a second direction along a second mechanical axis **852** without corresponding movement by the focusing objective **826** along the second mechanical axis. This simultaneous counter movement along the second mechanical axis **852**, in effect, keeps or maintains the field of view **831** of the visualization system **828** at its initial position relative to the target volume **60**. In other words, the field of view **831** does not move from its initial position.

[0226] With reference to the arrangement of FIGS. **8***b* and **8***c*, the first direction of movement of the visualization system **828** may be in either of two opposite directions as represented by the Z_A double arrow. More specifically for purposes of example only, with reference to FIG. **8***c* the visualization system **828** may be moved a first distance **860** in a first direction **862** along the first mechanical axis **850**. In the integrated surgical system **1000** of FIG. **8***b*, this first movement of the visualization system **828** is simultaneous or synchronous with the movement of the focusing objective **826** due to the each of the visualization system and focusing objective being associated with the same first movement mechanism, e.g., first plate **844** and first motor **845**.

[0227] Regarding the opto-mechanics of this second movement of the visualization system **828**, as shown in FIGS. **8***b* and **8***c* the second mechanical axis **852** is axially aligned with the telescope **842** of the visualization system **828** and is input to the dichroic mirror **843** of the focusing objective **826** to align with the first mechanical axis **850**. In the arrangement of FIGS. **8***b* and **8***c*, the second movement of the visualization system **828** in the second direction may be in either of two opposite directions as represented by the Z_B double arrow. More specifically for purposes of example only, with reference to FIG. **8***c* the visualization system **828** may be moved a second distance **864** in a second direction **866** along the second mechanical axis **852**. The focusing objective **826**, however, is not moved in the second direction. This movement of the visualization system **828** a second distance in a second direction along a second mechanical axis **852** keeps or maintains the field of view **831** of the visualization system **828** at its initial position and thus results in a subsequent image **1800***b*, **1800***c* of the region of the irido-corneal angle that has a field of view consistent with the initial image **1800***a* of FIG. **18***a*.

[0228] Considering further the opto-mechanical arrangement of FIG. **8***b*, any movement of the visualization system **828** in a first direction (e.g., either of two opposite directions

as represented by the Z_A double arrow in FIG. **8***b*) may be accounted for by a movement of the visualization system in a second direction (e.g., either of two opposite directions as represented by the Z_B double arrow in FIG. **8***b*) without corresponding movement of the focusing objective **826**. More specifically for purposes of example only, with reference to FIG. **8***b*, any movement of the first plate **844** that moves the visualization system **828** together with the focusing objective **826** is countered by movement of the second plate **846** that moves only the visualization system.

[0229] This movement of the second plate **846** keeps or maintains the field of view of the visualization system **828** at the initial position and thus results in a subsequent image **1800***b*, **1800***c* of the region of the irido-corneal angle that has a field of view consistent with the initial image **1800***a* of FIG. **18***a*. As noted above, in some embodiments movement of the visualization system **828** in the second direction along the second mechanical axis **852** is simultaneous or synchronous with movement of the focusing objective **826** in the first direction along the first mechanical axis **850** (at block **1704**). In other embodiments movement of the visualization system **828** in the second direction along the second mechanical axis **852** is separate from, or asynchronous with, movement of the focusing objective **826** in the first direction along the first mechanical axis **850** (at block **1704**).

[0230] In either of simultaneous/synchronous or separate/asynchronous movement, in some embodiments the second distance by which the visualization system **828** is moved (at block **1706**) in a second direction along the second mechanical axis **852** without corresponding movement of the focusing objective **826** is a transfer function of the first distance by which each of the focusing objective **826** and the visualization system **828** are moved (at block **1704**) in a first direction along the first mechanical axis **850**. With reference to FIG. **8***c*, in one configuration, this transfer function is simply a scalar value, such that the second distance **864** the visualization system **828** moves in the second direction **866** along the second mechanical axis **852** is a constant value, which is linearly proportional to the first distance **860** the focusing objective **826** (together with the visualization system **828**) moves in the first direction **862** along the first mechanical axis **850**.

[0231] In FIG. **8***c*, the transfer function is one in which the first distance **860** and the second distance **864** are equal. The two distances **860**, **864**, however, may not be equal. For example, in some configurations, the second distance **864** is less than the first distance **860**. In other words, the ratio of second distance/first distance is less than one (1.0) and may range, for example, from 0.2 to 0.6. Numerous other ratios outside of this example range are possible, as the ratio value is a function of characteristics of the visualization system **828**, such as magnification, and geometry, i.e., the angle between the first mechanical axis **850** of the focusing objective **826** and the second mechanical axis **852** of the visualization system.

[0232] With reference to FIG. **8***b*, in some embodiments, the control system **100** is configured to control operation of the second movement mechanism, e.g., the second plate **846** and the camera motor **847**, based on the operation of the first movement mechanism, e.g., the first plate **844** and the objective motor **845**, so that movement of the camera motor (and thus movement of the visualization system **828**) is triggered by movement of the objective motor (and thus movement of the focusing objective **826**). To this end, the control system **100** may be programmed to detect activation of the objective motor **845** and movement of the first plate **844** in a first direction **862** along the first mechanical axis **850** and to immediately activate the camera motor **847** and initiate a corresponding movement of the second plate **846** in a second direction **866** along the second mechanical axis **852**. Note, activation of the objective motor **845** and movement of the first plate **844** may be automatically controlled by the control system **100** in accordance with a scanning treatment pattern or activation may be operator initiated. The control system **100** may be further programmed to detect deactivation of the objective motor **845** and a stoppage of movement of the first plate **844** and to immediately deactivate the camera motor **847** to stop a corresponding movement of the second plate **846** in the second direction **866**.

[0233] Fixed Focus

[0234] As mentioned above, the integrated surgical system **1000** is configured to provide an image of the treatment site that has a consistent focus during laser scanning. Consistent focus means the sharpness or clarity of the subsequent image **1800***b*, **1800***c* is the same as those of the initial image **1800***a*. Quantitatively, this consistency in focus may be evidenced using a contrast-based spatial resolution approach. This is an industry standard, involving groups of line pairs (black and white) whose separation between lines gets successively smaller. The resolution limit is the line pair size at which one cannot distinguish between two black lines. The classic layout is the United States Air Force 1951 resolution target. Focus is a measure of resolution: when the image is defocused then the resolution has degraded. Experimental techniques to assess "best focus" typically involve moving an Air Force target in the imaging direction to see it go in and out of focus.

[0235] In accordance with embodiments disclosed herein, images having a consistent focus are obtained by configuring the visualization system **828** with a long depth of field relative to a dimension of the target volume **60** of ocular tissue. For example, the depth of field **829** of the visualization system **828** may be 2 to 10 times greater than the thickness of the target volume **60**, which from Table 3 above may range from 10 μm to 4000 μm. As such, any movement of the depth of field **829** that results from movement of the visualization system **828** does not cause the target volume **60** to fall outside the depth of field. Accordingly, the focus of the subsequent image **1800***b*, **1800***c* obtained by the visualization system **828** and displayed by the integrated surgical system **1000** is consistent with that of the initial image **1800***a*. Perceptually, this means the image on the display **110** of the integrated surgical system **1000** does not appear to change focus during laser scanning.

[0236] Comparison of Display Images

[0237] With reference to FIGS. **15***a* and **18***b*, a subsequent image **1800***b* of the region of an irido-corneal angle may be obtained, for example, by moving the visualization system **828** and the focusing objective **826** as described above with reference to blocks **1704** and **1706** of FIG. **17** to place the focus of a laser beam **201** at a shallow depth d_1 (referred to herein as a "shallow position"), while the field of view **831** of the visualization system **828** is kept or maintained at its initial position relative to the target volume **60** of ocular tissue, and the target volume remains within the depth of field **829** of the visualization system.

[0238] As described above, the field of view **831** of the visualization system **828** may be kept or maintained at its

initial position through movement of the visualization system that returns the field of view to its initial position after movement of the field of view, or that prevents movement of the field of view. Also, as described above, the target volume remains within the depth of field **829** of the visualization system **828** due to the long depth of field.

[0239] In comparing the initial image **1800***a* (shown in FIG. **18***a*) and the subsequent image **1800***b* (shown in FIG. **18***b*) it is noted that the respective images have the same or substantially the same focus characteristic and field of view. For example, the images inside of major sub-box **1804***b* and minor sub-box **1806***b* of FIG. **18***b* are consistent with the images inside the major sub-box **1804***a* and minor sub-box **1806***a* of FIG. **18***a*. Furthermore, the position of the treatment overlay **1810***b* of FIG. **18***b* is consistent with the position of the treatment overlay **1810***a* of FIG. **18***a*.

[0240] With reference to FIGS. **16***a* and **18***c*, a subsequent image **1800***c* of the region of an irido-corneal angle may be obtained by moving the visualization system **828** and the focusing objective **826** as described above with reference to blocks **1704** and **1706** of FIG. **17** to place the laser focus at a deep depth d_6 (referred to herein as a "deep position."), while the field of view of the visualization system **828** is kept or maintained at its initial position relative to the target volume **60** of ocular tissue, and the target volume remains within the depth of field **829** of the visualization system.

[0241] In comparing the initial image **1800***a* (shown in FIG. **18***a*) and the subsequent image **1800***c* (shown in FIG. **18***c*) it is noted that the respective images have the same or substantially the same focus characteristic and field of view. For example, the images inside of major sub-box **1804***c* and minor sub-box **1806***c* of FIG. **18***c* are consistent with the images inside the major sub-box **1804***a* and minor sub-box **1806***a* of FIG. **18***a*. Furthermore, the position of the treatment overlay **1810***c* of FIG. **18***c* is consistent with the position of the treatment overlay **1810***a* of FIG. **18***a*.

[0242] While the foregoing comparisons are between the initial image **1800***a* (shown in FIG. **18***a*) and each of the "shallow" subsequent image **1800***b* (shown in FIG. **18***b*) and the "deep" subsequent image **1800***c* (shown in FIG. **18***c*), it is noted that the "shallow" subsequent image **1800***b* and the "deep" subsequent image **1800***c* also have consistent field of view and focus. In other words, the images inside of major sub-box **1804***c* and minor sub-box **1806***c* of FIG. **18***c* are consistent with the images inside the major sub-box **1804***b* and minor sub-box **1806***c* of FIG. **18***b*. Furthermore, the position of the treatment overlay **1810***c* of FIG. **18***c* is consistent with the position of the treatment overlay **1810***b* of FIG. **18***b*. It is further noted that the integrated surgical system **1000** disclosed herein is configured to provide images with consistent field of view and focus, and a fixed overlay, at all depth positions between the shallow position and the deep position.

[0243] By comparison, in a surgical system that is not configured in accordance with embodiments disclosed herein (e.g., does not have a visualization system with a long depth of field and is not configured to keep or maintain the depth of field of its visualization system at its initial position relative to a volume of ocular tissue) subsequent images will have a shifted field of view and a different focus quality relative to the initial image. For example, with reference to FIGS. **15***a*, **18***a* and **18***d*, a subsequent image **1800***d* (shown in FIG. **18***d*) of the region of an irido-corneal angle that would be obtained after moving the visualization system **828** and the focusing objective **826** together to place the laser focus at a shallow depth d_2, without further independent movement of the field of view of the visualization system back to the initial position would have a shifted field of view and a different focus quality relative to the initial image **1800***a* (shown in FIG. **18***a*). The shifted field of view occurs because there is no further independent movement of the visualization system **828**, that keeps or maintains the field of view of the visualization system at its initial position while the change in focus may occur due to movement of the short depth of field of the visualization system that places all or a portion of the target volume **60** outside the depth of field.

[0244] In further comparing the initial image **1800***a* (shown in FIG. **18***a*) and the subsequent image **1800***d* (shown in FIG. **18***d*) it is noted that the respective images have different focus characteristics and fields of view. For example, the field of view of the images inside the major sub-box **1804***d* and the minor sub-box **1806***d* is shifted relative to the field of view of the images inside the major sub-box **1804***a* and the minor sub-box **1806***a* of the initial image **1800***a*. Likewise, the focus of the images inside the major sub-box **1804***d* and the minor sub-box **1806***d* is not as sharp as the images inside the major sub-box **1804***a* and the minor sub-box **1806***a* of the initial image **1800***a*. Furthermore, the position of the treatment overlay **1810***d* of FIG. **18***d* is shifted relative to the position of the treatment overlay **1810***a* of FIG. **18***a*.

[0245] Similarly, with reference to FIGS. **16***a*, **18***a*, and **18***e*, a subsequent image **1800***e* (shown in FIG. **18***e*) of the region of an irido-corneal angle that would be obtained by moving the visualization system **828** and the focusing objective **826** together to place the laser focus at a deep depth d_5, without further independent movement of the field of view of the visualization system back to the initial position would have a shifted field of view and a different focus quality relative to the initial image **1800***a* (shown in FIG. **18***a*).

[0246] In further comparing the initial image **1800***a* (shown in FIG. **18***a*) and the subsequent image **1800***e* (shown in FIG. **18***e*) it is noted that the respective images have different focus characteristics and fields of view. For example, the field of view of the images inside the major sub-box **1804***e* and the minor sub-box **1806***e* is shifted relative to the field of view of the images inside the major sub-box **1804***a* and the minor sub-box **1806***a* of the initial image **1800***a*. Likewise, the focus of the images inside the major sub-box **1804***e* and the minor sub-box **1806***e* is not as sharp as the images inside the major sub-box **1804***a* and the minor sub-box **1806***a* of the initial image **1800***a*. Furthermore, the position of the treatment overlay **1810***e* of FIG. **18***e* is shifted relative to the position of the treatment overlay **1810***a* of FIG. **18***a*.

[0247] Surgical Workflow

[0248] FIG. **19** is a flowchart of the workflow of surgical steps to complete a laser cut in a region of interest. The workflow is enabled by the integrated surgical system **1000** disclosed herein and may be performed by the integrated surgical system based on input received from a surgeon. As part of the workflow and with reference to FIG. **18***a*, a treatment box **1810***a* may be moved around by the user through the control system **100** of the integrated surgical system **1000** to place it over the region of interest, e.g., the trabecular meshwork. As described further below, the location of the treatment box **1810***a* may change due to movement of an azimuthal slider or movement of a circumferen-

tial slider. Also, as described above, the location of the treatment box **1810***a* may also shift due to movement of the focusing objective **826** during laser scanning.

[0249] At block **1902**, and with additional reference to FIG. **18***a*, a treatment box **1810***a* is positioned over a region of interest at an azimuthal location through a graphical user interface (GUI). To this end, the vertical scale **1802** may correspond to a GUI in the form of a vertical box with a vertical slider **1811** that is configured to move up and down in response to a user activation means, e.g., mouse pointer, keyboard up/down button, etc. The numerical values at the top and bottom of the vertical scale **1802** represent the azimuthal dimension of the treatable area of the surgical system, where the treatable area is between the parallel horizontal lines **1813***a*, **1813***b*. The center of the vertical scale **1802** is taken to be zero. Thus, placing the vertical slider **1811** at zero places the vertical center of treatment box **1810***a* at the azimuthal center of the treatable area. As the vertical slider **1811** is moved up and down, the value of the slider changes, and the treatment box **1810***a* azimuthal position moves in real time. Once the treatment box **1810***a* is at the desired azimuthal location, the value of the vertical slider **1811** is returned to system software and taken as parameter dA.

[0250] At block **1904**, and with continued reference to FIG. **18***a*, the treatment box **1810***a* is positioned over the region of interest at a circumferential location through a graphical user interface (GUI). To this end, the horizontal scale **1808** may correspond to a GUI in the form of a horizontal box with a horizontal slider **1815** that is configured to move side-to-side in response to a user activation means, e.g., mouse pointer, keyboard up/down button, etc. The numerical values at the ends of the horizontal scale **1808** represent the circumferential dimension of the treatable area of the surgical system, where the treatable area is along the length of the parallel horizontal lines **1813***a*, **1813***b*. The center of the horizontal scale **1808** is taken to be zero. Thus, placing the horizontal slider **1815** at zero places the horizontal center of the treatment box **1810** at the circumferential center of the treatable area. As the horizontal slider **1815** is moved side-to-side, the value of the slider changes, and the treatment box **1810***a* circumferential position moves in real time. Once the treatment box **1810***a* is at the desired circumferential location, the value of the horizontal slider **1815** is returned to system software and taken as parameter dC.

[0251] At block **1906**, a user interface, e.g., keyboard, of the control system **100** receives inputs corresponding to the height H (azimuthal dimension) and width W (circumferential dimension) of a 3D treatment pattern through which the surgical system will scan a laser. These parameters of the treatment pattern specify a two-dimensional plane (e.g., x-y plane) referred to as a 2D channel size. Upon receipt of these inputs, the software of the control system **100** resizes the azimuthal and circumferential dimensions of the treatment box **1810***a* displayed on the screen, while maintaining the location of the center of the box at its location set by the positioning of the vertical slider **1811** in block **1902** and the horizontal slider **1815** set respectively in block **1904**. The boundaries of the treatment box **1810***a* as displayed define the azimuthal and circumferential dimensions of the 3D treatment pattern.

[0252] At block **1908**, a user interface, e.g., push button, of the control system **100** is activated and in response to such activation, the control system **100** performs laser treatment of the ocular tissue within the treatment box **1810***a*. To this end, at block **1908***a* and with reference to FIG. **18***a*, the laser focus is placed at a depth location of the 3D treatment pattern and then at a starting location of the treatment box **1810***a*. For example, the laser focus may be placed at the top left corner **1817** of the treatment box **1810***a*. The top left corner **1817** of the treatment box **1810***a* has coordinates (dA+H/2, dC−W/2), where:

[0253] dA=the value of the vertical slider **1811** obtained in block **1902**

[0254] dC=the value of the horizontal slider **1815** obtained in block **1904**

[0255] H=height/azimuthal dimension obtained in block **1908**

[0256] W=width/circumferential dimension obtained in block **1908**

[0257] Regarding laser focus placement, the integrated surgical system **1000** includes two galvos—one for moving the laser beam in the azimuthal direction and the other for moving the laser beam in the circumferential direction. The galvos move when voltage is applied to them. Each galvo has an empirically determined calibration constant in units of micron/V. For example, a calibration of 700 um/V for azimuthal would mean that for a change of one volt, the laser beam would move 700 um along the azimuthal axis. Each galvo has a "zero" position, which corresponds to the center of its respective scale **1802**, **1808**. More specifically and with reference to FIG. **18***a*, the zero position of the azimuthal galvo corresponds to the zero position of the vertical scale **1802**, while the zero position of the circumferential galvo corresponds to the zero position of the horizontal scale **1808**. From a control standpoint, this "zero" position corresponds to a certain angle that the galvo sits at about which it deviates when the laser is scanned.

[0258] Thus, as part of placing the laser focus at the starting location in block **1908***a*, the control system **100** uses the azimuthal and circumferential calibration constants to calculate the required azimuthal and circumferential voltages to place the laser focus at a starting location, e.g., the top left corner **1817** of the treatment box **1810***a*.

[0259] At block **1908***b*, based upon laser spot separation settings, the laser focus is then raster scanned from the top left corner **1817** of the treatment box **1810***a* to an end location, e.g., the bottom right corner **1819**, of the treatment box. The bottom right corner **1819** of the treatment box **1810***a* has coordinates (dA−H/2, dC+W/2).

[0260] At block **1910**, the control system **100** determines whether additional layers of the 3D treatment pattern remain to be treated. If additional layers remain, the workflow returns to block **1908**, where laser treatment is performed at another depth location of the 3D treatment pattern. If no additional layers remain, the workflow ends at block **1912**.

[0261] As describe above with reference to FIG. **17**, during laser scanning in accordance with embodiments disclosed herein, the field of view of the visualization system remains fixed relative to the target volume **60** within the region of interest despite movement of the focusing objective during laser scanning. Because the field of view of the visualization system is fixed, the image on the display screen remains fixed, as shown in FIG. **18***a*-**18***c*. Therefore, the treatment box **1810***a* on the display screen remains fixed in place on the screen during laser scanning.

[0262] Control System

[0263] FIG. **20** is a schematic block diagram of an apparatus **2000** corresponding to the control system **100** of FIG. **8***b*. The apparatus **2000** is configured to execute instructions related to the imaging processes described above with reference to FIG. **17**. The apparatus **2000** may be embodied in any number of processor-driven devices, including, but not limited to, a server computer, a personal computer, one or more networked computing devices, a microcontroller, and/or any other processor-based device and/or combination of devices.

[0264] The apparatus **2000** may include one or more processing units **2002** configured to access and execute computer-executable instructions stored in at least one memory **2004**. The processing unit **2002** may be implemented as appropriate in hardware, software, firmware, or combinations thereof. A hardware implementation may be a general-purpose processor, a digital signal processor (DSP), an application specific integrated circuit (ASIC), a microprocessor, a microcontroller, a field programmable gate array (FPGA), a System-on-a-Chip (SOC), or any other programmable logic component, discrete gate or transistor logic, discrete hardware components, or any combination thereof, or any other suitable component designed to perform the functions described herein. Software or firmware implementations of the processing unit **2002** may include computer-executable or machine-executable instructions written in any suitable programming language to perform the various functions described herein.

[0265] The memory **2004** may include, but is not limited to, random access memory (RAM), flash RAM, magnetic media storage, optical media storage, and so forth. The memory **2004** may include volatile memory configured to store information when supplied with power and/or non-volatile memory configured to store information even when not supplied with power. The memory **2004** may store various program modules, application programs, and so forth that may include computer-executable instructions that upon execution by the processing unit **2002** may cause various operations to be performed. The memory **2004** may further store a variety of data manipulated and/or generated during execution of computer-executable instructions by the processing unit **2002**.

[0266] The apparatus **2000** may further include one or more interfaces **2006** that facilitate communication between the apparatus and one or more other apparatuses. For example, the interface **2006** may be configured to communicate with the laser source **200** and components of the second optical subsystem **1002**. The interface **2006** is also configured to transmit images captured by components of the second optical subsystem **1002** to the display **110** of FIG. **8***b*. Communication may be implemented using any suitable communications standard. For example, a LAN interface may implement protocols and/or algorithms that comply with various communication standards of the Institute of Electrical and Electronics Engineers (IEEE), such as IEEE 802.11.

[0267] The memory **2004** may store various program modules, application programs, and so forth that may include computer-executable instructions that upon execution by the processing unit **2002** may cause various operations to be performed. For example, the memory **2004** may include an operating system module (O/S) **2008** that may be configured to manage hardware resources such as the interface **2006** and provide various services to operations executing on the apparatus **2000**.

[0268] The memory **2004** stores operation modules such as a movement control module **2010**, an image/display module **2012**, a treatment plan module **2014**, and a laser control module **2016**. These modules may be implemented as appropriate in software or firmware that include computer-executable or machine-executable instructions that when executed by the processing unit **2002** cause various operations to be performed, such as the operations described above with reference to FIG. **17**. For example, the movement control module **2010** executes instructions that cause movement of the visualization system **828** that keeps or maintains the position of the field of view **831** of the visualization system relative to the target volume **60** of ocular tissue during a movement of a focus of a laser beam to a depth location within the target volume of ocular tissue. For example, the movement control module **2010** may execute instructions that cause a first movement mechanism, e.g., first plate **844** and objective motor **845**, to move the focusing objective **826** (together with the visualization system **828**), and a second movement mechanism, e.g., second plate **846** and the camera motor **847**, to move the visualization system **828** as a function of the movement by the first movement mechanism. The image/display module **2012** executes instructions that cause the visualization system **828** to capture and display (through a display **110**) an initial image of a region of an eye and subsequent images of the region. The treatment plan module **2014** executes instructions that cause the scanner component **830** and the objective motor **845** to scan the focus of a laser through a target volume of ocular tissue in accordance with a treatment plan. The laser control module **2016** executes instructions that cause the laser source **200** to delivery optical energy sufficient to affect treatment of the ocular tissue. For example, the laser source **200** may output energy that causes photodisruption of ocular tissue.

[0269] As an alternative to software or firmware, one or more of the modules **2010**, **2012**, **2014**, **2016** may be implemented as appropriate in hardware. A hardware implementation may be a general-purpose processor, a DSP, an ASIC, a FPGA or other programmable logic component, discrete gate or transistor logic, discrete hardware components, or any combination thereof, or any other suitable component designed to perform the functions described herein.

SUMMARY

[0270] Thus, disclosed herein is an integrated surgical system **1000** that provides an opto-mechanical coupling of a focusing objective **826** and a visualization system **828** that ensures a fixed, stable, real-time gonioscope imaging during surgery. Specifically, during a surgical procedure the initial image remains functionally the same throughout the procedure. In other words, the object of interest, e.g., the trabecular meshwork and the surrounding tissue, stays in focus and the field of view does not shift. Regarding the fixed field of view, in terms of imaging hardware, each feature of the object of interest is imaged to the same location of the sensor of the visualization system **828** as the focusing objective **826** moves along a second optical axis **706** in a depth direction, e.g., a z direction. Because of this, the image of the trabecular meshwork and the surrounding tissue itself is "locked"

in so that the image of the trabecular meshwork and the surrounding tissue captured by the visualization system **828** during the procedure does not change in a perceivable way. In other words, the gonioscope image appears fixed with a consistent focus quality and field of view.

[0271] In some embodiments, the opto-mechanical coupling of the focusing objective **826** and the visualization system **828** is accomplished by mounting the visualization system to a second plate **846** having a camera motor **847**, and then mounting the second plate **846** to a first plate **844** having the focusing objective **826** mounted thereto and an objective motor **845**. The objective motor **845**, operating under control of the control system **100**, moves the first plate **844** to thereby move the focusing objective **826** together with the second plate **846** (and the visualization system mounted to a second plate) in the Z_A direction. The camera motor **847**, operating under control of the control system **100**, moves the second plate **846** in the Z_B direction to thereby move the visualization system **828** relative to the first mechanical axis **850** of the focusing objective **826**, without moving the first plate **844** or the focusing objective.

[0272] As noted above in describing FIG. **18***a* verses FIGS. **18***d* and **18***e*, without this opto-mechanical coupling, movement of the focusing objective **826** would cause the gonioscope image to change during the procedure. For example, the image would vertically "shift" as the focusing objective **826** scans the depth of the treatment pattern. This shift would result from a combination of the off-axis imaging, where the chief optical ray angle of the visualization system **828** has an azimuthal component, and from the fact that the visualization system is mechanically attached to the first plate **844** and the objective motor **845** so that the visualization system has the same motion (direction and distance) as the motion of the focusing objective **826**. Other characteristics of the gonioscope image that may change include image magnification (field of view size remains the same), image quality factors such as distortion and optical aberrations, and resolution, contrast, and quality of focus.

[0273] If these imaging characteristics are not compensated for, the usability and functionality of the visualization system **828** is adversely affected. For example, the user's ability to discern anatomical features, such as the transition regions between trabecular meshwork, scleral spur and Schwalbe's line is degraded; the vertical location of the trabecular meshwork in the image shifts as the treatment proceeds making it confusing to discern; the field of view grows or shrinks with the scan, potentially vignetting important regions of the image; and finally, the position of system overlays generated on image screens are altered relative to the desired surgical zone changes, giving a misleading impression to the user where the surgery is actually taking place.

[0274] The control system **100** is further configured to control the movement of the treatment overlay **1810***a*, **1810***b*, **1810***c* on the gonioscope image **1800***a*, **1800***b*, **1800***c* so that the overlay tracks the surgical region or surgical channel as the focusing objective **826** moves the laser focus through the depth of the target volume of ocular tissue at the surgical channel. As mentioned previously, the treatment overlay **1810***a*, **1810***b*, **1810***c* or treatment box is a software construction, which is a rectangle representing the size of the 2D surgical channel and is not something that is captured by the camera of visualization system **828**. The treatment overlay **1810***a*, **1810***b*, **1810***c* is overlaid onto the gonioscope image **1800***a*, **1800***b*, **1800***c* by the control system **100** software and the user can control the position of the treatment overlay on the gonioscope image **1800** and the size of the overlay.

[0275] In accordance with embodiments disclosed herein, the software of the control system **100** is configured to apply a movement or transfer function to the treatment overlay **1810***a*, **1810***b*, **1810***c* that moves the overlay in such a manner that ensure the treatment overlay appears fixed in place relative to a location of the gonioscope image **1800***a*, **1800***b*, **1800***c* and maintains such appearance while the focusing objective **826** is moved during laser scanning. The transfer function of the treatment overlay **1810***a*, **1810***b*, **1810***c* may also be dependent on the azimuthal and circumferential galvo positions during the scanning of the laser in the x and y directions, along with laser scanning in the z direction by the objective motor and gonio stepper positions. In this case, movement of the treatment overlay **1810***a*, **1810***b*, **1810***c* by the control system **100** depends on the objective motor **845** position and the rate of change of azimuthal surgical position (y position) with objective motor position.

[0276] Without the overlay transfer function, the image field of view would vertically shift as the focusing objective **826** moves in the z direction and the treatment overlay **1810** would no longer occupy the same position on the gonioscope image **1800**. In other words, the treatment overlay would be offset. For example, in comparing the gonio scope images of FIGS. **18***a* and **18***d* note: 1) the field of view of the gonioscope image **1800***d* of FIG. **18***d* is vertically shifted upward relative to the field of view of the gonioscope image **1800***a* of FIG. **18***a*, where the shift is most notable from the shift in images inside of the respective major sub-boxes **1804***a*, **1804***d*; and 2) the treatment overlay **1810***d* in FIG. **18***d* is vertically shifted downward relative to the treatment overlay **1810***a* in FIG. **18***a*.

[0277] Considering the treatment overlay **1810***a*, **1810***b*, **1810***c* or treatment box further, as previously mentioned the treatment overlay physically represents the location and size of a laser cut. The resulting laser cut will have the same size and be in the same location relative to the displayed anatomy, as the treatment overlay **1810***a*, **1810***b*, **1810***c* on the display screen.

[0278] While the foregoing description details features of an integrated surgical system **1000** that provides consistent field of view and focus, the system also provides for consistency with respect to other visual characteristics of images, such as resolution, distortion, and magnification, of the subsequent image **1800***b*, **1800***c* is the same as or within an acceptable tolerance of those of the initial image **1800***a*. Quantitatively, consistency in resolution among the initial image **1800***a* and the subsequent image **1800***b*, **1800***c* may be evidenced through modulation transfer function (MTF) measurements, which are mathematical descriptions of contrast. Consistency in distortion among the images **1800***a*, **1800***b*, **1800***c* may be evidenced using standard, well known algorithms, while consistency in magnification among the images may be evidenced by imaging a ruler, measuring the length of the ruler in pixels, and then calculating its imaged length with knowledge of the detector pixel size.

[0279] The various aspects of this disclosure are provided to enable one of ordinary skill in the art to practice the present invention. Various modifications to exemplary embodiments presented throughout this disclosure will be

readily apparent to those skilled in the art. Thus, the claims are not intended to be limited to the various aspects of this disclosure but are to be accorded the full scope consistent with the language of the claims. All structural and functional equivalents to the various components of the exemplary embodiments described throughout this disclosure that are known or later come to be known to those of ordinary skill in the art are expressly incorporated herein by reference and are intended to be encompassed by the claims. Moreover, nothing disclosed herein is intended to be dedicated to the public regardless of whether such disclosure is explicitly recited in the claims. No claim element is to be construed under the provisions of 35 U.S.C. § 112, sixth paragraph, unless the element is expressly recited using the phrase "means for" or, in the case of a method claim, the element is recited using the phrase "step for."

[0280] It is to be understood that the embodiments of the invention herein described are merely illustrative of the application of the principles of the invention. Reference herein to details of the illustrated embodiments is not intended to limit the scope of the claims, which themselves recite those features regarded as essential to the invention.

What is claimed is:

1. A method of imaging a region of an eye including a target volume of ocular tissue, the method comprising:

placing a depth of field and a field of view of a visualization system at respective positions relative to the target volume of ocular tissue;

obtaining an image of the region of the eye with the visualization system;

maintaining the position of the field of view of the visualization system relative to the target volume of ocular tissue during a movement of a focus of a laser beam to a depth location within the target volume of ocular tissue; and

repeating the maintaining for each of a plurality of movements of the focus of the laser beam to different depth locations within the target volume of ocular tissue.

2. The method of claim **1**, wherein the visualization system is optically coupled to a focusing objective and placing the depth of field and the field of view of the visualization system at respective positions relative to the target volume of ocular tissue so the target volume is within the depth of field and within the field of view comprises one or more of:

moving the focusing objective along a first mechanical axis; and

moving the visualization system along a second mechanical axis.

3. The method of claim **2**, wherein moving the focusing objective along a first mechanical axis comprises moving the visualization system together with the focusing objective.

4. The method of claim **1**, wherein the laser beam and the visualization system are optically coupled to a focusing objective and maintaining the position of the field of view of the visualization system relative to the target volume of ocular tissue during a movement of a focus of a laser beam to a depth location within the target volume of ocular tissue comprises:

moving the focusing objective along a first mechanical axis to cause the movement of the focus of the laser beam, and

moving the visualization system along a second mechanical axis.

5. The method of claim **4**, wherein moving the focusing objective along a first mechanical axis comprises moving the visualization system together with the focusing objective.

6. The method of claim **4**, wherein moving the visualization system along a second mechanical axis comprises moving the visualization system without moving the focusing objective.

7. The method of claim **4**, wherein moving the focusing objective and moving the visualization system occur sequentially.

8. The method of claim **4**, wherein moving the focusing objective and moving the visualization system occur simultaneously.

9. The method of claim **1**, wherein the target volume of ocular tissue has a thickness, the depth of field has a center, and placing the depth of field relative to the target volume so the target volume is within the depth of field comprises positioning the center of the depth of field at or near the center of the thickness of the target volume.

10. The method of claim **9**, wherein the depth of field is greater than the thickness of the target volume.

11. The method of claim **10**, wherein the depth of field is in a range of 2 times to 10 times greater than the thickness of the target volume.

12. A system for imaging a region of an eye including a target volume of ocular tissue, the system comprising:

a laser source configured to output a laser beam;

a first optical subsystem configured to be coupled to the eye;

a focusing objective optically coupled with the first optical subsystem and the laser source;

a visualization system having a depth of field and a field of view, the visualization system optically coupled to the focusing objective and to the first optical subsystem through the focusing objective;

a movement subsystem configured to move the focusing objective and the visualization system; and

a control system configured to control the movement subsystem and the visualization system to:

place the depth of field and the field of view of the visualization system at respective positions relative to the target volume of ocular tissue so the target volume is within the depth of field and within the field of view,

obtain an image of the region of the eye with the visualization system, and

maintain the position of the field of view of the visualization system relative to the target volume of ocular tissue during movement of a laser focus of the laser beam to a depth location within the target volume of ocular tissue.

13. The system of claim **12**, wherein the movement subsystem comprises:

a first mechanism arranged to move the focusing objective together with the visualization system, and

a second mechanism arranged to move the visualization system without moving the focusing objective.

14. The system of claim **13**, wherein the control system controls the movement subsystem to maintain the position of the field of view of the visualization system by being further configured to:

control the first mechanism to move the focusing objective along a first mechanical axis together with the visualization system, and

control the second mechanism to move the visualization system along a second mechanical axis without moving the focusing objective.

15. The system of claim **14**, wherein the first mechanical axis and the second mechanical axis are one of parallel each other, at an angle relative to each other, or are co-axial.

16. The system of claim **14**, wherein movement by the first mechanism and movement by the second mechanism are one of sequential or simultaneous.

17. The system of claim **12**, wherein the movement subsystem comprises:

a first mechanism arranged to move the focusing objective, and

a second mechanism arranged to move the visualization system.

18. The system of claim **17**, wherein the control system controls the movement subsystem to maintain the position of the field of view of the visualization system by being further configured to:

control the first mechanism to move the focusing objective along a first mechanical axis, and

control the second mechanism to move the visualization system along the first mechanical axis and along a second mechanical axis.

19. The system of claim **18**, wherein the first mechanical axis and the second mechanical axis are of parallel each other, at an angle relative to each other, or are co-axial.

20. The system of claim **18**, wherein movement by the first mechanism and movement by the second mechanism is one of sequential or simultaneous.

21. A method of imaging a region of an eye including a target volume of ocular tissue, the method comprising:

moving a visualization system to place a field of view of the visualization system at a location relative to the region of the eye;

moving a focusing objective to place a laser focus of a laser beam at a depth location within the target volume of ocular tissue; and

moving the visualization system without moving the focusing objective to keep the field of view of the visualization system at the location relative to the region of the eye.

22. The method of claim **21**, wherein moving the focusing objective to place a laser focus of a laser beam at a depth location within the target volume of ocular tissue comprises:

simultaneously moving the visualization system and the focusing objective a first distance in a first direction along a first mechanical axis.

23. The method of claim **22**, wherein moving the visualization system without moving the focusing objective to keep the field of view of the visualization system at the location relative to the region of the eye comprises:

moving the visualization system a second distance in a second direction along a second mechanical axis, while maintaining the position of the focusing objective.

24. The method of claim **23**, wherein the second distance is a function of the first distance.

25. The method of claim **21**, wherein the visualization system is mechanically coupled to the focusing objective to move together with the focusing objective along a first mechanical axis and to move independent of the focusing objective along a second mechanical axis, and moving the visualization system to place a field of view of the visualization system at a location relative to the region of the eye comprises moving the visualization system along the second mechanical axis.

26. A system for imaging a region of an eye including a target volume of ocular tissue, the system comprising:

a laser source configured to output a laser beam;

a first optical subsystem configured to be coupled to the eye;

a second optical subsystem optically coupled to the first optical subsystem, and including: a) a focusing objective that is optically coupled to obtain the laser beam from the laser source, b) a visualization system that is optically coupled to the focusing objective, c) a first movement mechanism arranged to move the focusing objective and the visualization system, and d) a second movement mechanism arranged to move the visualization system; and

a control system coupled to the second optical subsystem and configured to control the visualization system, the first movement mechanism, and the second movement mechanism to:

move the visualization system to place a field of view of the visualization system at a location relative to the region of the eye;

move the focusing objective to place a laser focus of a laser beam at a depth location within the target volume of ocular tissue; and

move the visualization system without moving the focusing objective to keep the field of view of the visualization system at the location relative to the region of the eye.

27. The system of claim **26**, wherein the control system moves the focusing objective to place the focus of the laser beam at the depth location by being configured to activate the first movement mechanism to move the focusing objective and the visualization system a first distance in a first direction along a first mechanical axis.

28. The system of claim **26**, wherein the control system moves the visualization system without moving the focusing objective by being configured to activate the second movement mechanism to move the visualization system a second distance in a second direction along a second mechanical axis.

29. The system of claim **26**, wherein the first movement mechanism comprises:

a first structure carrying each of the visualization system and the focusing objective; and

a first motor coupled to the first structure and configured to move the first structure along a first mechanical axis.

30. The system of claim **26**, wherein the second movement mechanism comprises:

a second structure carrying the visualization system but not the focusing objective; and

a second motor coupled to the second structure and configured to move the second structure along a second mechanical axis.

31. The system of claim **30**, wherein the second movement mechanism is carried by the first movement mechanism.

* * * * *